Università degli Studi della Basilicata

Scuola di Dottorato di Ricerca

Dottorato di Ricerca in
"Rischio Sismico"

Analysis of dynamic behaviour of buildings and their soil-structure-soil interaction.

Settori Scientifico-Disciplinari
GEO/10, ICAR/07, ICAR/09

Coordinatore del Dottorato:

Prof.ssa Caterina DI MAIO

Candidato:

Dott. Rocco DITOMMASO

Tutors:

Prof. Vincenzo CAPUTO, Prof. Marco MUCCIARELLI, Prof. Felice C. PONZO

Relatore:

Prof. Marco MUCCIARELLI

Correlatori:

Prof. Vincenzo CAPUTO, Dr. Stefano PAROLAI, Prof. Felice C. PONZO

A.A. 2008/2009 - Ciclo XXII

SUMMARY

This thesis, entitled *'Analysis of dynamic behaviour of buildings and their soil-structure-soil interaction*', is the sum of the experiences, both theoretical and experimental, collected during the three years of my PhD in Seismic Risk, held at the Department of Structures, Geotechnics and Engineering Geology of the University of Basilicata.

The title reveals that the main issues addressed concern the analysis of the dynamic behaviour of structures and their nonlinear dynamic interaction with the soil. Too often this unique problem is treated, with a simplified approach, analyzing the building behaviour, modelled with fixed base, and using the soil just as a propagator that can change the seismic input.

It is obvious that this phenomenon requires adequate tools to characterize the dynamics of a system (soil and building) which can be very complex, due to the nonlinearity that soil and/or superstructure may have during the seismic motion. The result is a highly non-stationary behaviour that is ill-suited to be studied with the classical techniques for dynamic characterization.

The classical approach to study these kinds of problems concerning the dynamic soil-structure interaction is to subdivide the main problem into two sub-problems: kinematic and inertial interaction. This approach remains valid to estimate, using an approximate solution, the maximum values of the actions that superstructure and soil will mutually exchange during the seismic motion, but it is not adequate to properly evaluate the actions that instant by instant both systems are exchanging.

The approach proposed in this work is based on the idea postulated by Şafak, which consists in modelling both the structure and the soil as means for wave propagation. In this way, using a discrete approach, the system becomes a chain of mechanical oscillators, each having its mass, stiffness and damping. Obviously, using a discrete model it was necessary to introduce some variables that allow to take into account the attenuation of seismic motion with the distance and the ability of different buildings to radiate energy into the ground, accounting also for the mechanical properties and geometry of the foundation system and of the soil layers.

The proposed models were calibrated and validated using data collected during several experiments performed on real structures with different sizes: Bagnoli Experiment, Falkenhof Tower and housings of the Accelerometric National Network (RAN).

As for the analysis of the dynamic behaviour of structures and characterization of the main parameters that govern the linear and non-linear dynamic behaviour, several laboratory experiments and *in situ* tests have been carried out. Laboratory tests were performed at the Laboratory of Structures the University of Basilicata in the JET-PACS project that focused on the evaluation of the dynamic behaviour of a steel frame structure, 2:3 scaled and retrofitted by several seismic devices, for both semi-active and passive protection. During these tests the structure was monitored using accelerometers and displacement transducers that were located at all levels and all degrees of freedom relevant for the experiment. This structure was also used to validate an original technique for the expeditious evaluation of the rotational modes of the buildings.

For the evaluation of the dynamic characteristics of bridges and buildings *in situ* experiments (Fatih Bridge, Falkenhof Tower, housings of RAN, Municipality of Navelli) were also performed, using different kinds of sensors: accelerometers and velocimeters, and also a new wireless sensors. During these experiments it was possible to test the most widely diffused techniques and methodologies for the characterization of the dynamic behaviour of structures and for the expeditious evaluation of the safety of strategic buildings. In this regard, a new methodology has been proposed, which belong to the first level methods for the rapid assessment of the safety of strategic Italian buildings.

The progress of the work gave rise to the idea of researching new techniques that overcome some limitations of current techniques, allowing a proper evaluation of the dynamic systems response including the non-stationarity. Indeed, taking into account the severe limitations of using classical tools to study the non-stationary systems, a technique has been suggested both for analyzing and signal filtering.

This technique, based on S-Transform, allows to study the dynamic response of nonlinear systems and to monitor the temporal evolution of the main dynamic characteristics of systems during strong-motion.

In the first chapter the problem of numerical modelling of soil-structure system is addressed in detail and the main results obtained by numerical and experimental tests are shown. The problem was treated considering more than one building, and the interaction among different buildings was also accounted for. Chapter two still covers the dynamic soil-structure-soil interaction, focusing on issues relating to the characterization of the dynamic response of a tower forced both by environmental noise and by vibrations produced by an explosion. The structure interacted with a smaller

building, adjacent to the tower and having a common floor with the main structure. In this chapter a comparison among the results obtained using different techniques of signals analysis (with and without forcing) is presented.

Chapter three still deals with the issue of monitoring and dynamic characterization discussing the technologies, techniques and results of an experiment carried out on the Fatih bridge in Istanbul. The evaluation of the main features of the bridge was performed under normal traffic conditions. The ability to monitor the real-time response of a building subject to seismic actions using the same type of instrumentation is discussed in chapter four, showing the preliminary results of monitoring performed on the Municipality of Navelli during the L'Aquila seismic sequence, while in chapter five a new fast method for assessing the health status of building after a seismic event is presented. In particular, the methodology was calibrated for the Italian strategic buildings.

Chapter six discusses the purpose and techniques used during the Jet-Pacs project and, in particular, the techniques and configurations used for the estimation of the dynamic characteristics of the frame used to test the passive and semi-active control devices.

Chapter seven presents a fast technique for estimating both natural frequencies and the main rotational modes of existing buildings, in order to study their dynamic behaviour.

Chapter eight finally presents an innovative procedure to study the non-stationary behaviour of soil and structures, overcoming the limits of classical techniques. In particular, examples of applications to soils and buildings were shown.

The chapters of this thesis are based on already published (or submitted) papers on international journals or proceedings of international conferences:

Chapter 1: *Effect of vibrating buildings on "free-field" accelerometric recordings: from the Bagnoli experiment to many-buildings simulation. Proc. 4th Int. Conf. Earthq. Geot. Eng., CD-Rom edition, Paper No. 1388. Springer, ISBN 978-1-4020-5893-6; Effect of building-building interaction on "free-field" ground motion. Increasing Seismic Safety by Combining Engineering Technologies and Seismological Data. Springer, pp 141-145, ISBN 978-1-4020-9196 -4; Effect of a single vibrating building on free-field ground motion: numerical and experimental evidences. Bulletin of Earthquake Engineering, DOI: 10.1007/s10518-009-9134-5;*

Chapter 2: *Monitoring the response and the back-radiated energy of a building subjected to ambient vibration and impulsive action: the Falkenhof Tower (Potsdam, Germany). Bulletin of Earthquake Engineering - DOI: 10.1007/s10518-009-9151-4;*

Chapter 3*: Wireless technologies for the monitoring of strategic civil infrastructures: an ambient vibration test on the Fatih Sultan Mehmet Suspension Bridge in Istanbul, Turkey. Bulletin of Earthquake Engineering - DOI: 10.1007/s10518-009-9132-7;*

Chapter 4: *Real time monitoring of structures in task-force missions by wireless systems: the example of the mw = 6.3 central Italy earthquake, April 6, 2009. Natural Hazards - DOI 10.1007/s11069-009-9481-1.*

Chapter 5: *A fast method for structural health monitoring of Italian strategic buildings. Submitted to Bulletin of Earthquake Engineering.*

Chapter 6: *Jet-Pacs project: joint experimental testing on passive and semiactive control systems. The 14th World Conference on Earthquake Engineering. Beijing, China, October 12-17, 2008.*

Chapter 7*: Identification of building rotational modes using an ambient vibration technique. Accepted for publication in the Proceedings of the 14th European Conference on Earthquake Engineering. August 30 – September 03, 2010. Ohrid, Republic of Macedonia;*

Chapter 8: *S-Transform based filters applied to the analysis of nonlinear dynamic behaviour of buildings. Accepted for publication on The 14th European Conference on Earthquake Engineering. August 30 – September 03, 2010. Ohrid, Republic of Macedonia.*

ABSTRACT AND INTRODUCTION

This manuscript opens with the discussion, introduced in Chapter 1, on the problem of modelling soil-structure systems. Several authors have dealt with this problem, often tackled with different approaches that lead to different conclusions.

The idea that the buildings could somehow modify the free-field ground motion was postulated for the first time in 1975; almost all authors agree that buildings, and more generally all structures, are able to interact with the ground radiating energy and thus changing the motion on the surrounding area. Conversely, there are discrepancies about the effects of the radiation in an area when more than one buildings insists. Bearing in mind that the interference of radiation could be both beneficial and detrimental, and that buildings are systems with damping, some authors state that in the case of urbanized areas, the buildings would have a beneficial effect, helping dissipate a large part of the energy released from the source.

Other authors do not agree with these conclusions and, on the basis of experimental data and reliable numerical modelling, show that the effects of structures are not necessarily beneficial. In the presence of structures, the total energy of motion decreases with increasing number of buildings in the area, yet, as it might be expected from a physical viewpoint, in correspondence of the main frequencies of vibration a strong amplification of the seismic motion occurs.

The initial part of chapter 1 describes the numerical model used in the analyses and its implementation in Simulink. This model has been calibrated and validated against results obtained during tests performed on a real building located in the old industrial area of Bagnoli (Naples). After its validation, the model has been used to study the influence that three buildings could have on the response of an accelerometric station placed in the surrounding area.

Using a statistical approach (Montecarlo), the central part of chapter 1 presents the results concerning the study on the influence of three buildings on the response of an accelerometric station placed in the surrounding area; the difference with the previous analyses is that the buildings are assumed to interact with each other.

As previously outlined, it is known that medium and large size structures are able to modify the free-field ground motion in the surrounding areas, but few studies have been carried out about the ability of small buildings to influence the free-field response. The final part of chapter 1 presents a numerical and experimental study, performed during

the S4 Project (DPC-INGV 2007-2009), on the ability of the housings to contaminate the accelerometric recordings of instruments placed inside them. In general, the geometric characteristics of these structures are selected so that they should behave as small structures. Furthermore, on the basis of results derived from the analysis of recordings and on a model developed to study a generic soil-structure system, this section proposes some schedules aimed at evaluating in an approximate, yet quantitative way, the influence that a single building could have on a seismic station placed nearby.
Schedules are referred to two classes of structures: the former is referred to small-scale buildings, the latter related to medium and large size buildings. This section of the PhD thesis deals with the ability of structures to contaminate some interesting engineering parameters such as: PGA, Housner Intensity and Spectral Acceleration.
In the introductory section it was explicitly stated that the study of the dynamic response of a system composed by soil and superstructure requires analysis tools, with a different degree of complexity, adequate to characterize the most significant parameters in the different conditions faced by the system during its life.
These systems generally exhibit a stationary response when they are excited by an input with low intensity such, for example, ambient noise. On the contrary, these systems may exhibit a less stationary behaviour for higher values of the action (strong earthquakes) and/or when the constraint conditions are more complex than a single building with fixed base (for example: interacting buildings).
In chapter 2 the results related to the research carried out on the Falkenhof tower are presented. The structure is located in an uninhabited area of Potsdam city (Germany); for this experiment the dynamic response, both in ambient noise and forced vibration, was monitored. Furthermore, the results obtained using different techniques to analyze the signals were compared. It is interesting to observe that, although the intensity of the excitation is very low, the structure exhibits a behaviour completely different from that shown when forced with ambient noise. In this case the non-stationarity of behaviour is not related to nonlinear behaviour of the structure, but is due to the interaction with a small adjacent building. Using velocimetric stations located within the building and on the surrounding area, it has been possible to assess the interaction between the structure and the ground. Even in this case, it was demonstrated that the presence of a structure, while helping dissipate the total energy provided by another building, tends to focus most of the energy within the ranges close to its eigenfrequencies.

The problems related to the dynamic characterization are not only linked to classical structures but even more to large size structures, such as dams and bridges. These types of structures have often a strategic function, and hence their dynamic characterization has to be performed during normal operation.

In chapter 3 the strategies for monitoring and dynamic characterization of important bridges under normal traffic conditions are discussed, using innovative, low-cost technologies. In the example shown, tri-directional accelerometric sensors with wireless technology were installed on the deck; thanks to these sensors it was possible to identify the main frequencies of vibration of the bridge without causing inconvenience, such as the interruption of traffic.

The advantages of using such sensors to monitor large-scale works, and for unaccessible areas, has to be pointed out. After their installation, if the distances are not excessive, the sensors automatically constitute a mesh and, since they communicate with each other, it is not necessary to acquire the data recorded by each instrument, but it is possible to capture data from all stations just connecting to one of the stations that belong to the mesh.

These sensors were also used to monitor the response of buildings during the L'Aquila seismic sequence.

In particular, chapter 4 presents the preliminary results of the analyses performed processing the data obtained from the real-time monitoring carried out in the Municipality of Navelli. Also in this case, the use of this type of accelerometric stations turned out be very useful. After the installation of the stations it was no longer necessary to enter the building; a fortiori, when the structural damage had reached a relevant level after several shocks, this feature turned out to be extremely useful. Without unnecessary risks, operators working outside the building could acquire and download the data just connecting to an individual station.

It is worth noting that, as an alternative to power supply, the stations can run using portable batteries that last for several days. This occurred in Municipality of Navelli, where a station was installed outside the building to assess the response of the building itself and its interaction with the ground, and it was necessary equipped with portable batteries. The station was buried, and kept on recording for several days while continuing to interact, on request, with the operator without the need to move it every time on the surface.

Still dealing with monitoring and characterization of the dynamic behaviour of buildings, it has become extremely important to get some useful information to define the health of the structure, as soon as possible after a seismic event has occurred. This applies especially for strategic buildings, where the installation of a network for permanent monitoring within the structure feasible; chapter 5 presents a new methodology for monitoring the health of buildings. This methodology obtains information on the damage suffered by the structure by installing a few sensors at the last level of the building. Depending on the structural type, some parameters are defined.

These parameters are constants which take into account the conditions of the building upon installation of the sensors and which may vary with changing the conditions of the structure. Thanks to these parameters and thanks to the structural response recorded at the last level, during an earthquake, it is possible to evaluate the maximum inter-story drift which is strongly linked to the structural damage. The correlation laws used in this methodology have been obtained through a vast amount of numerical and experimental analysis.

The characterization of the dynamic behaviour of a structure is not only useful for monitoring goals but, in the author's opinion, to calibrate numerical models. This condition is needed to design correctly the seismic retrofitting of existing buildings.

In the structural laboratory of the University of Basilicata, taking advantage of the RELUIS project (research line 7), an experimental campaign was performed on a 2:3 scaled steel structure, with the purpose of studying the dynamic behaviour of building equipped with different seismic protection systems.

It this experimentation both passive and semi-active control systems were tested using several earthquakes as inputs. Obviously, in order to design the devices it was necessary to characterize the building and to develop a realistic numerical model on the basis of the experimental results.

Chapter 6 provides a brief description of the experiment campaign and discusses the several configurations and tests performed to characterize the dynamic behaviour of the steel-frame structure.

It is evident that only in the laboratory it is possible to change the configuration of the loads and to use several different types of input in order to characterize the structure completely. Yet, it is extremely difficult to perform this kind of operations on a real

structure. Faster and cheaper techniques are thus required for the assessment of existing buildings, especially if a large number of buildings have to be examined.

Many techniques have been proposed in the literature but, on the one hand, the ones which allow to perform detailed analyses require a large number of instruments installed on the building, yielding high cost and high calculation time, and are therefore unfeasible for quick analyses.

On the other hand, there are techniques that have cost and calculation time compatible with quick analyses, but have a low level of accuracy. Chapter 7s proposes a new technique for fast dynamic characterization of structures is proposed.

This technique is very especially useful to check the rotational modes, which might be very dangerous for structural safety. This technique needs a few sensors and allows to estimate in quasi-real-time the structural eigenfrequencies and to characterize those related to torsional modes. The technique was tested on a 2:3 scaled building, the same used for the experiment discussed in chapter 8. These analyses provided practically the same results which could be obtained using other more expensive and time consuming techniques and instrumentations.

This PhD thesis work closes with chapter 8. In this last chapter a new technique for signal analyses and extrapolation of the dynamic behaviour of a non-stationary system is presented.

It is known that the techniques based on Fourier analysis are adequate to study the stationary response, but do not provide acceptable result for the characterization of the dynamic response of a system whose characteristics evolve during time. In literature many techniques are available to study non-stationary systems, but suffer from severe limitations, arising from the assumptions on which they are based.

In order to study this kinds of systems, which deteriorating buildings, special interactions with ground or adjacent structures, soils that exhibit nonlinear behaviour associated with strong deformation or liquefaction deposit, a useful analytic instrument is generally the time-frequency analysis. The analytical tools most frequently used for this purpose are: Short Time Fourier Transform, Wavelet Transform and Wigner-Ville Distribution.

These three transformations have been used extensively over the years and also provide good results when the analysis is limited to qualitative observation of nonlinear dynamic behaviour of buildings or soil.

Yet, none of these techniques can be used to extract accurate information related to single modes of vibration, or in order to filter signal using a band-variable filter over time. Exploiting the mathematical characteristics of the Stockwell transform, a band-variable filtering method was implemented in a Graphical User Interface (GUI), and is presented in chapter 8.

This method allows to overcome all the limitations of previous methods and to filter the signal by varying the bandwidth over time. Thanks to these special properties, it is possible to can extract and monitor the dynamic behaviour of a non-stationary system, focusing on individual modes of vibration. In chapter 8 examples of application both for buildings and soil are provided.

CHAPTER 1

EFFECT OF DYNAMIC SOIL-STRUCTURE-SOIL INTERACTION

A release test on a 2-story R.C. building in Bagnoli (Italy) showed that a vibrating building may affect the "free-field" motion with an influence that may reach 20% of PGA (Gallipoli *et al.*, 2006). The data of that experiment were re-analyzed following the approach proposed by Şafak (1998) to model the building motion, described as propagation of up- and down-going S-waves. Waves are assumed to propagate in a multi-layered 1-d model that includes bedrock, soil and a layer for each floor of the structure. Numerical models have been implemented in Simulink, a toolbox of MatLab, thanks to which it has been possible to solve easily the differential equations of the case. The final model is a chain of SDOF oscillators, whose dynamic behaviour depends on mass, stiffness and damping. Both the tested structure and the reaction frame built to displace it were modelled. The sum of the two motion components was propagated to sensors taking into account geometrical spreading and inelastic damping.

The good agreement between synthetic and real data suggested to simulate a many-building situation. A virtual village composed of three structures of different height was modeled to study their effect on an accelerometer located among them. The structures have been designed and analysed with the SAP 2000 code that made possible to develop the models and to calculate all dynamic characteristics of the same models. These structures have been reduced to systems with a single degree of freedom, one for each structure. The excitation was provided by three earthquakes with different characteristics of intensity and duration. Multiple tests were carried out, varying the azimuth of incident waves and the coupling between building and soil, thus obtaining a statistical distribution of the influence of vibrating buildings on "free-field" ground motion. The effect induced on free-field ground motion by the interaction among buildings set in vibration by an earthquake was investigated. This is a refinement of the previous model where the building interacted with the soil, but not among each others. Waves are propagated in a multi-layered 1-d model that includes soil and a layer for each floor of the structure. Simulink, a toolbox of MatLab that easily allows solving the differential equations of the case was used to implement numerical models. The final model is a chain of SDOF oscillators, whose dynamic behaviour depends on mass, stiffness and damping. Comparing the results with the non-interacting case, a reduction of the mean and median of the ground motion enhancement and an increase of the

dispersion are observed. The influence of vibrating buildings on the free-field ground motion could affect the earthquake recordings collected inside or nearby the buildings. Some evidences are known for large structures, but also small buildings could adversely affect the quality of the recordings. An example is given for a station of the Italian Accelerometric Network whose recordings show a clear mark of the frequency of the host building. To tackle this problem in a more general way, numerical simulations were performed aiming to validate the empirical evidences derived from a test site. Gallipoli *et al.* (2006) monitored a release test on a 2-storey R.C. building in Bagnoli (Italy), showing that a single vibrating building may affect the "free-field" motion with an influence that reaches 20% of PGA (Peak Ground Acceleration). The data of that experiment were re-analyzed following the approach proposed by Şafak (1998) to building-soil motion, described as propagation of up- and down-going S-waves. The numerical model is a chain of SDOF (Single Degree Of Freedom) oscillators, whose dynamic behaviour depends on mass, stiffness and damping. The agreement between the synthetic and real data encouraged to use this model to reproduce generalised structures as systems with a single degree of freedom. Multiple tests were carried out varying the distance, between building and station, and the building-soil coupling, thus obtaining a statistical distribution of the influence of a single vibrating building on free-field ground motion taking into account the distance.

1.1 MODEL SET-UP

1.1.1 INTRODUCTION

During an earthquake, the vibration of buildings transmitted back to the soil is able to modify the free field ground motion. This idea was postulated theoretically by Wong and Trifunac (1975) and Wirgin and Bard (1996). During an earthquake it is difficult to measure and to separate the source and site effects from ground vibrations introduced by an oscillating building one (Chavez Garcia and Cardenas Soto; 2002).

Passive and active experiments have been carried out by Jennings (1970) during forced vibration of buildings, by Kanamori *et al.* (1991) studying the effects caused by the sonic boom of the Space Shuttle on high-rise buildings in Los Angeles, by Guéguen *et al.* (2000) and Guéguen and Bard (2005) on a five-story RC-building model (1:3) located in the EuroSeisTest site at Volvi (GR), by Mucciarelli *et al.* (2003) on a base isolated building during a release test, by Gallipoli *et al.* (2004) and Cornou *et al.*

(2004) using ambient noise. The conclusions of all these experiments confirm the importance that buildings may have as seismic sources.

On the other hand, numerical simulations were performed on idealised models, without comparison with real data (see, e.g., Kham *et al.*, 2006 and references therein). The main disagreement among modellers concerns the effects of summations of wave fields from several buildings, could be either a beneficial or a detrimental factory.

The availability of an existing R/C building to be demolished in the ex-Italsider steel works at Bagnoli-Naples, in the framework of ILVA-IDEM project (Mazzolani *et al.*, 2004), gave the chance to carry out in situ large-displacement tests on a R/C frame and to model the recorded waves.

1.1.2 MODELLING THE BAGNOLI EXPERIMENT

The building tested in Bagnoli was a two-story, reinforced-concrete former office building. The structure and the soil were monitored with several accelerometers and seismometers. Full details can be found in Gallipoli at al. (2006). The aim of this section is to reproduce the strong-motion time history recorded at 5 meters distance from the building. Several cyclic and release tests were performed for engineering purposes; the induced ground motion during a 7 cm displacement test was measured. This displacement is representative of the maximum excitation that this type of building might withstand during an earthquake. The highest PGA observed is 5% *g* with a 7 cm displacement of a structure, whose natural frequency was in the range 1-2 Hz. If the standard 5% damping response spectra provided by the Italian Seismic Code is considered, a 6 cm displacement at 1 Hz is obtained for the Zone 2 – Soil A spectrum, whose PGA is 0.25 *g*.

The observed PGA is about 20% of the theoretical unmodified free-field PGA. Both the building and the contrasting frame that was set in motion during the release were modelled using SAP2000 program. The frequency obtained for the first modes of the structures matched the ones observed from the experimental data, which are around 1 Hz for the building and 30 Hz for the frame. The frame was then reduced to a SDOF with equivalent mass, stiffness and damping, while the building was reduced to a Multiple Degree Of Freedoms system (one SDOF per floor). The approach suggested by Şafak (1998) was followed: the building and the foundation soil are idealised as propagators of up- and down-going waves. The whole system was modelled using Matlab Simulink. The advantage of this approach is that it can work on subsystems (i.e.,

soil strata or building floors), adding as many subsystems as it is necessary. The only unchanged sub-systems are the bedrock (half-space with inelastic attenuation) and the building roof. The whole system used for modelling the Bagnoli experiment is reported in Fig. 1.1.

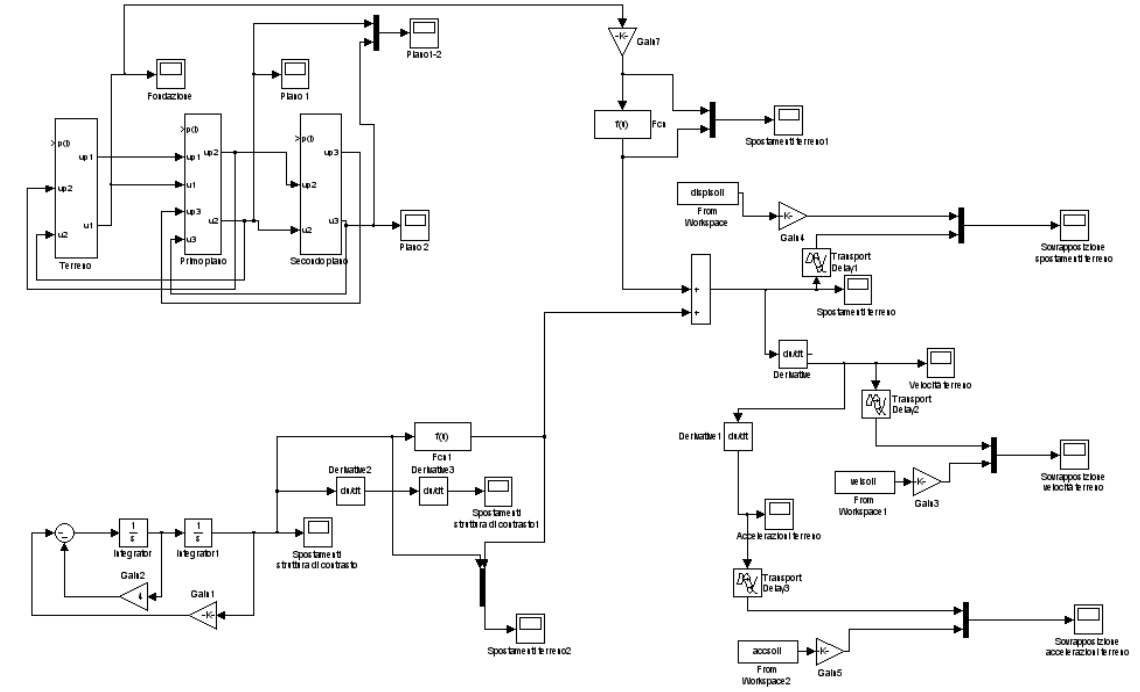

Figure 1.1: Matlab Simulink model used for the simulation of Bagnoli experiment

The two signals coming from the building and the contrasting frame were propagated in an inelastic medium reproducing the characteristics of the soil underlying the test site (volcanic ashes and alluvium). The distances were calculated from the centre of mass of the two structures projected on the ground to the accelerometer, with the attenuation given by:

$$A(r) = \frac{A_0}{r} \cdot e^{-\frac{f \cdot r}{Q \cdot v}} \qquad (1)$$

where A is the signal amplitude as a function of the travel distance r, A_0 is the initial amplitude of the signal, f is its frequency, Q is the quality factor and v is the shear wave velocity. The small strain involved allow for the assumption of soil linear behaviour. However, the model can be modified to take into account non –linearity if needed. The parameters used are reported in Tab. 1.1

Structure	*f (Hz)*	*r (m)*	*Q*	*v (m/s)*
Building	1.2	8	10	100
Contrasting frame	27	13	10	100

Table 1.1: Parameters used in the simulation

The initial condition reproduces the experiment: a 7 cm displacement of the building that is instantaneously released. The frame was dislocated according with the amount given by the SAP simulation.The equation where solved for a discrete model, a duration of 15 seconds, a variable step with Ode 45 resolution algorithm. The result for the displacements is shown in Fig. 1.2.

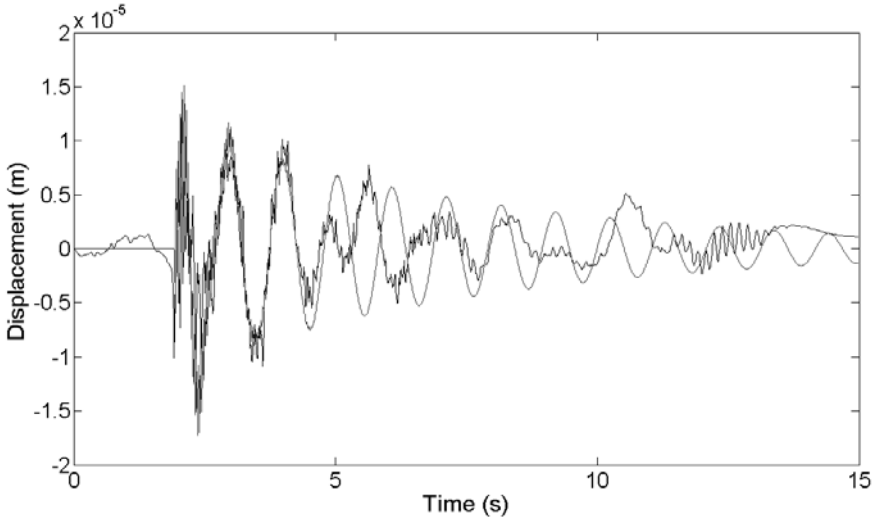

Figure 1.2: Comparison between real (black) and simulated accelerogram (red)

It has to be noted that this fit was achieved adjusting a free parameter, for which not information is available: the dynamic coupling factor between structures and soils.
The foundation system is unknown for the building (maybe isolated footings), while the frame was bolted to a pre-existing concrete slab running all along the dismissed building. This resulted in a greater coupling between frame and soil, with more than 90% of the energy transferred to the ground, while the coupling between building and soil is rather poor with just a small fraction of the energy radiated into the ground. The final fit is satisfactory, at least for the initial 4 seconds. After that, the real data show the effect of a possible reflection at the bedrock, which is not possible to simulate with the half-space soil model. It was deliberately chosen not to include a detailed stratigraphy, since no reliable information was available about the depth to the bedrock. The model

was able to reproduce the observed data, and this encouraged to go further, trying to solve another problem.

1.1.3 MODELLING A VIRTUAL VILLAGE

Gallipoli *et al.* (2006) pointed out three reasons why what had been observed could be a lower boundary value.

The first reason is that the total mass of the building plus the reaction structure reaches only 38,100 kg, which is twice the one of the Volvi model described by Guéguen *et al.* (2000) and Guéguen and Bard (2005), but still below the mass of a full-functional building, due to the lack of roof tiles, infills, services and internal loads.

The second reason concerns the coupling with the ground. This plays an important role in the efficiency of the structures as wave generators; taller buildings, besides having much larger masses, have deeper foundation, so in an actual city-soil interaction a higher coupling factor is expected.

The thirds reason is the lack of soil-building resonance in the Bagnoli test. Bard *et al.* (1996) and Cornou *et al.* (2004) pointed out the importance of trapped waves in a resonant layer as a cause for far away propagation of structure frequencies. In our case, no resonance is present between soil and building, and thus the observed values are a lower bound.

In order to clarify these issues, it was decided to setup a model for standard buildings, with varying dynamical coupling and with a resonant stratum above the bedrock.

Using SAP2000, 3 buildings of different mass and height were modeled, following the rules for anti-seismic design provided by the Italian code (largely similar to EuroCode8).

2 Storey			**4 Storey**			**6 Storey**		
(kg)	K (N/m)	c (%)	M (kg)	K (N/m)	c (%)	M (kg)	K (N/m)	c (%)
149,696	75,920,931	5	1,847,000	409,450,806	5	3,053,940	225,008,060	5

Table 1.2: Parameters used for the "virtual village" simulation

Again, the full model was reduced to a system of SDOFs to be used with the Simulink model. This time the input was provided by three real accelerograms with PGA equal respectively to 0.15 *g*, 0.25 *g* and 0.35 *g*.

To take into account the variability of the position of the buildings among them and with respect to the accelerometer, a random delay time was included in the model. The

output of each building was summed to the input ground motion with a variable delay, uniformly distributed from -0.1 to 0.1 sec. The velocity in the soil layer was set to 100 m/s, thus leading to simulated change in position in the range -10 to 10 m. To account for the variability in the dynamic coupling between building foundation and the soil, and thus to represent the different quantity of energy transferred back to the soil by the vibrating structure, a random coefficient was included in the simulation, with uniformly distributed values in the range from 1% to 90%.

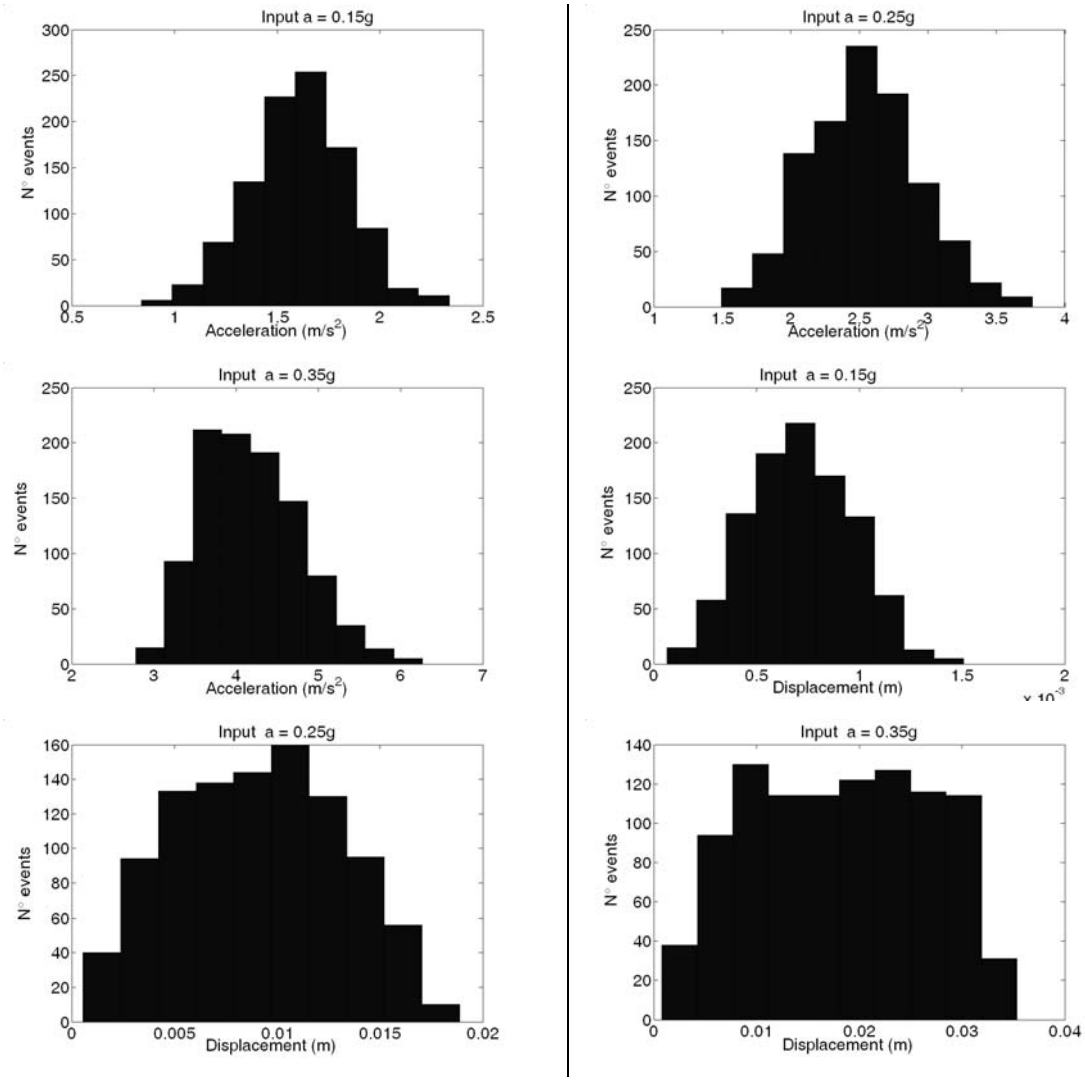

Figure 1.3: Distribution of simulated PGA and PGD

A Monte Carlo simulation was then performed, with 1000 runs of the Simulink model for each of the three inputs. From each run the Peak Ground Acceleration and the Peak Ground displacement were extracted, plotting the relevant histograms in Fig. 1.3. It is possible to note that the distribution is centred on the input value, with minimum and maximum variation of the order of 50% and with most of the values in the range ±25%.

This implies that real accelerogram recorded in free-field may be affected by the presence of building when the recording is made in a urbanised area.

The last step was the analysis of the spectral response. For each input 70 time histories were selected randomly and the relevant response spectra were calculated. Then the ratio between each spectrum and the one of the input signal (both in acceleration and displacement) was subsequently estimated, and the average of the ratios was finally computed. The results are plotted in Fig. 1.4. The values above unity are concentrated around the periods of the fundamental mode of the buildings, while the ratio tends to be lower for longer period.

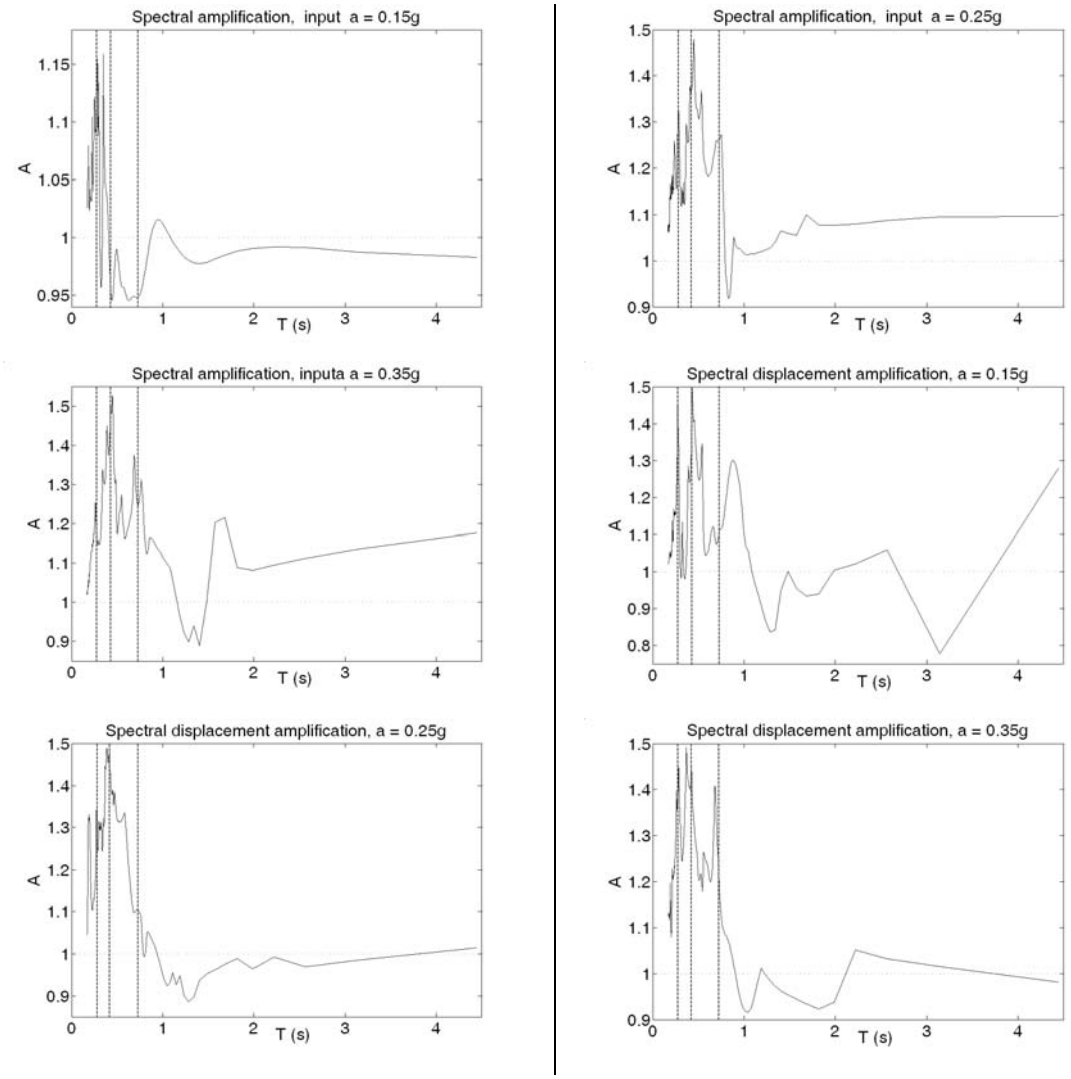

Figure 1.4: Difference in acceleration and displacement response spectra due to the presence of buildings. Red line are the buildings fundamental modes

This result was expected, with most of the back-radiated energy around the period of the buildings and, together with the distribution of PGA and PGD, leads to the main

conclusion of this work: the presence of buildings strongly affects the "free field" ground motion. Inside a urban area it is difficult to record a real free field motion. On average, the PGA remains similar, but it can be increased or reduced by the presence of buildings.

It is not possible to drawn general conclusion about the possibility of having larger or smaller PGA, since it depends on the typology and space pattern of the buildings. The energy balance is slightly increased, with energy added at the fundamental modes of the buildings and subtracted at longer periods.

1.2 SOIL-STRUCTURE-SOIL INTERACTION: STUDYING THE EFFECTS TAKING INTO ACCOUNT THE BUILDING INTERACTION

1.2.1 INTRODUCTION

During an earthquake, the vibration of buildings transmitted back to the soil is able to modify the free field ground motion. This idea was theoretically postulated by Wong and Trifunac (1975) and Wirgin and Bard (1996). Recent active experiments have been carried out by Guéguen *et al*. (2000) and Guéguen and Bard (2005) on a five-story RC-building model (1:3) located in the EuroSeisTest site at Volvi (GR), by Mucciarelli *et al.* (2003) on a base isolated building during a release test and by Gallipoli *et al.* (2006) taking advantage of a controlled demolition experiment at Bagnoli (IT). Recent passive tests using ambient noise are described in Gallipoli *et al.* (2004) and Cornou *et al.* (2005). The conclusions of all these experiments confirm the importance that buildings may have as seismic sources. On the other hand, numerical simulation on idealised models of city-soil interaction were performed: see, e.g., Kham *et al.* (2006). Ditommaso *et al.* (2007) reproduced with a numerical model the ground motion observed by Gallipoli *et al.* (2006) during a 7 cm top-floor displacement test of a real 2-stories building. This displacement is representative of the maximum excitation that this kind of building might withstand during an earthquake. The highest PGA (Peak Ground Acceleration) observed on the soil is 5% g with a 7 cm displacement of a structure whose frequency was in the range 1-2 Hz. If the standard 5% damping response spectra provided by the Italian Seismic Code is considered, a top-floor 6 cm displacement at 1 Hz is obtained for the Zone 2 – Soil A spectrum, whose PGA is 0.25 g. The observed PGA is thus about 20% of the hypothetical unmodified free-field PGA. After reproducing this result, Ditommaso *et al.* (2007) modelled a "virtual village" made of

three structures of different height to study their effect on an accelerometer located among them, varying the azimuth of incident waves and the coupling between building and soil, obtaining a statistical distribution of the influence of vibrating structures on "free-field" ground motion. The distribution of the output PGA is centred on the input value, with minimum and maximum variation of the order of 50% and with most of the values in the range ±25% input. The analysis of the ratios of response spectra (Out/In) showed that the values above unity are concentrated around the periods of the fundamental mode of the buildings, while the ratio tends to be lower for longer period. In this section an extension of the model proposed by Ditommaso *et al.* (2007) is described, including the feedback of each building on the others.

1.2.2 THE MODEL

The approach developed by Şafak (1998), where the building and the foundation soil are idealised as propagators of up- and down-going S-waves, The whole system was modeled using Matlab Simulink. The advantage of this approach is that it can work on subsystems (i.e., soil strata or building floors), adding as many subsystems as it is necessary. The only unchanged sub-systems are the bedrock (half-space with inelastic attenuation) and the building roof. To estimate the three parameters needed for each subsystem (mass, stiffness and damping), three buildings of different mass and height were designed using SAP2000 and following the rules for anti-seismic design provided by the new Italian code (largely similar to EuroCode8).

Structure	Mass (kg)	Stiffness (N/m)	Damping factor (%)
1	149696	75920931	5
2	1847000	409450806	5
3	3053940	225008060	5

Table 1.3: Parameter of the three buildings

To take into account the variability of the position of the buildings among them and with respect to the accelerometer, a random delay time was included in the model. The output of each building was summed to the input ground motion with a variable delay, uniformly distributed from 0 to 0.1 sec. The velocity in the soil layer was set to 150 m/s, thus leading to a simulated change in position in the range -15 to 15 m depending on the direction. The signals coming from the buildings were propagated in an inelastic

medium. The distances were calculated from the centre of mass of the structures projected on the ground to the accelerometer, with the attenuation given by:

$$A(r) = \frac{A_0}{r} \cdot e^{-\frac{f \cdot r}{Q \cdot v}}$$

where A is the signal amplitude as a function of the distance r, A0 is the initial amplitude, f is its frequency, v is the shear wave velocity and Q is the quality factor (taken equal to 18) . To account for the variability in the dynamic coupling between building foundation and the soil, and thus to represent the different quantity of energy transferred back to the soil by the vibrating structure, a random coefficient was included in the simulation, with uniformly distributed values in the range from 1% to 90%. The model is reported in Fig. 1.5.

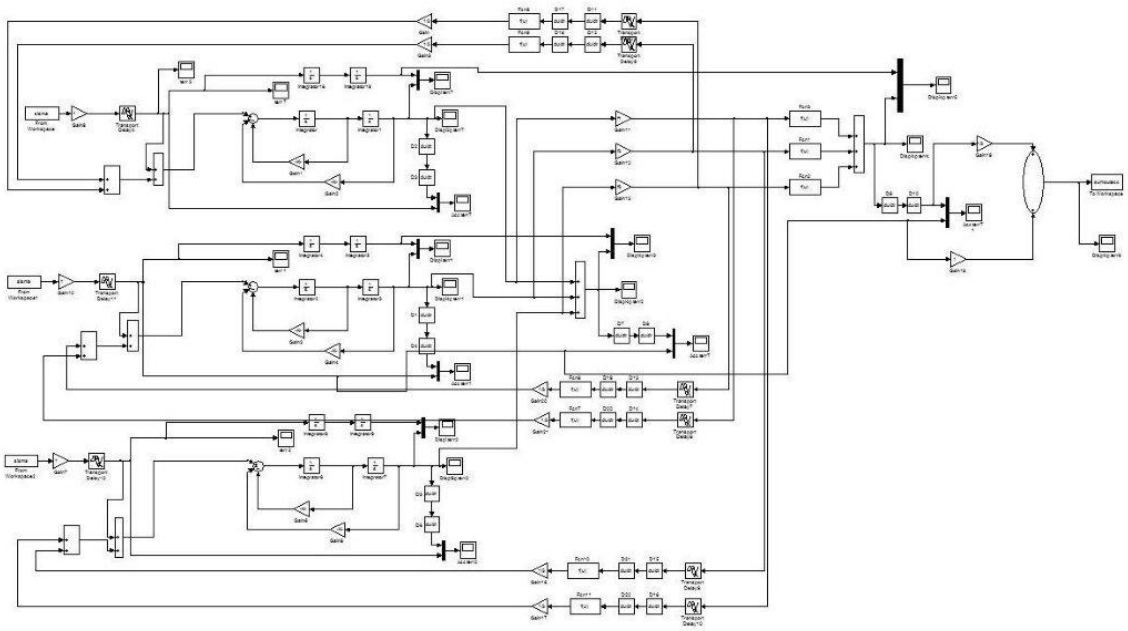

Figure 1.5: Matlab Simulink model used for the simulation

The input was provided by 11 real accelerograms with PGA ranging from 0.15 g to 0.35 g.

1.2.3 RESULTS

A Monte Carlo simulation was then performed, with 300 runs of the Simulink model for each input, obtaining 3300 possible combination of different position of the buildings with respect to the incoming wave, soil/foundations coupling and input. From each

simulated output accelerogram, the PGA, the Housner Intensity (H) and the maximum value of the acceleration response spectra (Sa) were extracted.

Fig. 1.6 reports the histograms and the Empirical Cumulative Distribution Functions (ECDFs) for the ratio between output and input values. The distribution are asymmetrical and well described by a log-normal model. The main point to consider is the percentage of results below 1, that means the output is reduced by the presence of the vibrating building. This kind of destructive interference occurs in 30% of the cases for PGA, 10% for H, never for Sa. The output is larger that 1.5 times the input in less than 10% of the cases for PGA, never for H and in half the cases for Sa. This is in agreement with the theoretical expectations: the energy is partly absorbed by the damping of the buildings, but in the range of frequency corresponding to the fundamental modes of the buildings, the spectral amplitude is enhanced.

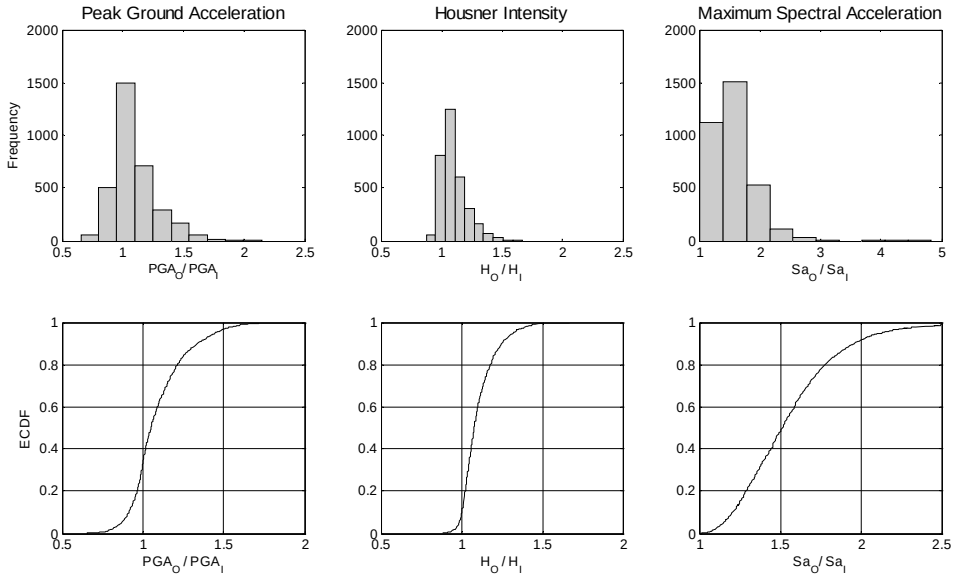

Figure 1.6: ECDFs of 3300 Monte-Carlo simulation

1.2.4 DISCUSSION

The results obtained in these simulations have been compared with those given by the model without feedback among the buildings (Ditommaso *et al.*, 2007). Fig. 1.7 reports the match between PGA, while Fig. 1.8 shows the comparison between Sa. For the previous model, the variation of the Housner intensity was not given.

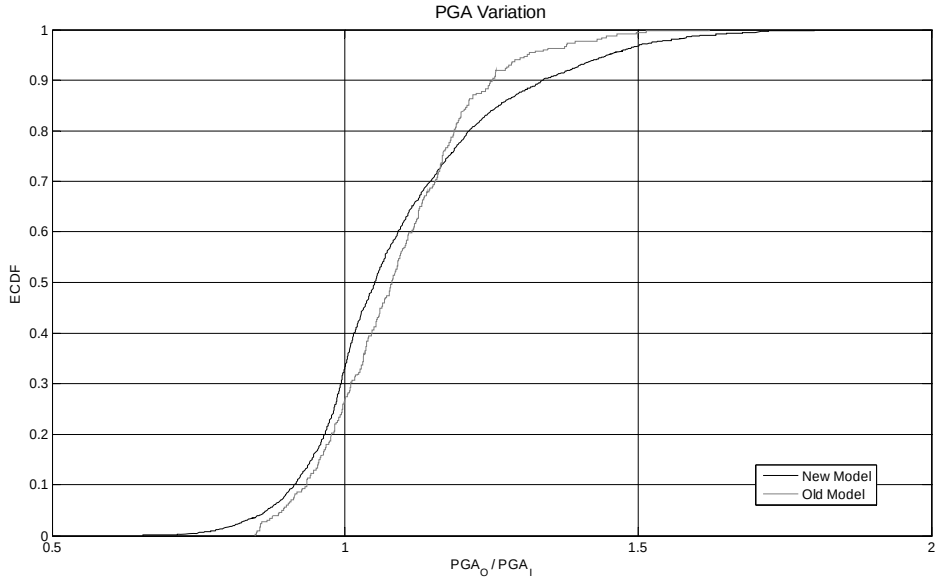

Figure 1.7: Comparison between this work and Ditommaso et al. (2007) for PGA

It is possible to note that the general pattern of the curve for PGA remains the same, with a small decrease of the median value and an increase of the dispersion with a larger probability of greater motion amplification due to the presence of buildings. The trend is the same also for Spectral Amplification.

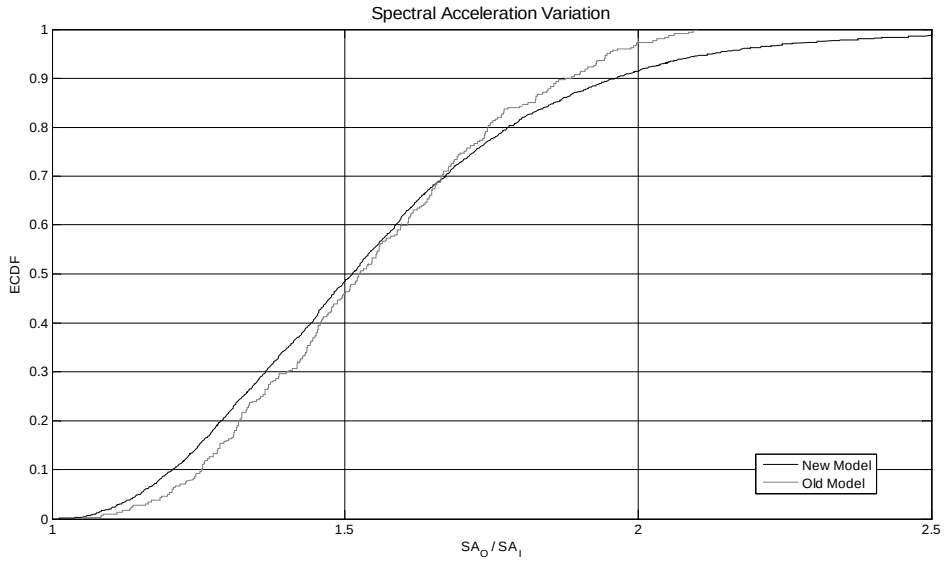

Figure 1.8: Comparison between this work and Ditommaso et al. (2007) for Sa.

In conclusion, this more refined model does not change the conclusion of previous works, but given the larger number of simulations allows for a deeper insight on the role that vibrating building may have in modifying the "free field" ground motion. The

energy back-radiated in the range of the fundamental periods of the buildings leads to the conclusion that inside a urban area it is difficult to record a real free field motion. The presence of buildings strongly affects the response spectra and, to a lesser extent, the PGA. The variation is always positive for the maximum spectral values, while for PGA it can be either positive or negative. The Housner Intensity tends to be increased rather than decreased, but the range of variation is smaller that the one observed for PGA and Sa. This result is obtained without selecting soil properties that may induce resonance between soil and buildings, and thus can be regarded as a lower limit of the modeled phenomenon.

1.3 NUMERICAL AND EXPERIMENTAL EVIDENCES

1.3.1 INTRODUCTION AND CASE HISTORIES

The influence of buildings on free-field ground motion recordings was postulated for the first time more than 30 years ago (Jennings, 1970; Wong and Trifunac, 1975). In the following years, several papers were devoted to the study of the vibration induced by an impulsive force on real buildings or on scale models (Kanamori *et al.,* 1991; Erlingsson and Bodare, 1996; Guéguen *et al.*, 2002; Mucciarelli *et al.*, 2003; Gallipoli *et al.*, 2006) given the difficulty of separating incoming and back-radiated wave field during an earthquake (Chavez-Garcia and Cardenas-Soto, 2002). Some works attempted to use ambient noise to identify the possible fingerprint of building vibration frequencies in the vicinity of the measurement point (Gallipoli *et al.*, 2004; Cornou *et al.*, 2004; Massa *et al.,* 2009). In the meantime, numerical simulation aimed to reproduce the phenomenon were carried out (Bard *et al.*, 1996; Wirgin and Bard, 1996; Guéguen and Bard, 2005; Kham *et al.*, 2006; Ditommaso *et al.*, 2007; Mucciarelli *et al.*, 2008; Ditommaso *et al.*, 2009).

In some cases, when an entire town is concerned, numerical simulations were performed on idealised models, without a possible comparison with real data (see, e.g., Kham *et al.*, 2006 and references therein). The main disagreement in the literature (Laurenzano *et al.*, 2009) concerns the effects of summations of wave fields from several buildings, which could be a beneficial or detrimental interference. Previous papers focused on the possible influence of built structures on the effects of the earthquake, in terms of greater or lesser damage. In this section the focus is only on the effect on free-field motion from a stand-alone building. This situation is of potential interest for seismometric or accelerometric stations installed inside or nearby a building. The Italian Civil Protection

has recently funded a research project aimed to build and maintain an online database of Italian accelerometric data (Working Group ITACA, 2008).

One of the tasks of the project is to study the influence of the structures on the accelerometric recordings. This effect has been already demonstrated for large engineered structures by Barnaba *et al.* (2007). They show how the presence of the Ambiesta dam and reservoir strongly affects the recording of the 1976 Friuli earthquake at the Tolmezzo accelerometric station. The problem to tackle now is if smaller structures can also produce a significant effect on free-field recordings.

Several accelerometric stations of the Italian national network are located in pre-cast housings (power substations), while others are installed nearby or inside buildings. Figure 1.9 shows a typical outside view of an accelerometric station, located in the Macchia Romana Campus of Basilicata University at Potenza, Italy. The housing is made of reinforced concrete, but there are no informations about its geometric characteristics (infill thickness, beam and pillar width and reinforcements, etc.), and it is located on stiff clay formation. In the considered frequency range there is not a clear peak related to a superficial impedance contrast. The orientation of the building is N50°. Within the housing there is an accelerometer connected to an Etna data logger, sampling data at 50 Hz up to a maximum of 1g.

Two 3-directional 24-bit digital tromometers (Tromino – Micromed) were used in order to characterise the main frequencies of the structure. Using ambient noise we assessed the first and the second structural frequency were assessed using a twenty minutes time window sampled at 128 Hz. The acquired signals were pre-processed with baseline correction, trend removal, and 0.1-20 Hz band-pass filter.

After these preliminary operations, signals were processed using a 15 s moving window with an overlap equal to 50% of moving window length. The spectral ratio between the measurement atop the building and the free-field taken as reference was used(Figure 1.9). Figure 1.10 shows the transfer functions that provided a first mode along the WE direction at 12 Hz and a second mode along the NS direction at 14 Hz.

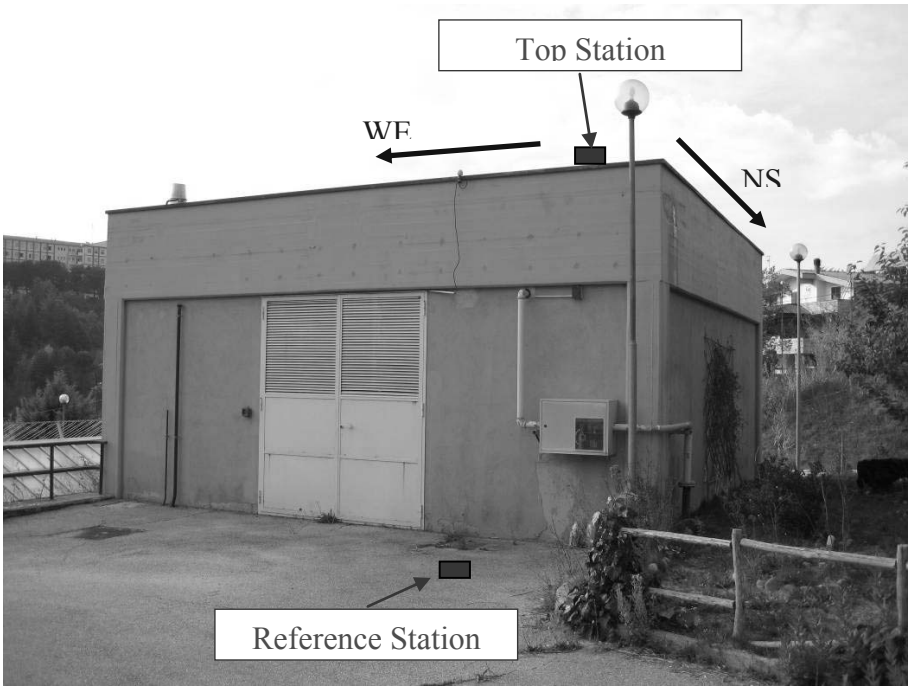

Figure 1.9: RAN (Accelerometric Italian Network) - Station Code PTZ (Potenza – Italia)

After evaluating the dynamic characteristics of the housing, the earthquakes recorded by the accelerometer installed inside were analyzed. Table 1.4 summarizes the earthquake characteristics.

Recordings were pre-processed (de-trended, filtered and tapered) and then analysed using the rotational HVSR (Horizontal to Vertical Spectral Ratio) using a 15 s moving window with an overlap equal to 50% of moving window length. For each event rotational HVSR was calculated and then the average for all the events was performed.

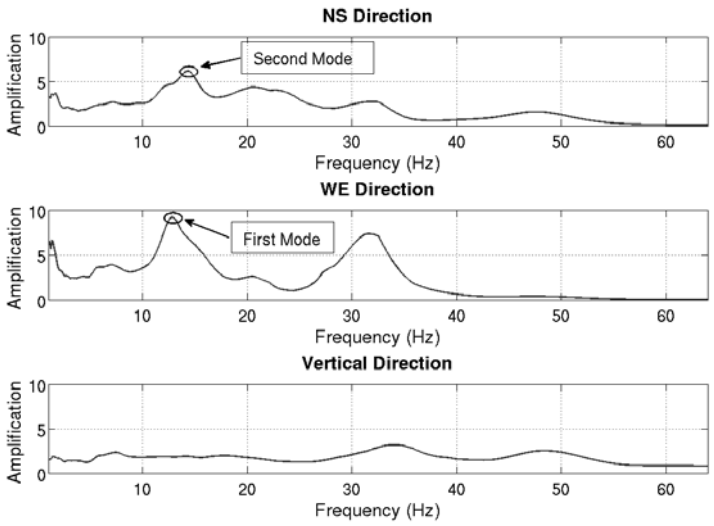

Figure 1.10: SSR (Standard Spectral Ratio) evaluated between the roof and free-field

Date Time	Event name	Epicentral location	Epicentral distance (±0.2 km)	Lat	Long	Province	PGA (g)	M_L
03/02/2003 11.24	POTENTINO	BELLA	16.18	40.73	15.65	PZ	0.00224	3.6
03/02/2003 12.18	POTENTINO	BELLA	15.51	40.74	15.67	PZ	0.00132	3.5
24/02/2004 5.21	VALLO DI DIANO	SAN GREGORIO MAGNO	35.67	40.69	15.39	SA	0.00136	3.9
03/09/2004 0.04	POTENTINO	PICERNO	13.86	40.68	15.65	PZ	0.00877	4.1
27/09/2004 23.20	POTENTINO	RUOTI	9.44	40.70	15.72	PZ	0.0180	2.6

Table 1.4: Earthquakes recorded at PTZ station

The results are reported in Figure 1.11, which shows a very clear peak at 12 Hz that coincides with the fundamental mode of the housing. The peak is the highest of the entire HVSR; the recordings are thus strongly influenced by the building frequency.

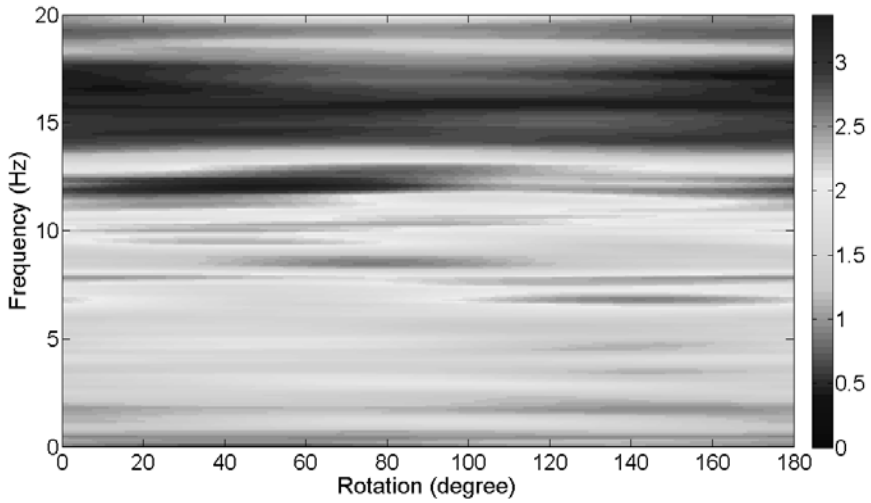

Figure 1.11: Average of rotational HVRS evaluated on all events recorded at PTZ

Since it is not possible to perform measurement in all the buildings near a station, it is preferable to have a more general model based on a numerical simulation validated by comparison with experimental data. An additional aim of the model is to provide a statistical study of the probability that a generic building may influence free-field recordings, focusing on possible effects on different parameters (peak motion values, integral/energy parameters or spectral ordinates).

1.3.2 A MODEL VALIDATING REAL DATA

The availability of an existing R/C (Reinforced Concrete) building to be demolished in the ex-Italsider steel factory at Bagnoli-Naples in the framework of ILVA-IDEM project (Mazzolani *et al.*, 2004), gave the chance to carry out *in situ* large-displacement tests on a real R/C frame, to model the recorded waves and then to prepare a more general model.

The building tested in Bagnoli was a two-story, reinforced-concrete former office building, linked to a moment resisting steel frame (used as contrast frame). The structure and the soil were monitored with several accelerometers and seismometers.

Structure	f (Hz)	r (m)	Q	v (m/s)
Building	1.2	8	10	100
Contrast frame	27	13	10	100

Table 1.5: Parameters used in the simulations of the Bagnoli experiment

Full details can be found in Gallipoli *et al.* (2006). The aim of this section is to reproduce the strong-motion time history recorded at 8 meters distance from the building. Several cyclic and release tests were performed for engineering purposes. The induced ground motion was measured during a 7 cm displacement test. This displacement is representative of the maximum excitation that this type of building might withstand during an earthquake. The highest PGA observed in ground motion recordings was 5% g with a 7 cm displacement of the structure, whose natural frequency was in the range 1-2 Hz. Considering the standard 5% damping response spectra provided by the Italian Seismic Code, a 6 cm displacement at 1 Hz is obtained for the Zone 2 – Soil A spectrum, whose PGA is 0.25 g; the observed PGA is thus about 20% of the theoretical unmodified free-field PGA.

The building and the contrast frame were both modelled using SAP*2000* finite element program. The frequency obtained for the first modes of the structures matched the ones observed from the experimental data, which are around 1 Hz for the building and 30 Hz for the frame. The frame was then reduced to a SDOF with equivalent mass, stiffness and damping, while the building was reduced to a MDOF system (one SDOF per floor). The approach proposed by Şafak (1998) was followed: the building and the foundation soil are idealised as propagators of up- and down-going waves. This leads to the need of solving a system of recursive differential equations. The whole system was modelled

using Matlab® Simulink. The advantage of this approach is that it can work with subsystems (i.e., soil strata or building floors), adding as many subsystems as it is necessary. The only unchanged sub-systems are the bedrock (half-space with inelastic attenuation) and the building's roof.

The two signals coming from the building and the contrasting frame were propagated in an inelastic medium reproducing the characteristics of the soil underlying the test site (volcanic ashes and alluvium).

The distances were calculated from the centre of mass of the two structures projected on the ground to the accelerometer, with the attenuation given by equation 1:

$$A(r) = \frac{A_0}{r} \cdot e^{-\frac{f \cdot r}{Q \cdot V}} \qquad (1)$$

where A is the signal amplitude as a function of the travel distance r, A_0 is the initial amplitude of the signal, f is its frequency, Q is the quality factor and V is the shear wave velocity. The small strains involved allow for the assumption of soil linear behaviour. However, the model can be modified to take into account non–linearity if needed. The parameters used are reported in Table 1.5.

The initial condition reproduces the experiment: a 7 cm displacement in the middle of the building that is instantaneously released. The frame was dislocated according with the amount given by the SAP*2000* static simulation.

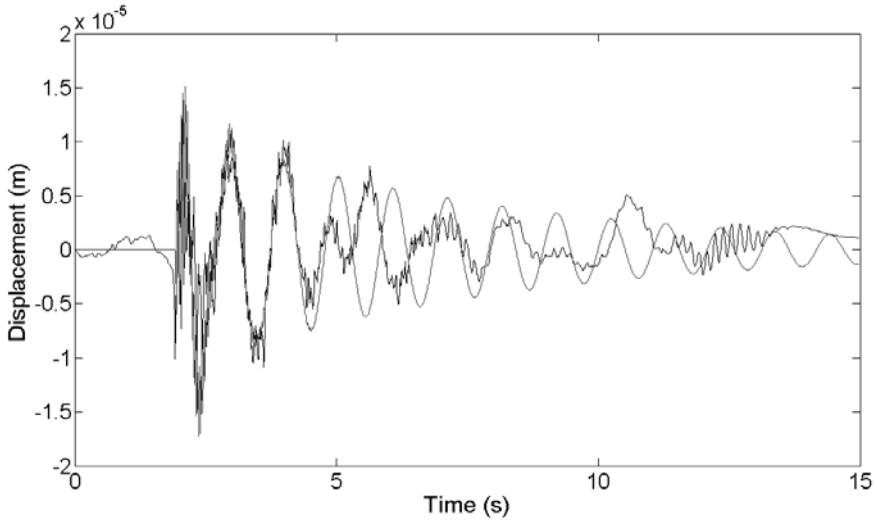

Figure 1.12: Comparison between real (black) and simulated displacement (red)

The equations were solved for a discrete model, a duration of 15 seconds, a variable step with Ode 45 resolution algorithm. Figure 1.12 shows the result for the modelled displacements compared with the recorded ones.

It has to be noted that this fit was achieved adjusting a "free" parameter, for which not information is available: the dynamic coupling factor between structures and soils (range of variation 0 to 1, see Şafak, 2006). The foundation system is unknown for the building (maybe isolated footings), while the frame was bolted to a pre-existing concrete slab running all along the dismissed buildings. This resulted in a greater coupling between resisting frame and soil, with more than 90% of the energy transferred to the ground, while the coupling between building and soil is rather poor with just a small fraction of the energy radiated into the ground. The final fit is satisfactory, at least for the initial 4 seconds. After that, the real data shows the effect of a possible reflection at the bedrock, whose depth is not known and thus not considered in the model. The model was able to reproduce the observed data, and this encouraged to go further, trying to use it to answer practical questions. As observed for Potenza station several questions arise: can ground motion recordings be contaminated by building frequency? How often may this happen, and which parameters (peak values, integral parameters or spectral ordinates) could be the most affected? How can the problem of unknown foundation systems be tackled?

1.3.4 MONTE-CARLO SIMULATION OF A BUILDING INFLUENCE ON GROUND MOTION

Using the Matlab® Simulink model prepared to reproduce the ground motion induced by the release test as described in the previous chapter, several analyses were performed to study the effect of a building on free-field ground motion recordings. The variation of the effects as a function of the distance between a single building and the accelerometric station was investigated. The 0.1 – 25 Hz frequency range was investigated.

Two different buildings, respectively with 2 and 10 storeys, designed according to the most recent Italian seismic code were considered. Each structure was modelled as a single degree of freedom oscillator equivalent to the main vibration mode of the structure. The 2 floors building is representative of electrical power distribution stations, while the 10 floors building simulates a structure that may host a station in the basement or in the vicinity.

2-STOREY BUILDING			10-STOREY BUILDING		
Mass (kg)	**Stiffness (N/m)**	**Damping (%)**	**Mass (kg)**	**Stiffness (N/m)**	**Damping (%)**
149696	75920931	5	6260610	204056563	5

Table 1.6: Linear equivalent parameters of oscillators

Table 1.6 shows the dynamic characteristics of equivalent oscillators in terms of mass, stiffness and damping, while Table 1.7 shows the ground parameters. It is important to note that a half-space approximation for the soil was assumed. A layered soil with impedance contrast at the interfaces would produce possible resonances between buildings and soil frequency, thus enhancing the contribution of the back radiated energy. This makes the problem more complicated because each building could be resonating or not, and in case of building damage or soil non-linearity both frequencies could vary. In this model, the back-radiated energy is attenuated away from the building and there is no trapping of energy in the upper soil layers. The absolute value of ground motion perturbation that will be obtained is thus a lower bound for this problem. The analysis were performed using 11 different earthquakes (Table 1.8), randomly extracted from the European Strong Motion Database to sample uniformly the PGA range 0.05-0.35 *g*.

SOIL PARAMETERS		
Density (kg/m3)	**Shear Wave Velocity (m/s)**	**Quality Factor**
1900	1000	10

Table 1.7: Soil Parameters

Event Code	Event Name	PGA (g)
359	000359a	0.066
365	000365a	0.099
361	000361a	0.157
123	000123a	0.232
159	000159a	0.237
1313	001313a	0.265
27	000027a	0.294
196	000196a	0.306
501	000501a	0.346
1226	001226a	0.361
199	000199a	0.363

Table 1.8: Earthquakes extracted from the European Strong Motion Database

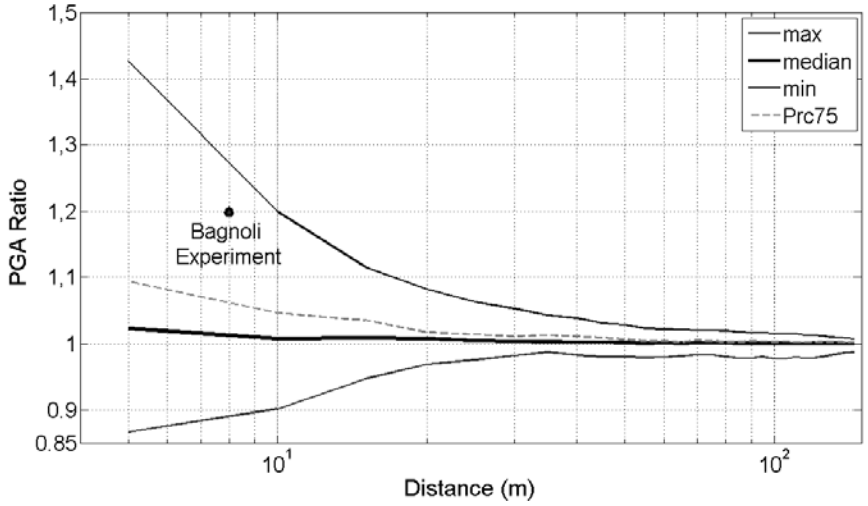

Figure 1.13: Ratio between PGA with and without the presence of the 2-storey building

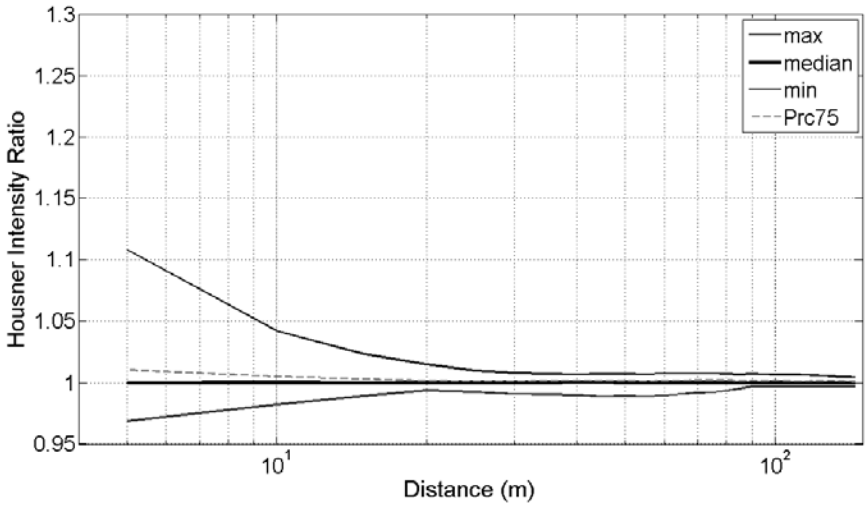

Figure 1.14: Ratio between HI with and without the presence of the 2-storey building

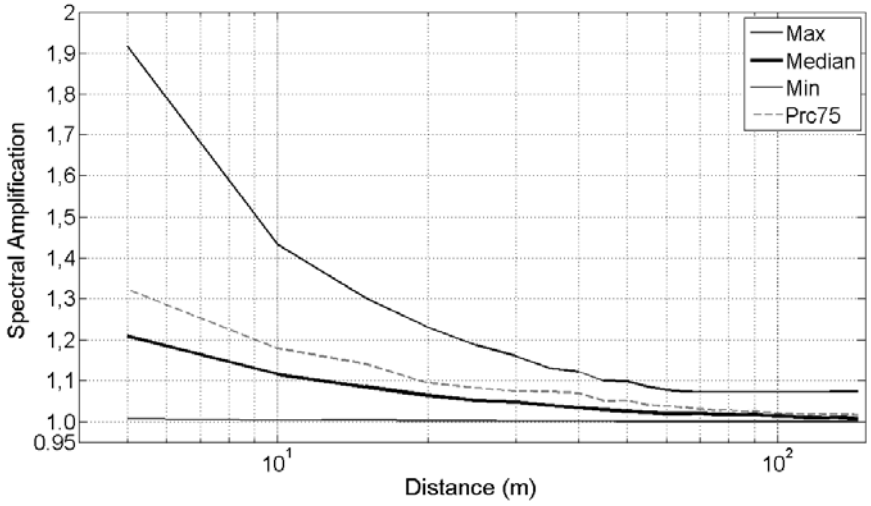

Figure 1.15: Ratio between maximum Sa with and without the presence of the 2-storey building

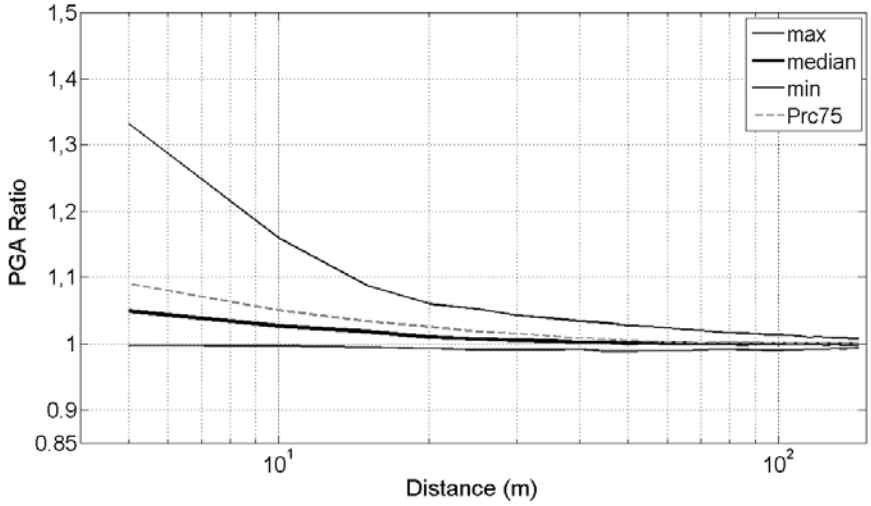

Figure 1.16: Ratio between PGA with and without the presence of the 10-storey building

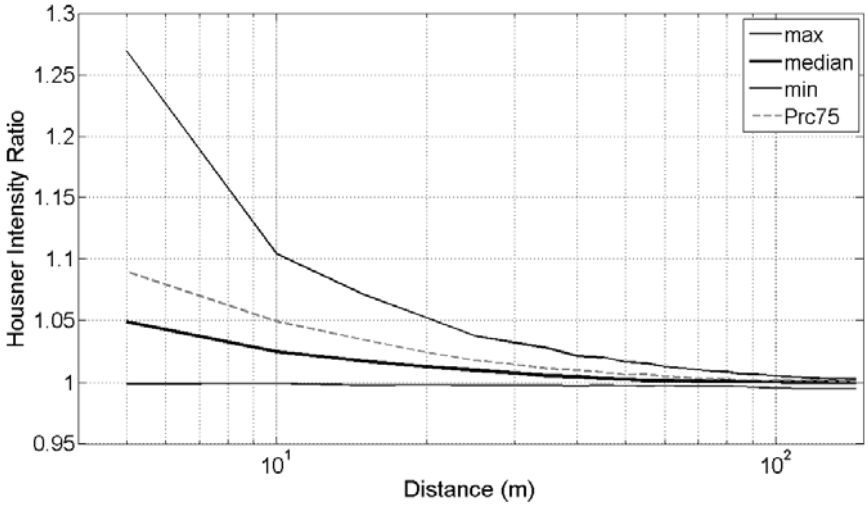

Figure 1.17: Ratio between HI with and without the presence of the 10-storey building

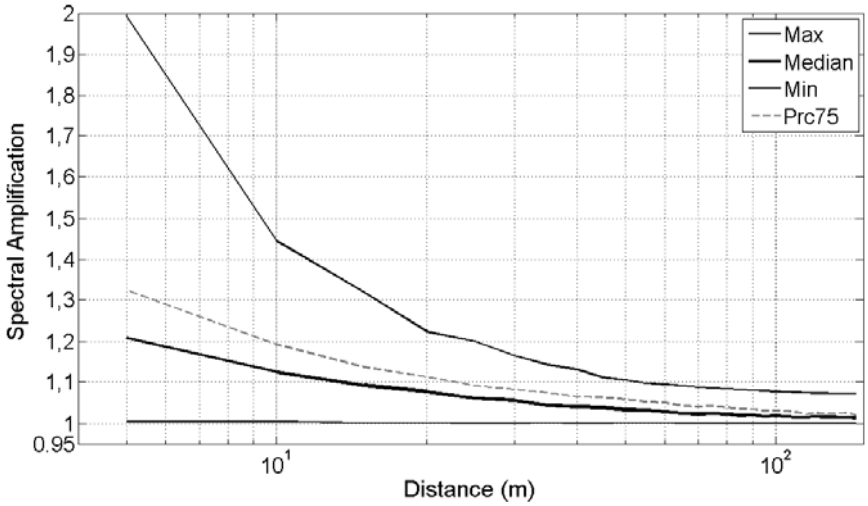

Figure 1.18: Ratio between Sa with and without the presence of the 10-storey building

Using a random coefficient of structure-soil coupling (0.01-0.99) and a building-accelerometer random distance (5 to 150 m), 1000 simulations for each building and for each earthquake were carried out, for a total of 22000 simulations.

For each simulation, hence for each distance, Peak Ground Acceleration (PGA), Housner Intensity (HI) and the spectral acceleration at 5% damping (Sa) were calculated. The ratio between each value and the related free-field recording was then computed. For each distance between building and accelerometer, having more than one value, four statistical parameters were calculated: the maximum value, the minimum value, the 75^{th} and 50^{th} percentile (median) values.

Figures from 1.13 to 1.15 show the results related to the two-storey building, while Figures 1.16 to 1.18 are relevant to the 10-storey building.

From the graphs related to the acceleration ratio (Figures 1.13 and 1.16) it is clear how the possibility of having beneficial or detrimental interference leads both to amplification and de-amplification. For small distances, the median shows an increase around 10% that decreases with distance. For exceptional cases, an increase of 40% (maximum) or a decrease around 5% (minimum) can occur. Similar comments are valid for the graph that represents the HI ratio, but in this case the increase is lower and median values start from 2% and decrease with distance.

Different considerations apply to Sa graphs (Figures 1.15 and 1.18). In this case the curve of minimum values does never decrease below unity, while the curve of maximum values highlights the possibility, for extreme cases, of an increase around 90%. Median curve starts from an increase of 20% and decreases with distance.

The 10-storey building has a very different influence on free-field ground motion. For example, both in terms of PGA and HI a decrease never occurs, even for extreme cases. On the contrary, an increase of the observed parameters always occurs. A slight increase in terms of PGA amplification, compared with those observed in case of 2-storey building, can also be noted. This was to be expected, because the frequency of the 10-storey building is lower and thus not affecting the high frequency end of the spectrum. In this case the median curve starts with an increment of 5% and decreases with distance. Housner Intensity has significant increases compared with those observed for the 2-storey building, both for median curve and for extreme cases. Median HI ratio curve starts from an increment of 5% for small distance. Regarding the spectral amplification values, a good agreement with those evaluated for the 2-storey building can be observed. Only a little increment occurs for the most extreme values.

1.3.5 DISCUSSION

Both the numerical and experimental aspect of the dynamic building-soil interaction were investigated. The experimental evidence regarding the ability of buildings to back-radiate energy into the soil, thus modifying the free-field ground motion, as shown for the case of Potenza accelerometric station was preliminary discussed.

A numerical model, was subsequent defined and validated comparing the synthetic signal with the time-history recorded during the release test of a real RC frame.

Finally, a Monte-Carlo simulation was performed starting from the same model applied to realistic buildings with different masses and fundamental period. The random parameters varied during the simulation were the impedance function of the foundation system and the building-station distance. The variation of extreme values, median and 75%, was plotted against distance for PGA, HI, and Sa.

As shown in Ditommaso *et al.* (2009) for the effect of a building set in motion by a nearby explosion, the spectral parameters are the most affected, while the integral ones are not so disturbed. This is due to the fact that the presence of the structure has both the effect of a damper (thus reducing the total energy) and of a filter, focusing energy in the band of building eigenfrequencies.

In conclusion it can be stated say that buildings are able to modify the free-field ground motion, contaminating the signals recorded near or within them. The less affected parameter by the presence of buildings is the Housner intensity, however, PGA and Sa are more contaminated. In order to give recommendations on the use of signals contaminated by the back-radiated energy from buildings, further numerical studies and in situ experiments are needed.

ACKNOWLEDGMENTS

This study was been funded by the Italian Department of Civil Protection within the DPC-INGV 2007-2009 (S4 Project).

REFERENCES

Bard, P.-Y., Gueguen, P. and Wirgin, A. (1996). A note on the seismic wavefield radiated from large building structures into soft soils, in Proc. of the Eleventh World Conference on Earthquake Engineering, Acapulco, Mexico, Paper No. 1838.

Barnaba, C., Priolo, E., Vuan, A. and Romanelli, M. (2007). Site effect of the Strong-Motion Site at Tolmezzo-Ambiesta Dam in Northeastern Italy, Bull. Seism. Soc. Am., 97, 339-346.

Chavez-Garcia, F.J. and Cardenas-Soto, M. (2002). The contribution of the built environment to the free-field ground motion in Mexico City, Soil Dyn. Earthq. Eng., 22, 773–780.

Cornou, C., Guéguen, P., Bard, P.-Y., and Haghshenas, E. (2004). Ambient noise energy bursts observation and modeling: Trapping of harmonic structure-soil induced–waves in a topmost sedimentary layer, J. Seismol., 8(4), 507–524.

Ditommaso, R., Gallipoli, M. R., Mucciarelli, M., Ponzo, F. C. (2007). Effect of vibrating building on "free-field" ground motion: from the Bagnoli experiment to many-buildings simulation. Proc. 4th Int. Conf. Earthq. Geot. Eng., CD-Rom edition, Paper No. 1388. Springer, ISBN 978-1-4020-5893-6.

Ditommaso, R., Parolai, S., Mucciarelli, M., Eggert, S., Sobiesiak, M. and Zschau, J. (2009). Monitoring the response and the back-radiated energy of a building subjected to ambient vibration and impulsive action: the Falkenhof Tower (Potsdam, Germany). Bulletin of Earthquake Engineering, submitted to this issue.

Dolce, M., Cardone, D., Marnetto, R., Mucciarelli, M., Nigro, D., Ponzo, C.F. and G. Santarsiero (2004). Experimental static and dynamic response of a real r/c frame upgraded with SMA re-centering and dissipating braces, in Proc. 13th World Conf. on Earthq. Eng., Vancouver, B.C., Canada August 1-6, 2004, Paper No. 2878, CD-Rom Edition.

Erlingsson, S. and Bodare, A. (1996) Live load induced vibrations in Ullevi stadium – Dynamic soil analyis; Soil Dyn Earthq. Eng., 15, 171-188.

Gallipoli, M. R., Mucciarelli, M., Castro, R.R., Monachesi, G. and Contri, P. (2004). Structure, soilstructure response and effects of damage based on observations of horizontal-to-vertical spectral ratios of microtremors, Soil Dyn. Earthq. Eng., 24, 487-495.

Gallipoli, M. R., Mucciarelli, M., Ponzo, F., Dolce, M., D'Alema, E., Maistrello, M. (2006) Buildings as a seismic source: analysis of a release test at Bagnoli, Italy, Bull. Seism. Soc. Am., 96, 2457-2464.

Guéguen, P., Bard, P.-Y. and C.S. Oliveira (2000). Experimental and numerical analysis of soil motion caused by free vibration of a building model, Bull. Seism. Soc. Am., 90, 6, 1464-1479.

Guéguen, P., Bard, P.-Y. and Chavez-Garcia, F.J. (2002). Site-city seismic interaction in Mexico Citylike environments: An analytic study, Bull. Seism. Soc. Am., 92, 2, 794-811.

Gueguen, Ph. and Bard, P-Y (2005). Soil-structure and soil-structure-soil interaction: experimental evidence at the Volvi test site, Journ. Earthq. Eng., 9, 5, 657–693.

Jennings, P.C. (1970). Distant motion from a building vibration test, Bull. Seism. Soc. Am., 60, 2037-2043.

Kanamori, H., Mori, J., Anderson, D.L., and Heaton, T.H. (1991). Seismic excitation by the space shuttle Columbia, Nature, 349, 781–782.

Kham, M., Semblat, J.-F., Bard, P.-Y., and Dangla, P. (2006); Seismic site–city interaction: main governing phenomena through simplified numerical models, Bull. Seism. Soc. Am., 96, 1934-1951.

Laurenzano, G., Priolo, E., Gallipoli, M. R., Mucciarelli, M., Ponzo, F. C. (2009). Effect of vibrating buildings on free-field motion and on adjacent structures: the Bonefro (Italy) case history, submitted to bull. Seism. Soc. Am.

Massa M., Marzorati S., Ladina, C. and Lovati, S. (2009) Urban seismic stations: soil-structure interaction assessment by spectral ratio analyses, submitted to Bull. Earthq. Eng., this issue.

Mazzolani, F.M., Della Corte, G. and Faggiano, B. (2004). Seismic upgrading of RC buildings by means of advanced techniques: the ILVA-IDEM project, in Proc. 13th World Conf. on Earthq. Eng., Vancouver, B.C., Canada August 1-6, 2004, Paper No. 2703, CD-Rom Edition.

Mucciarelli, M., Gallipoli, M. R., Ponzo, F.C. and Dolce, M. (2003). Seismic waves generated by oscillating building. Soil Dyn. Earthq. Eng., 23, 255-262.

Mucciarelli, M., Ditommaso, R., Gallipoli, M. R. and Ponzo, F. (2008). Effect of Building-Building Interaction on "Free-Field" Ground Motion. Increasing Seismic Safety by Combining Engineering Technologies and Seismological Data. Springer, pp 141-145, ISBN 978-1-4020-9196 -4

Şafak, E. (1998), New approach to analyzing soil-building systems; Soil Dyn.and Earthq. Engin. 17,509-517.

Şafak, E. (2006), Time-domain representation of frequency-dependent foundation impedance function; Soil Dyn. and Earthq. Engin. 26, 65-70.

Wirgin, A. and Bard, P-Y (1996). Effects of building on the duration and amplitude of ground motion in Mexico City, Bull. Seism. Soc. Am., 86, 914-920.

Wong, H.L. and Trifunac, M.D. (1975). Two dimensional antiplane building-soil-building interaction for two or more buildings and for incident plane SH waves, Bull. Seismol. Soc. Am., 65, 1863-1865.

Working Group ITACA (2008). Data Base of the Italian strong motion data: http://itaca.mi.ingv.it

CHAPTER 2

SOIL-STRUCTURE-SOIL INTERACTION: OBSERVING THE STATIONARY AND NON-STATIONARY BEHAVIOUR OF A TOWER INDUCED BY NOISE AND EXPLOSION

The response of the soil-structure system near the Falkenhof Tower, Potsdam, Germany, has been monitored during the controlled explosion of a bomb dating back to World War II.

Eight 3-component velocimetric stations were installed in the building and three in the surrounding area. Several hours of seismic noise were recorded before and after the explosion, thus allowing the dynamic characterization of the structure, with both ambient noise and forced vibration. We then compared the frequencies values and modal shapes of the structural modes evaluated both by analysing in the frequency domain the transfer functions and in the time-domain the different signals. Moreover, an interferometric analysis of the recorded signals was also carried out, in order to study the structural behaviour and to characterize the soil-structure interaction. Furthermore a normalized Short Time Fourier Transform (STFT) was also used for the continuous monitoring of the structural response, in order to highlight possible frequency variations of the structural mode of vibration, and therefore of the structural behaviour.

To assess structural frequencies and to compare them with those evaluated by transfer functions, azimuth-dependent Fourier spectra were used. It was also verified the suitability of the Horizontal-to-Vertical Spectral Ratio (HVSR) for estimating the dynamic characteristics of buildings when only single station seismic noise measurements are available.

Regarding the structure-soil interaction, the presence of a wave field back-radiated from the structure within the low amplitude seismic noise signal was identified. In fact, in the free-field seismic noise recording spectra, peaks at frequencies consistent with those of the first two modes of the structure were recognized.

2.1 INTRODUCTION

The problem of energy back-radiated from vibrating structures has been studied from both the theoretical (e.g. Wong *et al*., 1975) and the experimental point of view. Due to the intrinsic difficulties in separating the building-radiated field from the incoming motion during an earthquake, alternative sources have been used: impulsive sources (Kanamori *et al.,* 1991), ambient noise (Chavez-Garcia *et al*., 2002; Gallipoli M.R. *et*

al., 2004; Cornou C. *et al.*, 2004), or snap-back test on both models (Guéguen. *et al.*, 2002) and real buildings (Mucciarelli *et al.*, 2003; Gallipoli *et al.*, 2006; Ditommaso *et al.,* 2009).

Several authors have used seismic recordings or artificial sources to identify the dynamic properties of buildings (Trifunac, 1972; Hans *et al.*, 2005; Clinton *et al.*, 2006; Kohler *et al.*, 2005 - 2007) and their interaction with the surrounding soil (Safak, 1995 - 1999; Todorovska *et al.*, 2001; Trifunac *et al.*, 2007). However, while there is a vast literature on the effects of a nearby blast (tens of meters) on building behaviour, the use of large explosions (up to some hundred of meters from the target structure) to study dynamic characteristics of a building is rather unusual (Potapov, 1974; Dhakal, 2004; Davoodi *et al.*, 2007; Davoodi *et al.*, 2008).

In this study, it was possible to take advantage of the disposal of an unexploded ordnance from WWII near the town of Potsdam, Germany, in a sparsely inhabited area, were only one tall structure is present, to perform an experiment whose aim is twofold:

1) To verify if the dynamic characteristics estimated using ambient noise differ from those retrieved using a motion in the range from hundredth- to milli-*g*.
2) To study the propagation of back radiated energy both from ambient noise and the impulsive source.

2.2 EXPERIMENT DESCRIPTION

On the 9th of July, 2008, several kilometres outside of the inhabited area of Potsdam, a bomb dating back to World War II was destroyed.

In order to investigate how the seismic signal propagates into and out of a building, and how this could affect the recording in the free field, 11 velocimetric stations were installed by the Helmholtz Centre Potsdam GFZ (German Research Centre for Geosciences).

Eight stations were installed inside a building located in an area near the location of the explosion, while 3 stations were used to monitor free-field motions. In Figure 2.1 a satellite image shows the area of the experiment.

The north-south direction coincides with the direction joining the building and the explosion site, and it was used to orient the sensors. Each station is equipped with a 24 Db digitizer and a 1Hz geophone. The sampling rate was set to 100 sample per second.

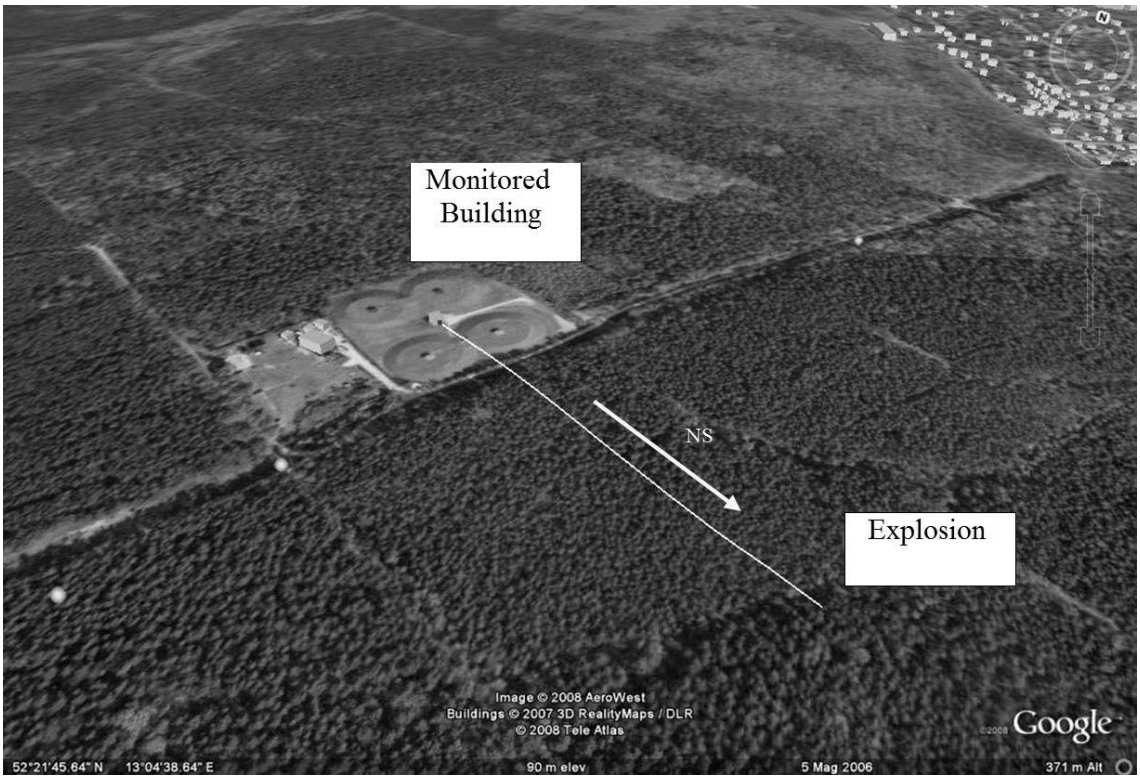

Figure 2.1: Satellite site image showing the relative location of the monitored building and the site of the explosion.

PGA (g)		
z	**ns**	**we**
0.00032987	0.00052496	0.00032522
PGV (m/s)		
z	**ns**	**we**
3.7668E-05	5.5438E-05	3.7887E-05
PGD (m)		
z	**ns**	**we**
6.7034E-07	5.3751E-07	7.4905E-07

Table 2.1: Parameters of peak ground movement in the vicinity of the Tower

The bomb was exploded about 300 m from the building and the radial direction between the location of the explosion and the building coincides with one of the main structural direction.

The bomb had a mass of about 10 kg, while the energy released was estimated to be around 40 MJ. The maximum amplitude recorded is similar to what can be expected for a magnitude 3 earthquake at 30 km distance (see Table 2.1 for some details on PGA, PGV and PGD).

The building (Figure 2.2), subsequently henceforth refered to as the Tower, is a brick-masonry, bearing-wall structure. It has a square plant (4m x 4m) and is about 16 m high. It was founded sandy ground and has no underground level.

The structure consists of 6 storeys used as residential apartments and an additional level for the roof. The inter-storey height is 2.70 m. The thickness of the walls and the characteristics of the stairwell are unknown. Adjacent to the tower, along the NS direction, there is a 2 storey building that was not monitored.

The structure was monitored installing the sensors along two vertical directions, indicated as A and B in the plan view shown in Figure 2.3. Along vertical direction A, stations were located at all storeys, starting from the ground level, up to the roof, with the only exception being the first floor where access was denied by the owner for privacy reasons. In the vertical direction B, stations were installed at the ground level and at the sixth floor. As show in Figure 2.3, vertical direction B coincides with the stairwell, and therefore closer to the estimated stiffness centre of the building than vertical direction A. Figure 2.3, also depicts the position of the stations installed outside the building. Station T1 was located at the bottom of an existing well at 2.5 m depth.

It is worth noting that the installation preceded by several hours the explosion, and that the de-installation of the network was done the day after. Therefore, a large amount of seismic noise data was available for the analysis together with the explosion generated signal.

2.3 DATA ANALYSIS

Figure 2.4 shows some examples of the recorded signals, from the ground level (top) to the uppermost storey (bottom) of the structure on +/- 5 sec around the explosion.

At first glance, there is an effect that might appear inconsistent with general expectations, that is, amplitude decreases with increasing height. As we will discuss later, this is mainly due to the fact that the energy released during the explosion is concentrated in a frequency band outside the eigenfrequencies of the building.

All records were first corrected by the following operations:

- baseline correction;
- trends removal;
- 0.1-30 Hz band-pass filter;
- smoothing with a Tukey-window.

Figure 2.1: Monitored building.

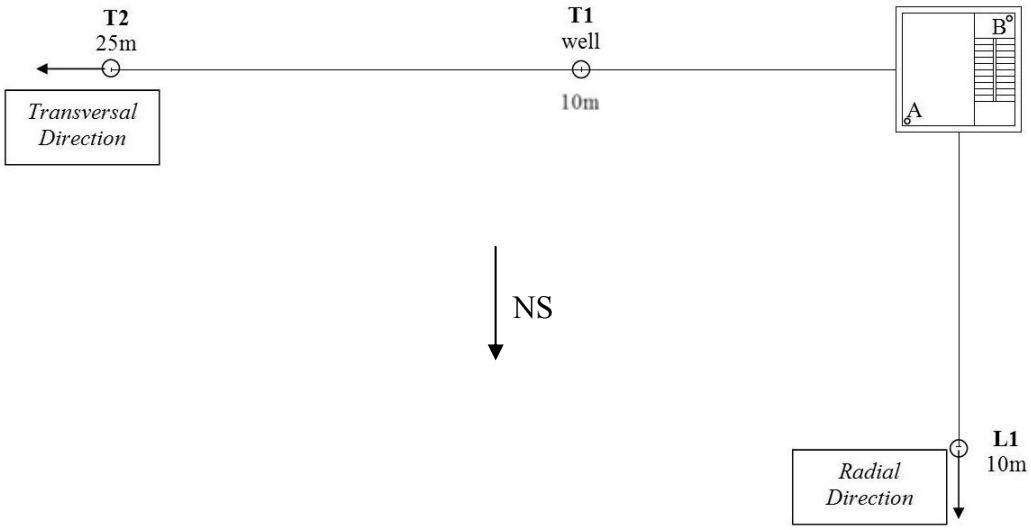

Figure 2.2: Instrumentation plan view.

The length of the analysed time window pre- and post-explosion is 1600 sec. The seismic noise was divided into 20 sec moving windows, with 50% overlap before analysis. The window including the explosion-generated signal was chosen to be 30 sec.

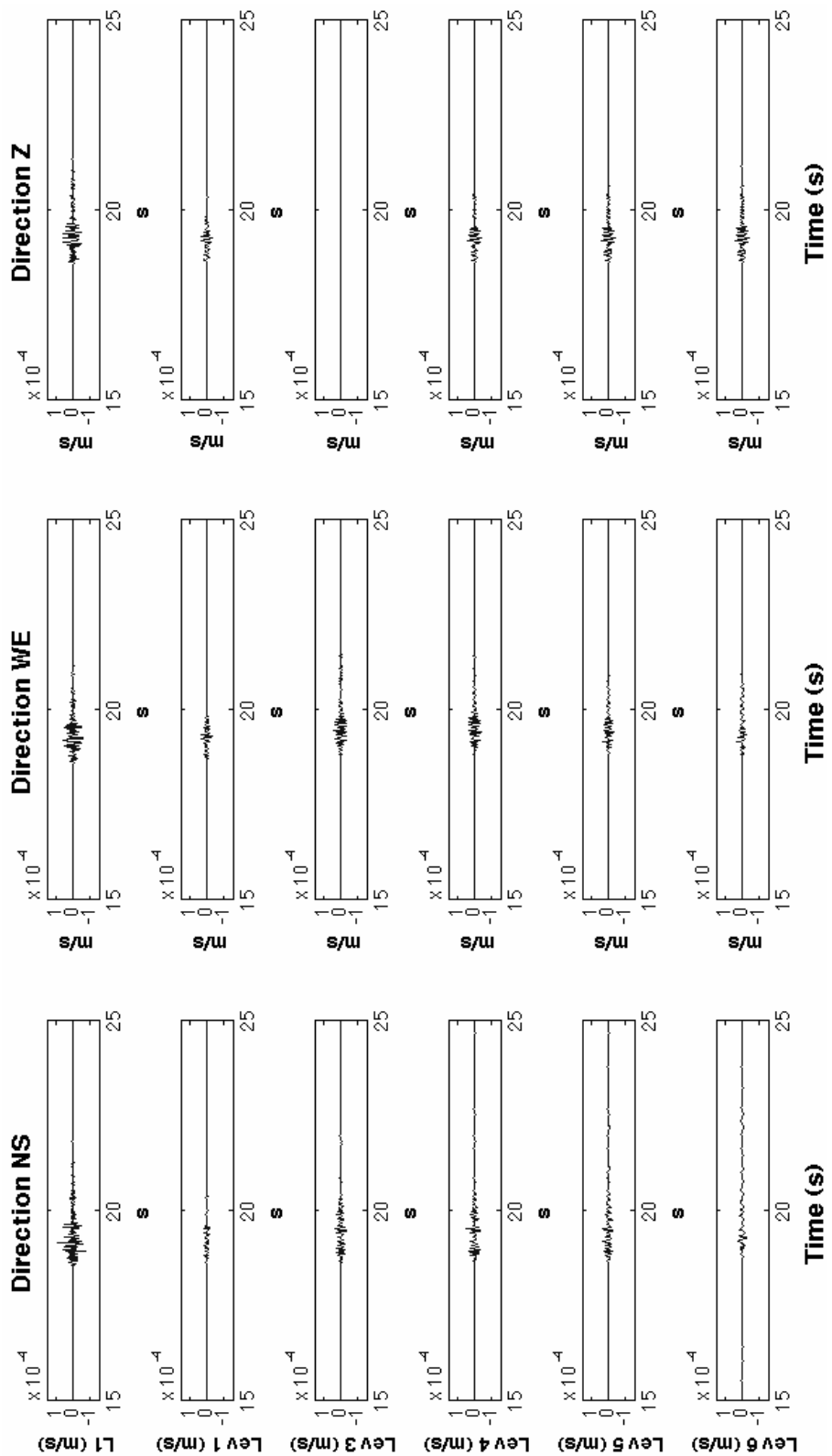

Figure 2.3: Example of the recorded signals at the L1 station and along vertical A.

The transfer functions for different storeys were then estimated by calculating the spectral ratio between each station and the station installed in the ground floor of the building, the latter being chosen as the reference. The transfer functions were calculated separately for the vertical direction A and B. However, since the results obtained are very similar, for sake of simplicity only the results relevant to direction A will be discussed in the following section.

2.4 IDENTIFICATION OF THE DYNAMIC CHARACTERISTICS OF THE BUILDING

The transfer functions calculated using seismic noise signal collected before and after the explosion are identical, as shown in Figures 2.5 and 2.7. This result implies that the structural behaviour remains unchanged after the explosion and that, therefore, no damage occurred.

A close look at the transfer functions allows to identify the first vibration mode of the structure when, along one chosen direction, the amplitude of a peak occurring at a particular frequency increases with increasing storey level. In the case at hand, this can be observed along the WE direction for the peak occurring at 2.73 Hz (first mode – WE1), and along the NS direction at 2.87 Hz(second mode – NS1). Furthermore, in both horizontal components an increase in the peak amplitude occurs at 6.20 Hz. This evidence indicates the existence of a rotational mode (third mode – R1). Over the frequency range 10 to 15 Hz, there are several peaks that might be attributed to the interaction between the tower and the adjacent structure.

The analysis of the transfer functions (Figure 2.6) obtained using the explosion signal allows us to identify the main modes of the buildings at frequencies consistent with those estimated by the seismic noise analysis. Moreover, the large amplitudes of the spectral peaks over the frequency range 5 to 20 Hz highlight the interaction between the second translational modes (of the tower) along the WE and NS directions and the adjacent structure. In fact, within this frequency band lies the resonance frequency of the small adjacent structure as assessed by seismic noise measurements not shown here.

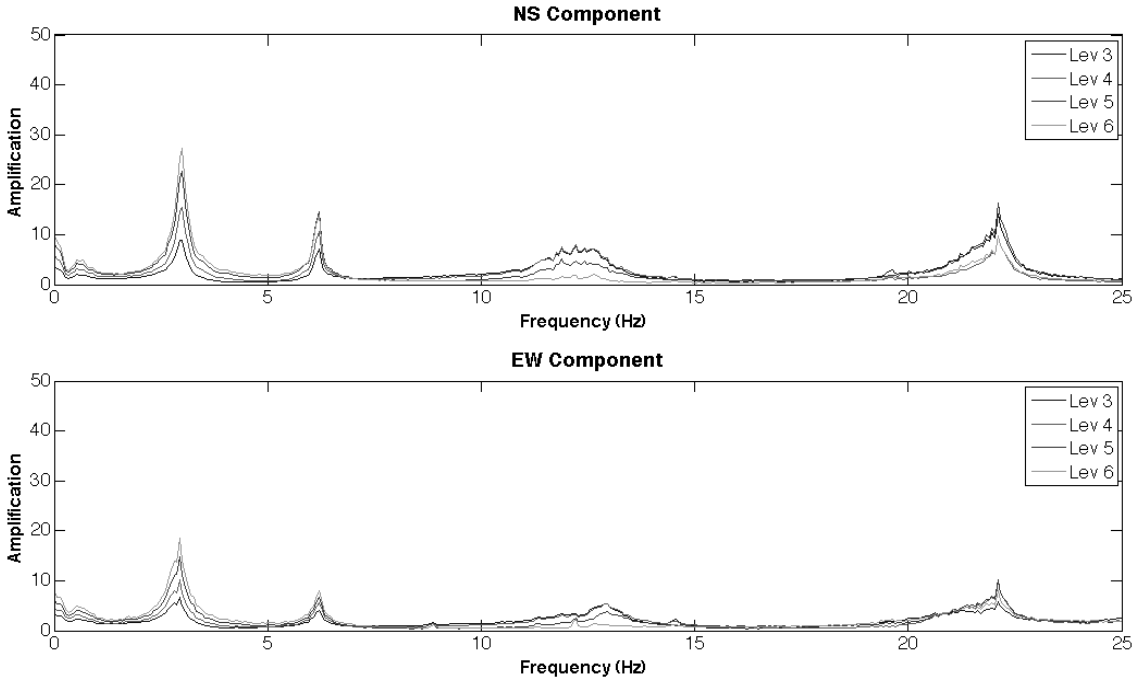

Figure 2.4: Transfer functions evaluated from noise recordings before the explosion.

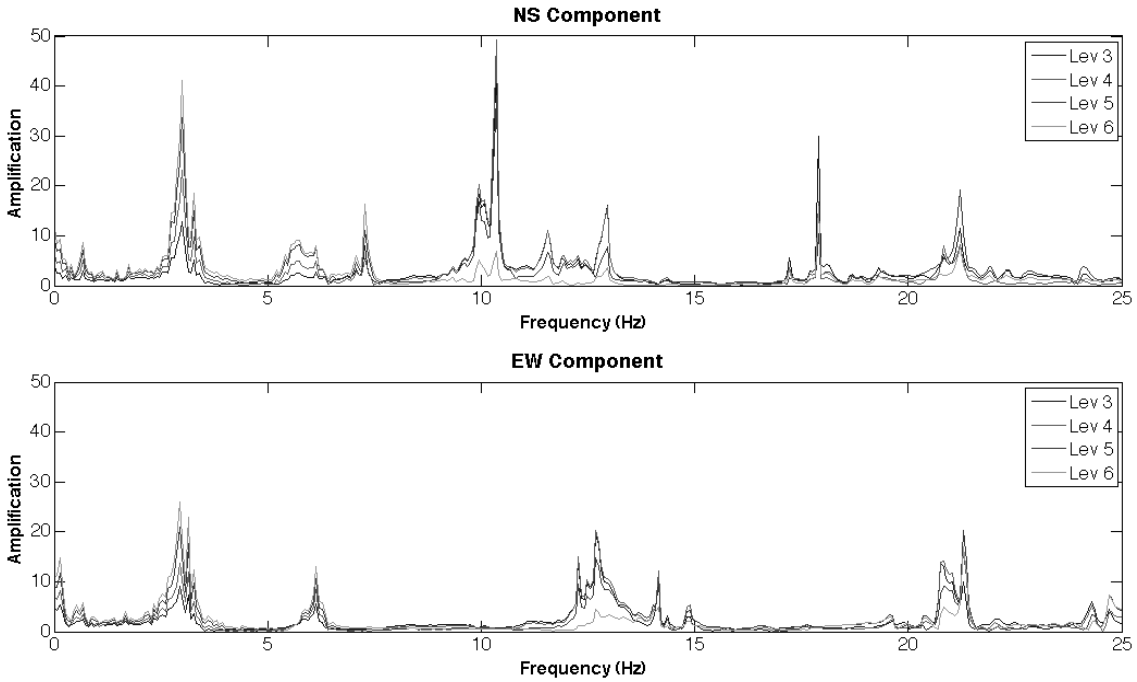

Figure 2.5: Transfer functions evaluated from the signal recorded during the explosion.

It is worth noting that the main frequencies of the structure (Figure 2.6) do not change when they are excited by the larger amplitude transient vibrations, confirming the results obtained for ambient noise and impact described in Boutin and Hans (2008). It also highlights that higher modes of the structure are strongly excited by the explosion (Figure 2.7).

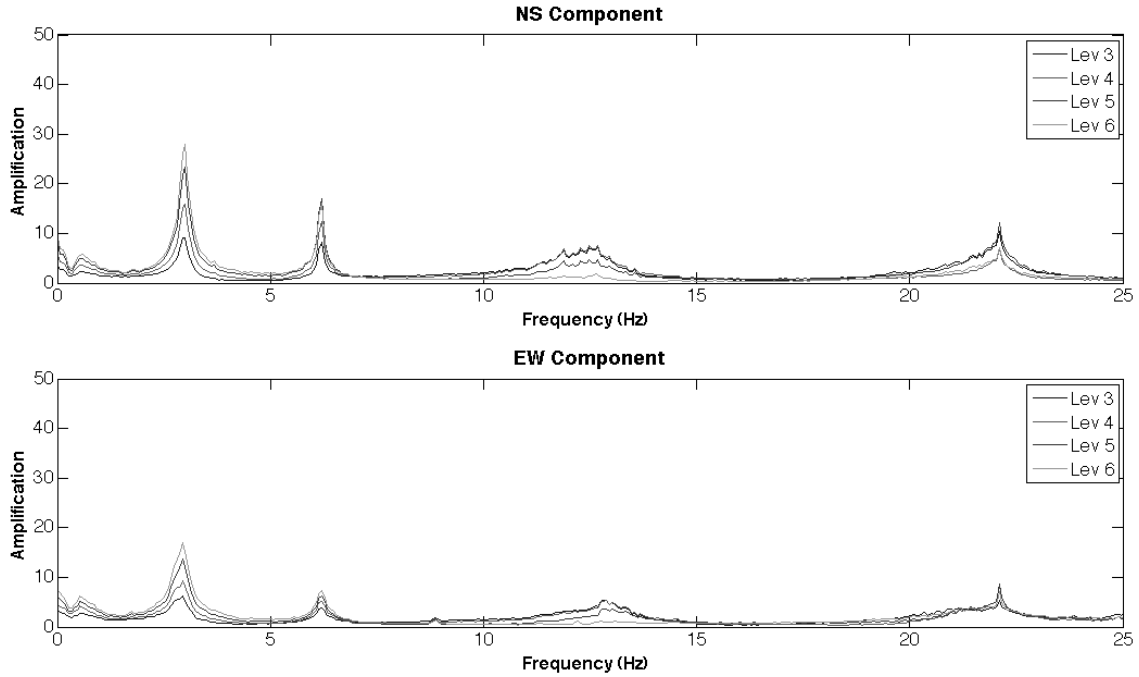

Figure 2.6: Transfer functions evaluated from recordings after the explosion.

This behaviour can be easily explained considering that most of energy released during the explosion, differently from the noise spectrum, is concentrated within 5-20 Hz frequency range (Figure 2.17).

I Mode (WE1) Translational WE	**II Mode (NS1) Translational NS**	**III Mode (R1) Rotational Z**	**IV Mode (NS2) Translational NS**	**V Mode (WE2) Translational WE**	**VI Mode (R2) Rotational Z**
f (Hz)	**f (Hz)**	**f (Hz)**	**f (Hz)**	**f (Hz)**	**F (Hz)**
2,73	2,87	6,20	12,22	12.95	22.10

Table 2.2: Main frequencies of vibration of the structure.

Using frequency-domain analysis, several peaks that could be related to higher modes of the structure were identified in the transfer functions estimated by the seismic noise and explosion data analysis. By performing a time domain analysis, filtering the signal around these peaks, it was then possible to assign the corresponding frequencies to the higher modes (the fourth at 12.22 Hz in the NS direction and the fifth one at 12.95 Hz in the EW direction) of the structure.

On the contrary, a clear spectral peak at 22.10 Hz indicating the second rotational mode of the structure (VI mode) is easily identified in the transfer functions of both the seismic noise and the explosion signal.

Summarizing, the spectral ratio analysis allowed to identify six frequencies of vibration of the tower (Table 2.2) at 2.73, 2.87, 6.20, 12.22, 12.95 and 22.10 Hz.

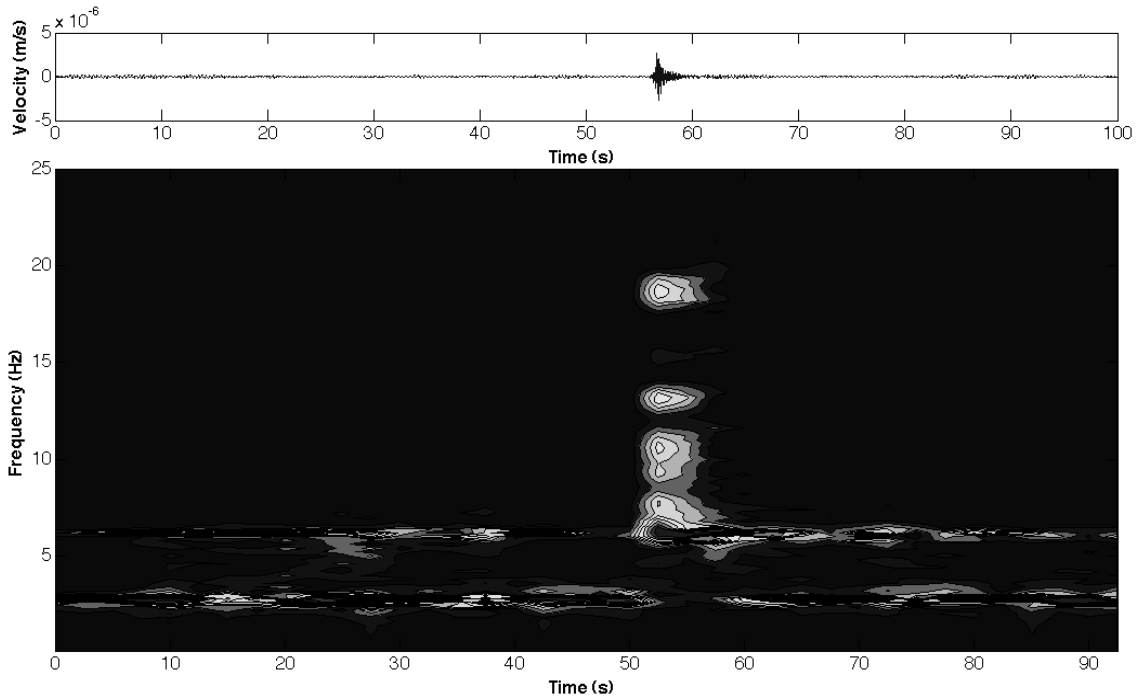

Figure 2.8: STFT evaluated during the explosion at the top floor – WE direction.

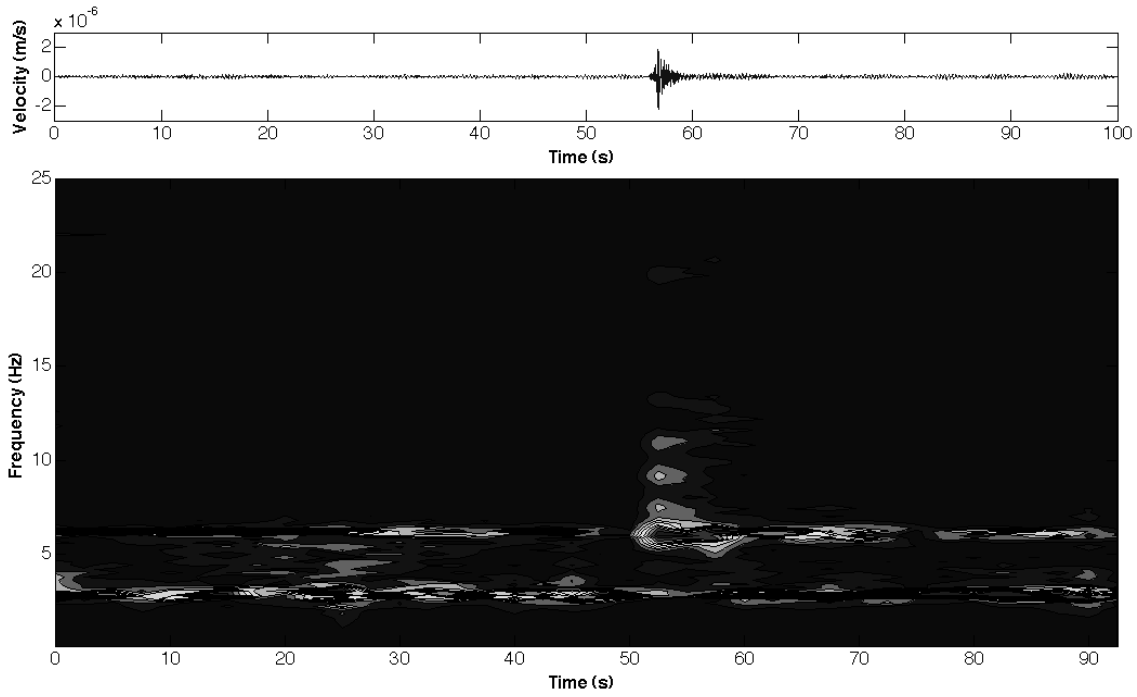

Figure 2.9: STFT evaluated during the explosion at the top floor – NS direction.

The time-frequency analysis (normalized Short Time Fourier Transform, STFT) of signals starting before and ending after the explosion (Figures 2.8 and 2.9) confirms that

during the explosion, while the resonance frequencies of the building do not vary, a strong interaction between the tower and the adjacent structure takes place. In fact, only during the explosion (between 50 and 55 sec) along the two main orthogonal directions were the frequencies of vibration of the small adjacent structure strongly excited.

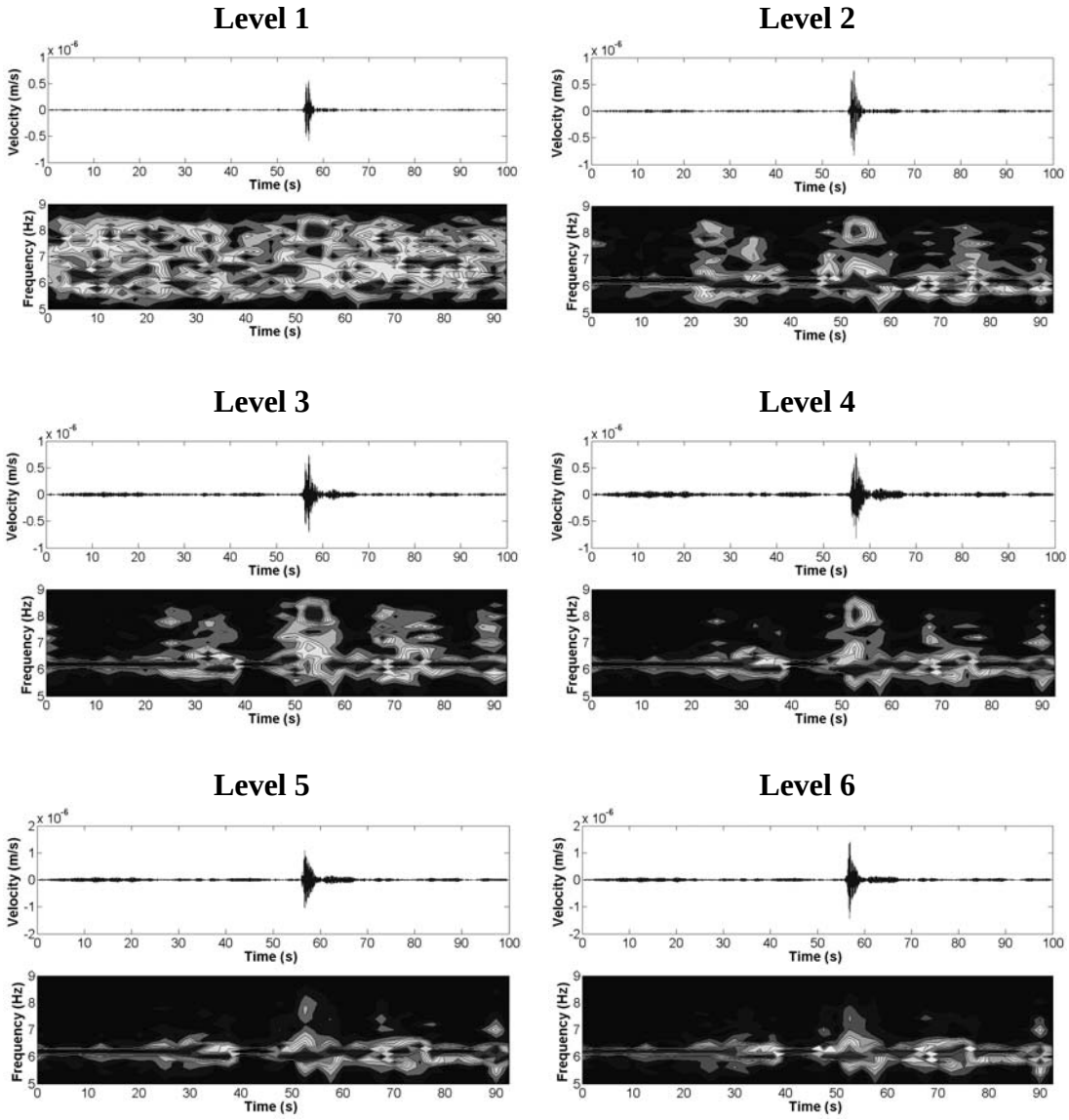

Figure 2.10: STFT of the filtered signal (5 – 9 Hz) recorded at each level of the building – NS Direction.

Calculating the STFT over narrow-band filtered signals recorded at different levels inside the building allows to confirm the interaction between the two structures. As an example, Figure 2.10 shows the results obtained by filtering the signal with a pass-band filter (5-9 Hz) around the peak at 7.5 Hz. The spectral amplitude at 7.5 Hz clearly decreases with increasing distance between the storey and the adjacent building,

therefore confirming that this frequency cannot be regarded as a mode of vibration of the tower, but is due to the interaction between the two structures. Similar results, not shown here for the sake of brevity, were obtained for the other peaks at 10 and 18 Hz shown in Figure 2.6.

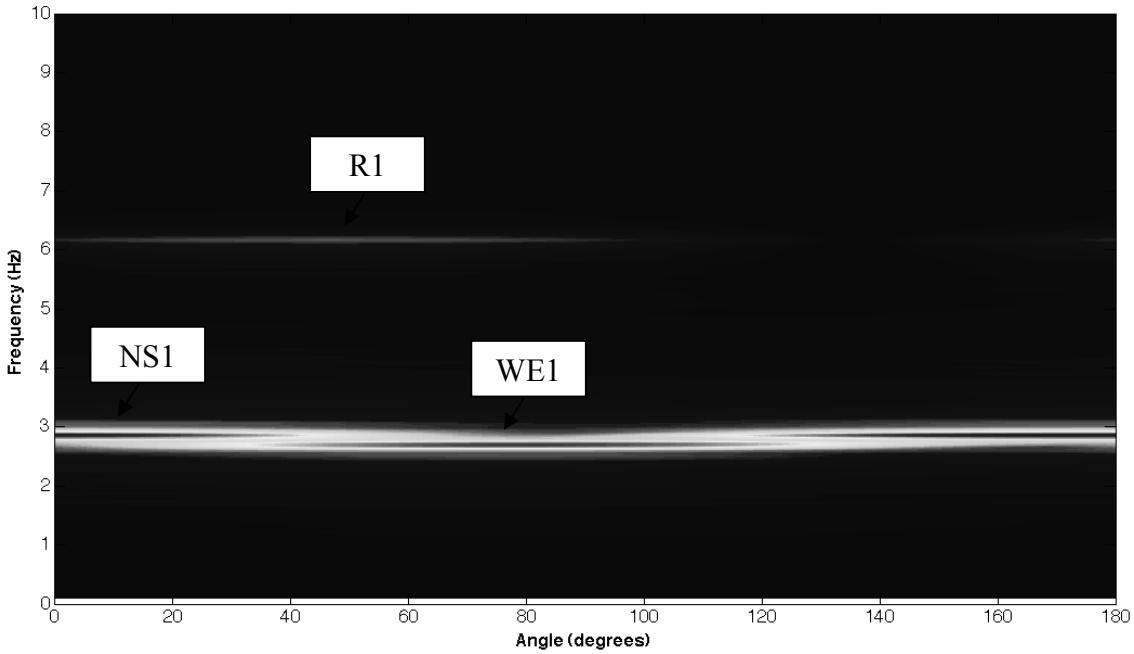

Figure 2.11: Rotational Fourier spectra.

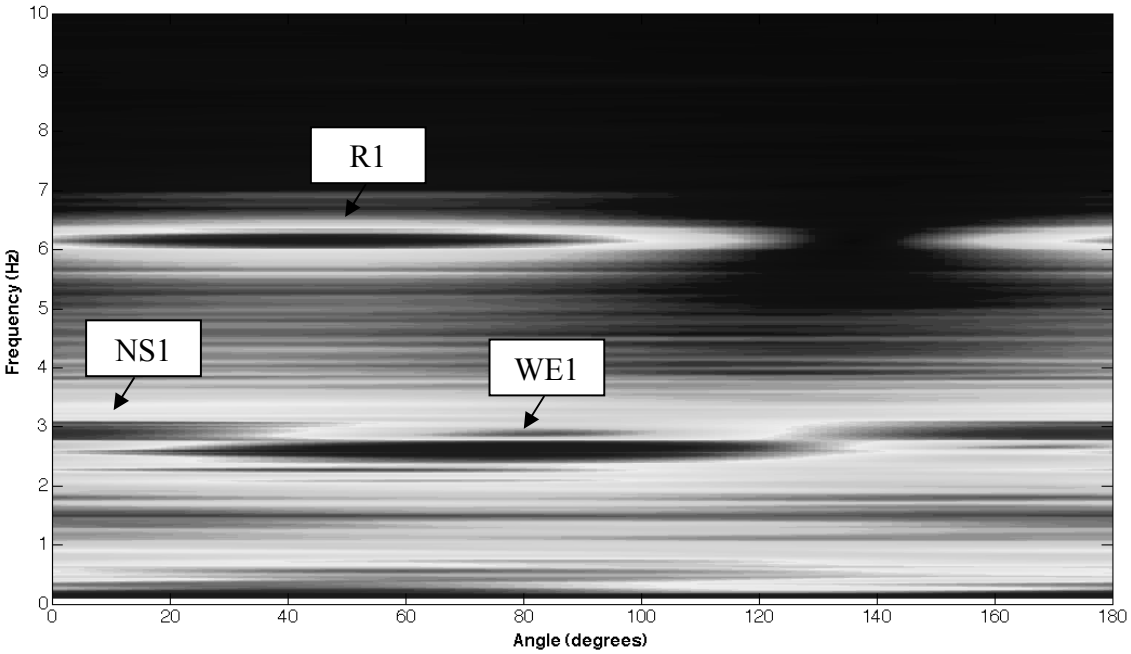

Figure 2.12: Rotational HVSR.

These results show that a frequency-time analysis can provide a deeper insight into the dynamic characteristics of a building, more than a simple frequency domain analysis which is not able to follow the time-dependent variation of the seismic input and of the related building response. In particular, in this case, the use of seismic noise alone cannot get the effect of the adjacent building on the tower behaviour.

Thanks to the large available data set, it was possible to evaluate if single station noise measurements, processed according the HVSR technique, might be suitable for multi-mode identification in the structure. The main frequencies of vibration were evaluated by rotating the horizontal component of the recorded motion and then performing both a spectral and a HVSR analysis. Both analyses were carried out by considering only the recordings collected on the topmost storey (Figure 2.3) along the vertical direction A. Figures 2.11 and 2.12 show the Fourier spectra of the horizontal component after rotation for the back-azimuth, and the corresponding HVSR, respectively.

Figures 2.11 and 2.12 show that both methods allow an estimation of the frequencies of vibration in agreement with those obtained by the standard spectral ratio method. It is worth noting that simple rotational HVSR allows us to identify the structural frequencies highlighting the peaks related to the first three main modes of vibration.

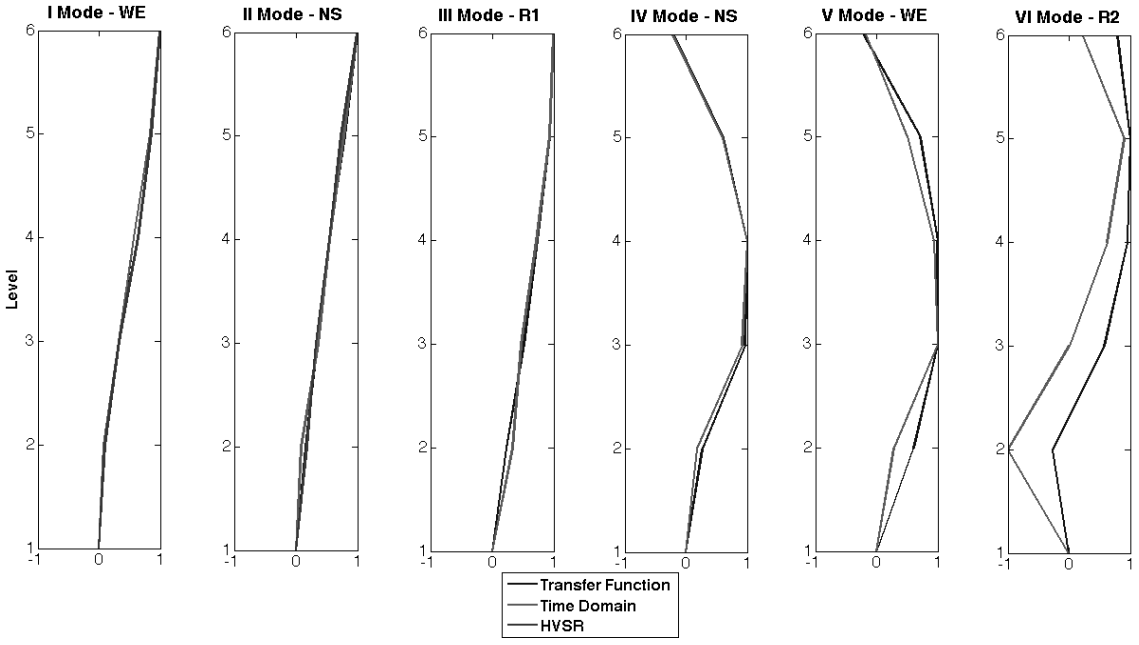

Figure 2.13: Modal shapes with respect to level. Note the change in slope after the second level for the higher modes.

However, it should also be observed that the relative amplitudes of the HVSR peaks might be different from those estimated by the transfer function method, due to the

amplification of the vertical component of the motion in the building; furthermore, during the measurements it was also verified that no-strong source of noise was acting inside the building.

Figure 2.13 shows the structural modal shapes evaluated by the transfer function and the time domain analysis, with both techniques providing consistent results.

The modal shapes derived using the eigenfrequencies previously estimated are consistent with the expected ones for the kind of structure at hand. That is, the first 3 modes feature nearly linear shapes with increasing level. Interestingly, the slope of the modal shape for higher modes changes after the second level in the building, indicating that there is a vertical change in the global stiffness (mainly along the NS direction) of the structure due to the adjacent small building.

Furthermore, it was also attempted to estimate the first two modal shapes by using HVSR. In order to characterize the modal shapes using the HVSR technique, at the second level a linear interpolation was necessary, because the signal recorded at this level was not reliable due to a malfunctioning of the sensor Z component.

Interestingly, the HVSR results are consistent with those obtained by the transfer function and the time domain analysis. Using H/V ratio it is possible that the estimate of both resonance frequencies and modal shapes can be biased, if the vertical component has large spectral amplitudes in the range of frequencies close to the main frequencies of horizontal vibration. For example this can happen when the independent membrane vibrations of the floor can be large. It is therefore advisable, when H/V measurements are carried out, to place the instrumentations as close as possible to structural elements like columns, beams and walls.

Finally, the damping of the structure was estimated by using the method proposed in Mucciarelli and Gallipoli (2007). Damping was also evaluated for signals recorded by station L1 located outside of the building. The damping value evaluated for the Tower, with both signals in good agreement (~3%) and the estimated damping consistent with the small amplitude ground motion analysed. On the contrary, the damping values estimated from seismic noise (~6%) and the explosion signal (~3.5%) are different. Since higher damping might be expected in the case of larger amplitude ground motion, this result could indicate that the estimated damping is an effective one, biased by the larger amount of energy radiated back to the soil by the Tower during the explosion.

2.5 BUILDING-SOIL INTERACTION

In order to verify if the Tower returned a significant amount of energy back into the ground, the rotational HVSR were also calculated for the recordings of station L1 (Figure 2.3) in the ambient noise window.

The results, reported in Figure 2.14, show that the first and second modes of the building can be tracked in the signal recorded at 10 meters distance outside it.

In order to study both the structural behaviour and soil-structure interaction, an interferometric analysis (e.g. Curtis *et al.*, 2006; Snieder and Safak, 2006) was performed using signals recorded in the tower and at station L1.

The signal at different levels was deconvolved for the signal recorded at the top of building using a regularized Tikhonov deconvolution (Tikhonov and Arsenin, 1977; Bertero and Boccacci, 1998; Parolai *et al.*, 2009).

Figure 2.15 shows the results obtained comparing the analysis performed with seismic noise and the explosion signal. While there is good agreement between the results provided by both analyses for the WE and NS components, the results obtained for the Z component show some discrepancies. However, this might be explained by taking into account that at each level of the Tower the mass was different, thus implying different frequencies of vibration of the floor.

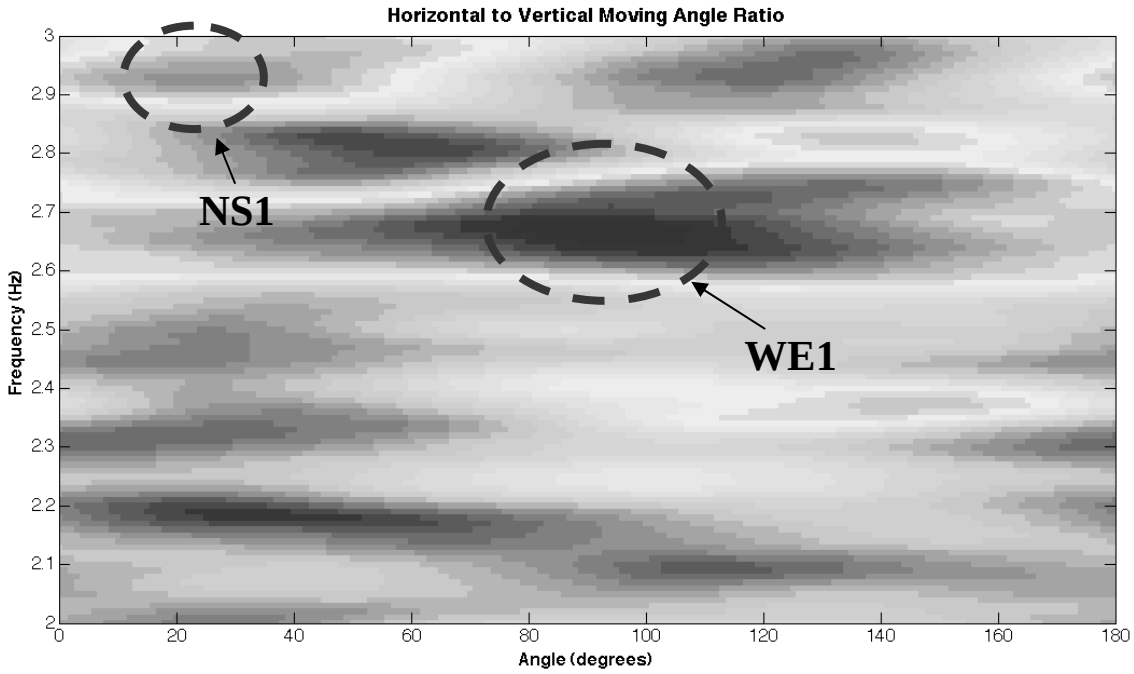

Figure 2.14: Rotational HVSR evaluated for L1 station.

In this case, each floor has exhibited a membrane behaviour, depending from its mass and stiffness. Stiffness was the same at each floor, while masses were very different.

It is worth noting, for example on the WE component of the explosion signal recordings, the differences between the simple pulse in the acausal part of the Green's function and the long lasting oscillation in the causal one due to the structural response. Also in the deconvolved wavefield the dominance of higher modes in the explosion signal is highlighted.

These analysis are in good agreement with the modal analysis presented in Figure 2.13. Performing a spectral analysis of the deconvolved traces depicted in Figure 2.15 (here not shown), it is possible to find the structural eigenfrequencies and the related modes (Figure 2.13); e.g. the ringing of the WE component, during the explosion (Figure 2.15), is a frequency related to the V mode (f=12.95 Hz) showed in Figure 2.13.

It was finally investigated the possibility of detecting the "fingerprint" of soil-structure interaction using the FFT of the signals recorded on the ground surrounding the structure before the explosion. Figure 2.16 clearly shows two spectral peaks: the former occurring at the same frequency of the fundamental mode of the structure, the latter at 22.10 Hz, the second rotational mode of the Tower. Thus, confirming the results of the rotational HVSR analysis, it can be seen that ambient vibrations already indicate the capability of the structure to modify the free-field ground motion. This ability, however, disappears with distance. At station T2, located 25 m away from the building, the peak due to the fundamental period of the structure has vanished.

It can also be observed that the amplitude of the peak at 22.10 Hz decreases with increasing distance for stations located outside the tower (Figures 2.16 and 2.18), while it varies within the building, depending on the storey. The amplitude is thus believed to be due to the structure and not to an external source.

Figure 2.17 shows the spectra of the signal generated by the explosion recorded at the free-field stations. The transient energy is concentrated within the 5-20 Hz frequency band, i.e., at frequencies higher than those corresponding to the lower modes of the structure. This might explain why only the higher modes (third and fourth) were excited (Figure 2.17) and released a large amount of energy back to the soil.

The Fourier spectra of the signal recorded after the explosion are shown in Figure 2.18. Spectra are again similar to those calculated for seismic noise collected before the explosion with the first and fourth modes of the structure easily identified by a large peak in the spectra of all stations.

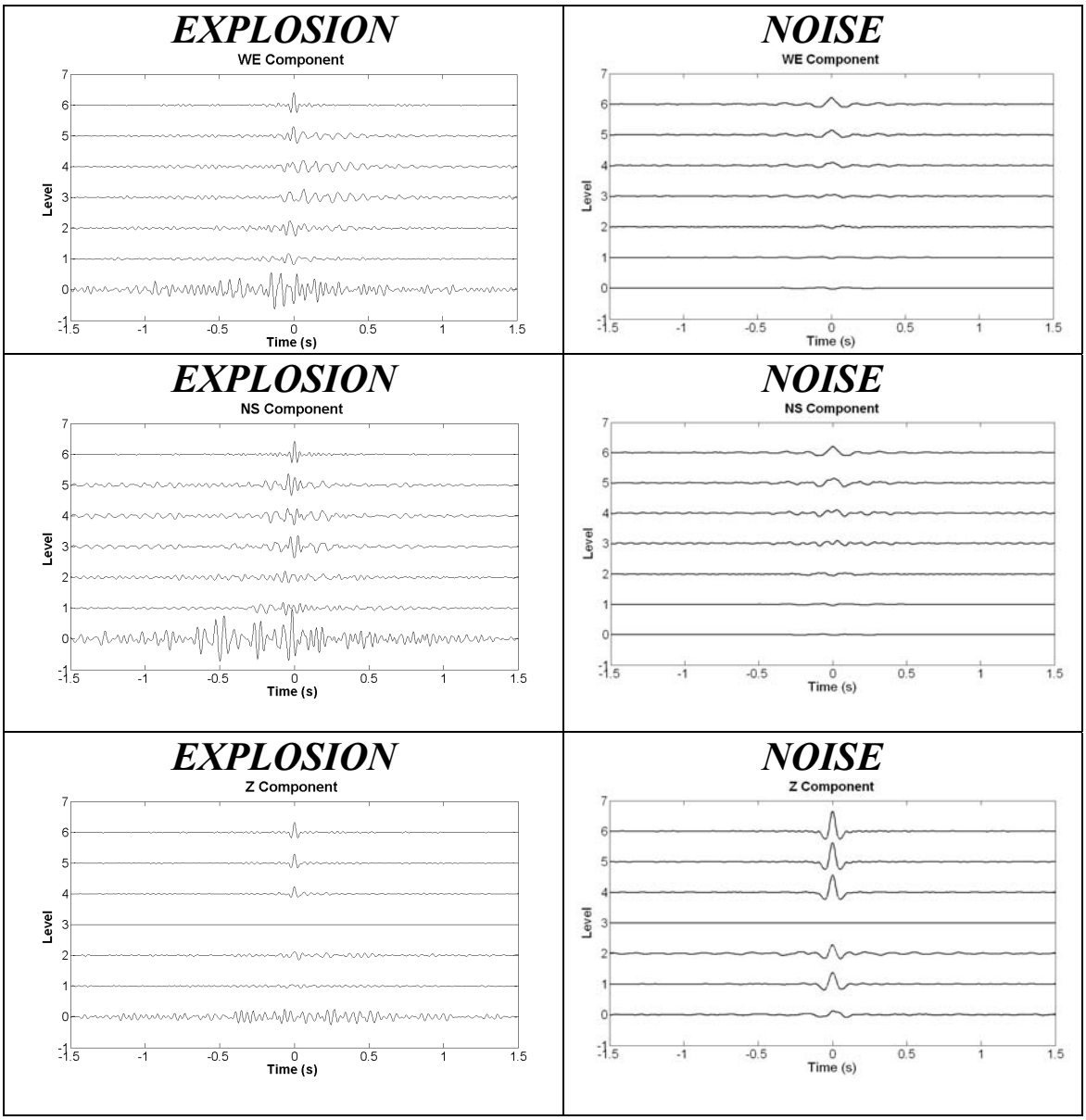

Figure 2.15: Comparison of the interferometric analysis of signals recorded within the building and the station L1 (Level 0) using noise (right) and explosion signals (left). Signal recorded at Level 3 (Z Component) was not reliable due to malfunctioning of the sensor.

Finally, Figure 2.19 shows one example of the results obtained by calculating the spectral ratio between the recordings of the explosion at the closest station (L1) and the most distant one (T25). The radiated energy is visible also in the vertical component because the building-radiated wave field is a mix of body and Rayleigh waves (Guèguen *et al.*, 2000, Mucciarelli *et al.*, 2003; Gallipoli *et al.*, 2006). Amplifications peaks occur close to the main frequencies of vibration of the building. This result is consistent with the findings of Mucciarelli *et al.* (2008) and Ditommaso *et al.* (2009), who noticed that, although the soil-structure interaction in inhabitated areas might act in general as a dampener for the recorded wavefield (Semblat *et al.*, 2008), there is a shift

of energy that concentrates at frequencies close to the frequencies of the buildings, yielding local peaks of amplification in the Fourier spectrum.

2.6 DISCUSSION

The analysis of ambient and transient vibrations performed with different techniques showed that there was no change in the resonant frequencies of the investigated structure. In this case, the dynamic characteristics estimated using ambient noise are not different from those retrieved using ground motion in the range from centi- to milli-*g*.

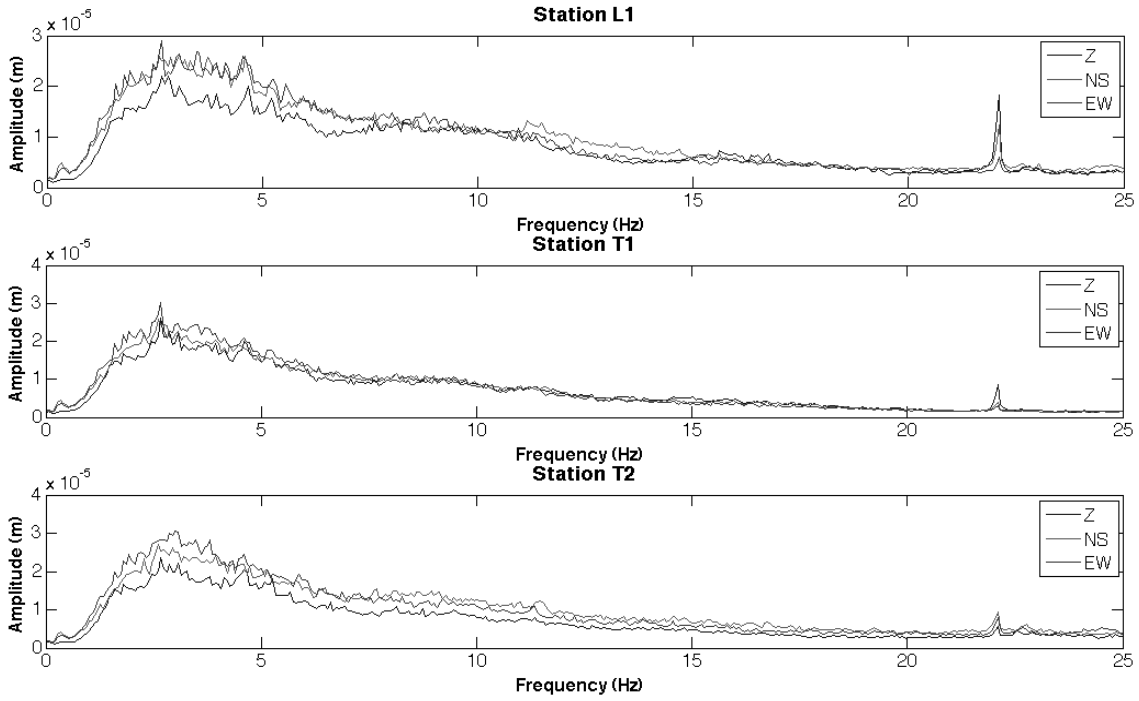

Figure 2.16: Spectra evaluated with noise before the explosion.

However, in the case of the presence of adjacent buildings, it was shown that seismic noise analysis on a single building might not fully explain its structural behaviour. With regards to this, it was also shows that a frequency-time analysis provides more information than standard time domain or frequency domain investigations.

The presence of the Tower proved to be able to modify the free-field ground motion. It is important to note that the frequencies most affected during the ambient noise recording were those around the fundamental periods, because the structure of the noise reveals a broad peak in the same range of frequency.

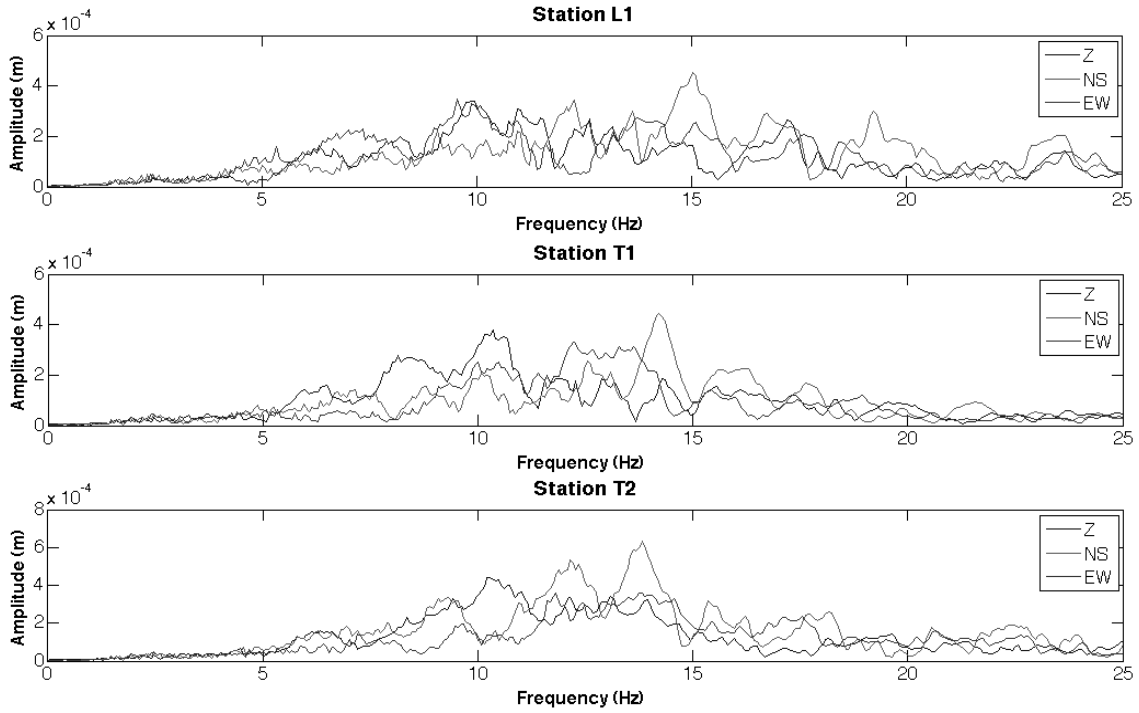

Figure 2.17: Spectra evaluated during the explosion.

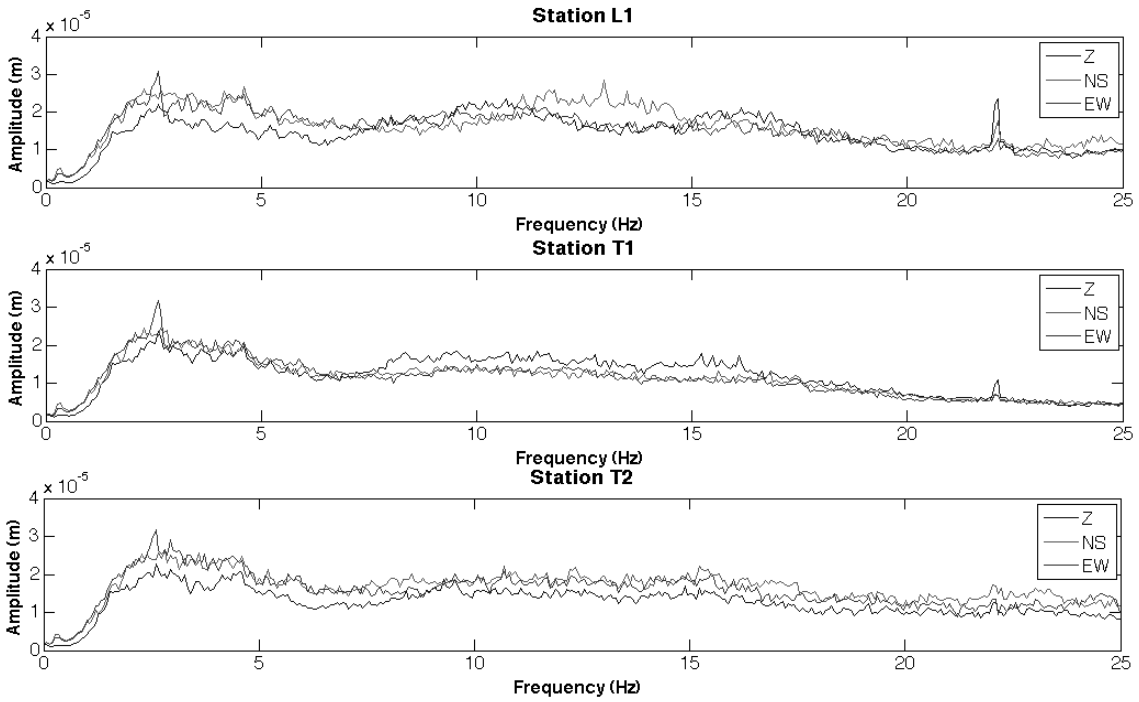

Figure 2.18: Spectra evaluated with noise after the explosion.

During the explosion, more energy is carried at higher frequencies, thus exciting the higher modes of the structure, whose contribution to the back-radiation also increases. While the global effect is a decrease in energy due to the added damping of the

structure, there is a strong increase in spectral values in the frequency band close to the eigenfrequencies of the building.

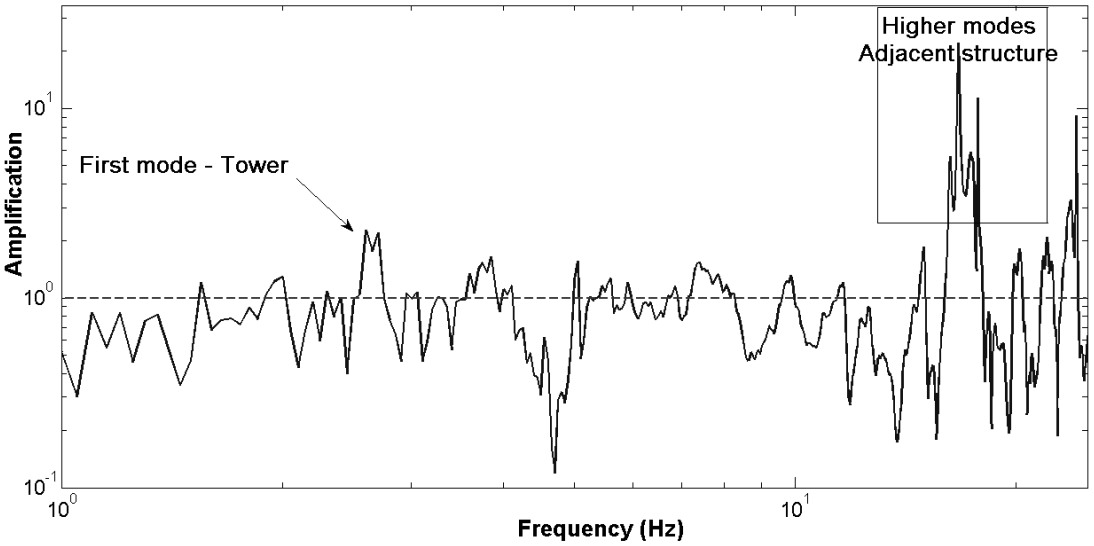

Figure 2.19: Spectral ratio between the L1 and T25 stations (vertical component).

The modification of the observed motion can be considered interesting for the effect that it may have on accelerometric stations located inside or nearby stand-alone buildings. A more quantitative modelling of this effect is described in Ditommaso *et al.*, (2009).

REFERENCES

Bertero, M. and P. Boccacci (1998). Introduction to inverse problems in imaging. Bristol:IOP Publishing.

Boutin, C. and Hans, S. (2008). How far ambient noise may help to assess building vulnerability? "Increasing Seismic Safety by Combining Engineering Technologies and Seismological Data". Springer, ISBN 978-1-4020-9196-4, 151-180.

Chavez-Garcia, F.J. and Cardenas-Soto, M. (2002). The contribution of the built environment to the free-field ground motion in Mexico City, Soil Dyn. Earthq. Eng., 22, 773–780.

Clinton, F., Case, Bradford, S., Heaton, T. H. and Favela, J. (2006). The observed Wander of the Natural Frequencies in a Structure. Bulletin of Seismological Society of America, February 2006, Vol. 96, No. 1, pp. 237-257.

Cornou, C., Guéguen, P., Bard, P.-Y., and Haghshenas, E. (2004). Ambient noise energy bursts observation and modeling: Trapping of harmonic structure-soil induced–waves in a topmost sedimentary layer, J. Seismol., 8(4), 507–524.

Curtis, A., Gerstoft, P., Sato, H., Snieder, R. and Wapenaar, K. (2006). Seismic interferometry-turning noise into signal. The Leading Edge, 25, 1082-1092.

Davoodi, M., Jafari, M. K., Amel Sakhi, M (2007). Using TFD signal processing to evaluate dynamic characteristics of Masjed Soleiman embankment dam by blasting tests' Five International Conference on Seismology and Earthquake Engineering, IIEES Tehran.

Davoodi, M., Jafari, M. K., Amel Sakhi, M. (2008). Using new signal processing techniques in analyzing Masjed Soleyman Embankment dam's explosion records. The 6th International Conference on Case Histories in Geotechnical Engineering,, USA.

Dhakal, R.P. (2004). Explosion-induced structural response: An overview. Proceedings of 2004 NZSEE Conference. Paper No. 40.

Ditommaso, R., Gallipoli, M. R., Mucciarelli, M., Ponzo, F. C. (2007). Effect of vibrating building on "free field" ground motion: from the Bagnoli experiment to many-buildings simulation. Proc. 4th Int. Conf. Earthq. Geot. Eng., CD-Rom edition, Paper No. 1388. Springer, ISBN 978-1-4020-5893-6.

Ditommaso, R., Gallipoli, M. R., Mucciarelli, M., Ponzo, F. C. (2009). Effect of a single vibrating building on free-field ground motion: numerical and experimental evidences. Bulletin of Earthquake Engineering, DOI: 10.1007/s10518-009-9134-5

Gallipoli, M.R., Mucciarelli, M., Castro, R.R., Monachesi, G. and Contri, P. (2004). Structure, soilstructure response and effects of damage based on observations of horizontal-to-vertical spectral ratios of microtremors, Soil Dyn. Earthq. Eng., 24, 487-495.

Gallipoli, M. R., Mucciarelli, M., Ponzo, F., Dolce, M., D'Alema, E., Maistrello, M. (2006). Buildings as a seismic source: analysis of a release test at Bagnoli, Italy, Bull. Seism. Soc. Am., 96, 2457-2464.

Guéguen, P., Bard, P.-Y. and Oliveira, C. S. (2000). Experimental and numerical analysis of soil motions caused by free vibrations of a building model. Bull. Seism. Soc. Am. 90(6), 1464-1479.

Guéguen, P., Bard, P.-Y. and F.J. Chavez-Garcia (2002). Site-city seismic interaction in Mexico Citylike environments: An analytic study. Bull. Seism. Soc. Am., 92, 2, 794-811.

Guéguen, P. and Bard, P.-Y. (2005). Soil-structure and soil-structure-soil interaction: experimental evidence. Journal of Earthquake Engineering, Vol. 9, No. 5 (2005), 657–693.

Hans, S., Boutin, C., Ibraim, E. and Rousillon, P. (2005). In situ experiments and seismic analysis of existing buildings. Part I: Experimental investigations. Earthquake Engineering and Structural Dynamics, 2005, 34, pp. 1513-1529.

Kanamori, H., Mori, J., Anderson, D.L., and T.H. Heaton (1991). Seismic excitation by the space shuttle Columbia, Nature, 349, 781–782.

Kohler, M. D., Davis, P. M. and Safak, E. (2005). Earthquake and Ambient Vibration Monitoring of the Steel-Frame UCLA Factor Building. Eqrthquake Spectra, August 2005, Vol. 21, No. 3, pp. 715-736.

Kohler, M. D., Heaton, T. H. and Bradford, S. C. (2007). Propagating Waves in the Steel, Moment Frame Factor Building Recorded during Earthquakes. Bull. Seismol. Soc. Am., August 2007, 97, 1334-1345.

Mucciarelli, M., Gallipoli, M.R., Ponzo, F. C. and Dolce, M. (2003). Seismic waves generated by oscillating building. Soil Dyn. Earthq. Eng., 23, 255-262.

Mucciarelli, M., Ditommaso, R., Gallipoli, M. R. and Ponzo, F. (2008). Effect of Building-Building Interaction on "Free-Field" Ground Motion., in "Increasing Seismic Safety by Combining Engineering Technologies and Seismological Data". Springer, ISBN 978-1-4020-9196-4, 141-145.

Mucciarelli, M. and Gallipoli, M.R. (2007), Non-parametric analysis of a single seismometric recording to obtain building dynamic parameters, Annals of Geophisics,Vol. 50, N. 2, April 2007.

Parolai, S., A. Ansal, A. Kurtulus, A. Strollo, R. Wang and J. Zschau (2009). The Ataköy vertical array (Turkey): insights into seismic wave propagation in the shallow-most crustal layers by waveform deconvolution. Geophys. J. Int. doi:10.1111/j.1365-246X.2009.04257.x.

Potapov, V.A. (1974). Investigation of the explosion-induced vibration of buildings. Soil Mechanics and Foundation Engineering. Volume 11, Number 3, 170-173.

Safak, E. (1995). Detection and Identification of Soil-Structure Interaction in Buildings from Vibration Recordings. Journal of Structural Engineering, May 1995, pp. 899-906.

Safak, E. (1999). Wave-Propagation Formulation of Seismic Response of Multistory Buildings. Journal of Structural Engineering, April 1999, pp. 426-437.

Semblat, J.-F., Kham, M. and Bard, P.-Y. (2008). Seismic-Wave Propagation in Alluvial Basins and Influence of Site-City Interaction. Bulletin of the Seismological Society of America, Vol. 98, No. 6, pp. 2665–2678, December 2008.

Snieder, Roel and Safak, Erdal (2006). Extracting the building response using seismic interferometry: teory and application to the Millikan Library in Pasadena, California. Bull. Seismol. Soc. Am., Apr. 2006, 96, 586-598.

Tikhonov, A.N. and V.Y. Arsenin (1977). Solution of ill-posed problems. Washington:Wiston/Wiley.

Trifunac, M. D., Ivanovic, S. S., Todorovska, M. I. (2007). Apparent periods of a building. I: Fourier Analysis. Journal of Structural Engineering, May 2001, pp. 517-526.

Tifunac, M. D. (1972). Comparison between ambient and forced vibration experiments. Earthquake Engineering and Structural Dynamics, 1972, Vol. 1, pp. 133-150.

Todorovska, M. I., Ivanovic, S. S., Trifunac, M. D. (2001). Wave propagation in a seven-story reinforced concrete building I. Theorethical models. Soil Dynamics and Earthquake Engineering, 2001, 21, pp. 211-223.

Wong, H.L. and M.D. Trifunac (1975). Two dimensional antiplane building-soil-building interaction for two or more buildings and for incident plane SH waves, Bull. Seismol. Soc. Am., 65, 1863-1865.

CHAPTER 3

APPLICATION OF NEW WIRELESS SENSOR UNITS FOR SYSTEM IDENTIFICATION: THE CASE OF FATIH SULTAN MEHMET SUSPENSION BRIDGE

Rapid improvements in telemetry technology and the general decrease in communication costs have raised a growing interest in low-cost wireless sensing units. This is especially the case for structural monitoring purposes, where they are becoming a more valuable alternative to conventional wired monitoring system.

The main advantages associated with the use of wireless sensing unit include a considerable decrease in installation costs, decentralization of data analysis, and the possibility of broadening the functional capabilities by exploiting the use, at the same time and place, of different sensors. In this work, the design of a low-cost wireless sensing unit able both to collect, analyze, store, and communicate data and estimated parameters is presented. The suitability of a network of these low-cost wireless instruments for monitoring the vibration characteristics and dynamic properties of strategic civil infrastructures has been validated during a ambient vibration recording field test on the Fatih Sultan Mehmet Bridge in Istanbul, Turkey.

3.1 INTRODUCTION

The monitoring of strategic civil infrastructures to ensure their structural integrity is a task of major importance, especially in earthquake-prone areas. In fact, after earthquakes, only by real-time structural health monitoring systems it is possible to obtain the critical data necessary for a rapid condition assessment, damage and structural degradation detection in structures (Safak and Hudnut, 2006).

However, traditional wired systems have the main drawbacks of being relatively expensive, time consuming to install, and are limited to a centralized data server where data are collected and analyzed that can become the main critical point of failure for the whole system.

In contrast to wired system, Straser and Kiremidjian (1996, 1998) first explored the application of wireless communications technology for structural monitoring, showing that wireless monitoring systems are feasible, reliable and cost-effective. From those pioneering works, several other studies have dealt with the development of such systems, taking also advantage of the continuous and rapid improvements in wireless technology (e.g. Lynch *et al.*, 2002; Lynch *et al.* 2003; Grosse *et al.*, 2004; Krűger *et*

al., 2005). A further significant step was made by Lynch *et al.* (2003) who, in order to attain an optimal usage of power, introduced the idea of performing the real-time processing of data locally by embedded engineering algorithms in lieu of transmitting wirelessly the complete time-history records to centralized data servers.

Prototype structural wireless monitoring systems have been already validated by tests performed on bridges and other structures (e.g. Lynch *et al.*, 2006; Wang *et al.* 2006; Loh *et al.*, 2007), where they have been found to be a highly cost-competitive, completely autonomous and very reliable alternative to traditional wired systems.

In this study a new low-cost Wireless Sensing Unit (WSU) designed to form dense wireless mesh networks is presented. These innovative instruments have the capability to rearrange automatically their communication scheme, and allow the analysis and storage of data to be decentralized. The work for the development of such instruments, together with the organisation and routing protocols necessary to obtain a wireless mesh network, involves significant technical efforts, which are being carried out within the framework of the earthquake early warning projects Seismic eArly warning For EuRope (SAFER, 2006, http://www.saferproject.net/index.htm) and Earthquake Disaster Information systems for the Marmara Sea region, Turkey (EDIM, 2007, http://www.cedim.de/EDIM.php), by the Helmholtz Centre Potsdam GFZ German Research Centre for Geosciences (GFZ, http://www.gfz-potsdam.de), and the Department of Informatics, at the Humboldt University Berlin (HU, http://www.informatik.hu-berlin.de), both in Germany.

The reduced sensitivity of these sensors, arising from the use of low-cost components, is compensated by the possibility of deploying high-density self-organizing networks performing real-time data acquisition and analysis. Such characteristics make systems of WSU of great interest for the monitoring of strategic civil infrastructure.

In the first part of this chapter the hardware that make up the individual WSU is described, and the main characteristics of the software adopted for the routing protocols and the data archiving are introduced. This is followed by a section describing the execution of a ambient vibration field test in Istanbul, Turkey.

Istanbul is a mega-city (population about 14 million), prone to significant risk from earthquakes, being located at its nearest point only a few kilometers from the North Anatolian Fault, along which there have been a number of large earthquakes over the past century, the most recent being the 1999 Izmit (August 17th, Mw=7.4) and 1999 Dűzce (November 12th Mw=7.2) Earthquakes (Milkereit *et al.*, 2000; Tubi *et al.*, 2001;

Erdik, 2003 a,b). For these reasons, together with the development of an earthquake early warning network made up of low-cost WSUs, it was considered worthwhile to explore the possibility of using these instruments for the structural monitoring of strategic civil infrastructures. Therefore, the second part of this chapter, is devoted to describe the findings of an experimental ambient vibration test carried out on the Fatih Sultan Mehmet Suspension Bridge in Istanbul, the second gravity-anchored suspension bridge spanning the Bosporus Strait, in collaboration with the Kandilli Observatory and Earthquake Research Institute (KOERI). Suspension bridges are often critical nodes of major transportation systems, hence their failure during strong earthquake is a major threat for both the potentially high number of fatalities and the substantial interruption of emergency activities (Erdik and Apaydin, 2005).

Therefore, the monitoring systems of bridge's design parameters vibration characteristics and dynamic properties represent a valuable tool for assessing their wind and earthquake safety. However, the size and the very low vibration frequencies of suspension bridges rules out the use of forced vibration techniques (such as harmonic excitation or impulsive loading) commonly used for other bridges and viaducts. On the contrary, one of the best methods utilized to assess the dynamic characteristics of such massive structures is the measurement of the structural response to ambient excitations, such as wind and traffic. The structural vibrations caused by such excitations are termed the 'Ambient Vibrations'. Previous works (e.g. Petrovski *et al.*, 1974; Tezcan *et al.*, 1975; Abdel-Ghaffar and Housner, 1978; Brownjohn *et al.,* 1987; Erdik and Uckan, 1988) showed that full-scale dynamic testing of suspension bridge by ambient vibration recording represents a reliable approach for the assessment of the free vibration characteristics (i.e. vibration mode shapes, frequencies and associated damping ratios), the calibration of the analytical and finite element models, and the detection of changes in vibration characteristics. Similar ambient vibration tests were conducted on the Fatih Sultan Mehmet Bridge (e.g. Brownjohn *et al.*,1990; Brownjohn *et al.*,1992; Apaydin and Erdik, 2001; Apaydin, 2002; Kaya and Harmandar, 2004; Erdik and Apaydin, 2005). In particular, Brownjohn *et al.* (1992) outlined, performing a direct comparison with theoretical results provided by Dumanoglu *et al.* (1992), the importance of the experimental validation of such mathematical modeling. In fact, these authors showed that the theoretical study was able to predict correctly the modes of vibration in the frequency range below 1 Hz, but an increasing divergence for increasing frequencies was observed.

Thanks to the versatility of the developed system, using a network of 24 WSUs, it has been possible to perform contemporary recordings of the ambient vibrations at the different structural elements of the Fatih Sultan Mehmet Suspension Bridge (i.e. with instruments installed both along the two side of the deck, on top of the four towers, and at the base of the two vertical cables in the middle of the bridge).

Then, from the analysis of the data-set collected, it is shown that the WSUs provide robust and reliable estimates concerning the main modal properties of the bridge, and that these latter are in remarkable agreement with the results of Brownjohn *et al.* (1992), and Erdik and Apaydin (2005).

3.2 HARDWARE

The WSU consists of three main parts: the sensors, the digitizer board, and the wireless router applications platform (WRAP-board). All components are bought off-the-shelf, with the exception of the digitizer board's Analogue-Digital Converters (ADC), which have been developed within GFZ, making to them much cheaper than standard seismometers (about 600,00 Euro per unit). Figure (3.1) provides a view of the main components of a WSU, with some technical details listed in Table 3.1.

The sensors incorporated into the WSU include accelerometers arranged to provide three component data, and an additional sensor to measure some environmental parameter, such as anemometers, humidity, strain gauges, temperature etc. The accelerometers are based on MEMS (Micro Electro Mechanical Systems), originally designed to serve as controllers for air bag safety units, but have also been successfully incorporated into various seismic networks (e.g. Holland, 2003), as well as for field acquisition by the exploration sector (Hons *et al.*, 2008). The units used in the WSUs have a measurement range of +/- 1.7 g, with a bandwidth of 25 Hz and a noise-level of 0.5 mg.

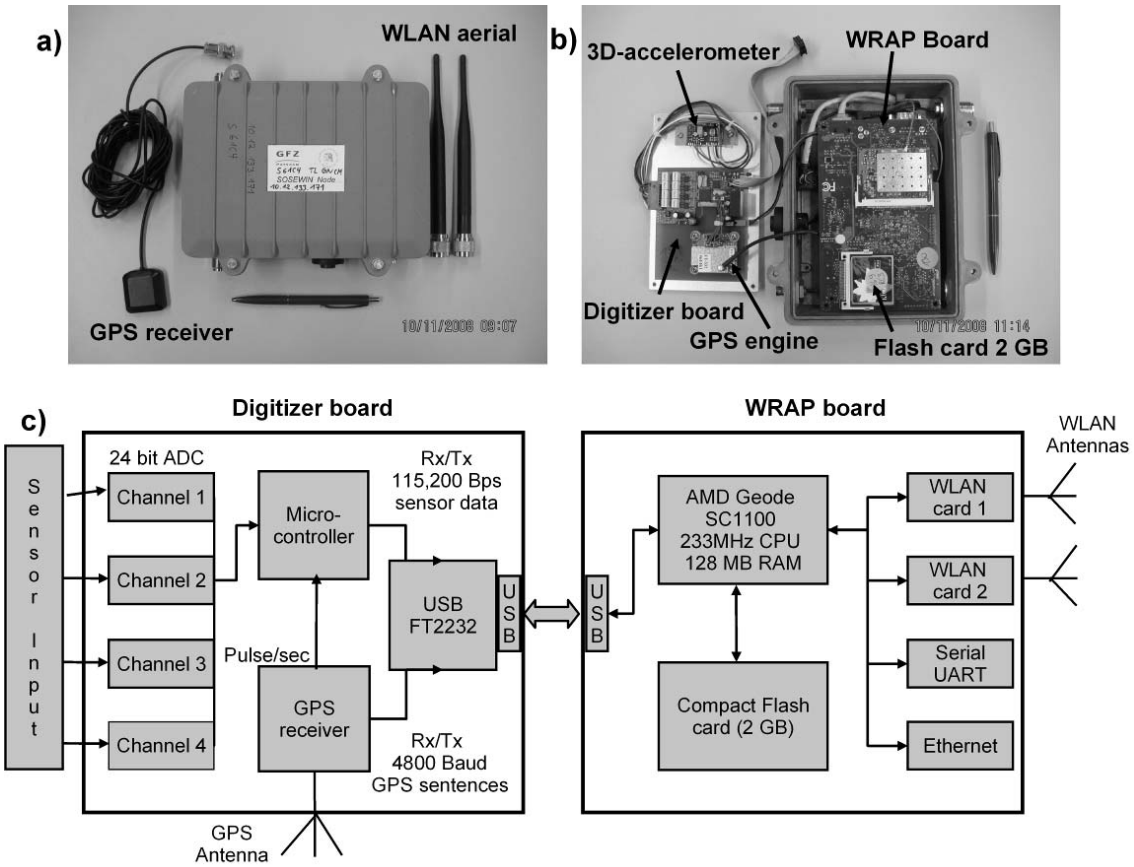

Figure 3.1: The prototype Wireless Sensing Unit (WSU): (a) the complete unit and (b) an internal view. (c) A schematic overview of the architecture of the WSU. Technical details of its various components are listed in Table 3.1.

The digitizer board consists of four ADCs, a GPS unit that provides time and geographical coordinates, and a USB interface (Figure 3.1). The ADCs have a resolution of 24 bits (effectively 19 bits), with sampling variable between 50 to 400 samples per second (sps), although at present 100 sps is being used. The USB chip combines the readings from the ADC units and the GPS device and sends them in two streams (one for the sensor data, one for the GPS) to the WRAP board. While ideally all WSUs should have the GPS signal, some may not be able to use it, for example those installed inside a building or other structure.

Accelerometers (MEMS ADXL203 chip)	
Bandwidth	25 Hz (up to 2.5 kHz)
Sensitivity	1 V/g
Measurement range	+/- 1.7 g
Output noise	0.5 mg (rms) @20 Hz
Digitizer board	
Number of channels	4
AD converter resolution/effective resolution	24/19 bits
Input voltage range	+/- 5V
Input impedance	50 kΩ
Bit weight	0.6 μV
Sample rate	50 to 400 sps, standard is 100 sps
Signal bandwidth (-3dB)	20 Hz
Stop bandwidth attenuation	>80dB @ 80 Hz or higher
Analogue anti-alias filter	2nd order 30 Hz low-pass Butterworth
Timing	GPS NMEA messages and PPS
Timing accuracy	+/- 5 msec @ 100 sps
Digital output	USB (2x virtual com-port, 115 kBaud data/4800 baud GPS)
Temperature range	-20° to +70°C
Power supply	+5V (USB) or 9 to 18 V (on board DC/DC converter)
Power consumption	50 mA @ 5V plus 70MA @ 5 V for the GPS module
WRAP board	
CPU	266 MHz AMD Geode SC1100 (486er core)
DRAM (dynamic random access memory)	128 MB SDRAM (synchronous dynamic random access memory)
Operating system	
Storage	CompactFlash card, currently 1 GB
Power consumption	3 to 5 W @ 12 V DC (excluding miniPCI cards)
Safety features	Watchdog timer built into the CPU, LM77 thermal monitors
User interface	3 front leds, console I/O redirected to serial port
Possible expansions	LPC bus for adding more serial ports, ISA style I/O, GPIO and I^2C bus
Connectivity	1 Ethernet channel (National DP83816), 2 miniPCI slots, 1 serial port
BIOS	tinyBIOS version 1.11

Table 3.1: Technical specifications of the various components that make up the Wireless Sensing Unit.

Hence, in order to guarantee the full performance of all WSUs, procedures have been planned to cover the situation of a WSU without GPS timing, but able to synchronize itself with a WSU which has this feature.

The WRAP board (PC Engines, 2008) has the three roles of analysis, communication, and storage of data (Figure 3.1). It is made up of an embedded PC (i.e. a 233 MHz

AMD Geode x86 CPU, 128 MB RAM) that uses a Compact Flash card (currently 2 GBytes, but can be easily increased) as a hard disk. Moreover, the WRAP board is equipped with two positions for WLAN Mini PCI cards (i.e. Routerboard R52 wireless 802.11a/b/g, 2.4 and 5GHz combo cards that use the Atheros AR5414 chipset, MikroTik, 2008), a power supply plug, a serial port and 100 MBit/s Ethernet.

The software operating on the WSU currently consists of the following:

- OpenWRT: The operating system for the WRAP boards (OpenWrt, 2007) with Linux kernel 2.6.22 (Torvalds, 2007). OpenWRT is an open-source freely available having a highly configurable distribution. By default, it contains only the minimum that is required to run Linux, so it can also run on very size-limited systems. Moreover, it provides an environment for building your own Linux distribution for several platforms, including our x86er target platform for the WRAP boards.
- Data-provider: The program that handles the data streams from the digitizer board, and then archives them via SeisComP/SeedLink.
- SeisComP/SeedLink: A software package and concept for near real time seismic data distribution, (http://geofon.gfz-potsdam.de/geofon//seiscomp/seedlink.html) developed by the GFZ. SeedLink protocol is based on TCP (Heinloo, 2000) and data are sent in the form of 512-byte Mini-SEED packets with a 8-byte SeedLink header. The header contains the packet sequence number, which allows the unit to resume transmission where it left off (i.e. the recovering of the connection in the event of network errors, and the support of non-permanent connections as the “dialup mode”). It has a client-server architecture and is capable of many possible tasks (data acquisition, data recording, monitoring and controlling, real-time communications, user access, near-real-time data processing). In the WSU, the SeedLink server stores the data in a ring buffer of configurable size on the Compact Flash card, which currently is 2GB. The data in the ring buffer will be kept for the order of 20 days. If more storage is found to be necessary, a larger Compact Flash card can be simply used.
- Optimized Link State Routing (OLSR, 2004): OLSR is a table-driven pro-active routing protocol currently chosen for the wireless mesh network (http://www.olsr.org). As a proactive protocol, it periodically assesses and maintains the network topology by flooding information about its direct neighborhood throughout the whole network. OLSR has proven to be capable of running with hundreds of nodes, and it is also widely accepted by several mesh networking communities, i.e. Freifunk (http://www.freifunk.net) and the Funkfeuer (http://www.funkfeuer.at) projects.

Additional secondary software is MadWifi version 0.9.3 (MadWifi, 2007) as WiFi driver. MadWifi's regdomain setting was changed to the ETSI domain in order to obtain 13 channels for 802.11b/g. The packet generation and capturing was done with the Click Modular Router software version 1.5 (Kohler, 2006).

All boards were installed in waterproof outdoor metal cases. Omni-directional dual-band antennas with a gain of 5 dB were mounted with opposite vertical polarization.

The amount of power required by a WSU when all operational activities are fulfilled (recording and real-time communication of data) has been experimentally measured to be about 4 W.

3.3 REAL-TIME PROCESSING

Since for structural monitoring applications portable batteries are usually the preferred power source, wireless monitoring system must be designed with special attention in the optimization of their power consumption. The work of Lynch *et al.* (2003) showed that computational power must be distributed throughout the network in order to preserve battery lifespan. They showed that a high system energy efficiency can be obtained, saving 98% of energy, when local data analysis is performed (e.g. by a fast Fourier transform, FFT) and only the transmission of modal frequencies is performed instead of the whole time-history.

Following Lynch *et al.* (2003), and considering that WSUs include low-cost components, the general scheme of the real-time processing designed for a WSU within the framework of structure monitoring involves a local, relatively simple, rapid, and robust analysis of data suitable for real-time processing (Figure 3.2). This involve, first filtering the accelerometer data using a 4^{th} order band-pass (i.e. selected for the bridge experiment to be 0.01 – 3 Hz) IIR Butterworth filter, followed by its integration to velocity and displacement using the recursive formulation of Kanamori *et al.* (1999). In the meantime, raw accelerometric data are continuously stored in the ring buffer.

For the long-term monitoring of structural modal properties, the Cooley-Tukey version of the FFT (Press *et al.*, 1992) is applied to the signals. Thus, the main frequency peaks for the three components of motion can be continuously extracted using an approach based on pattern recognition, and can be communicated through the other nodes towards a final target by a gateway (Figure 3.2).

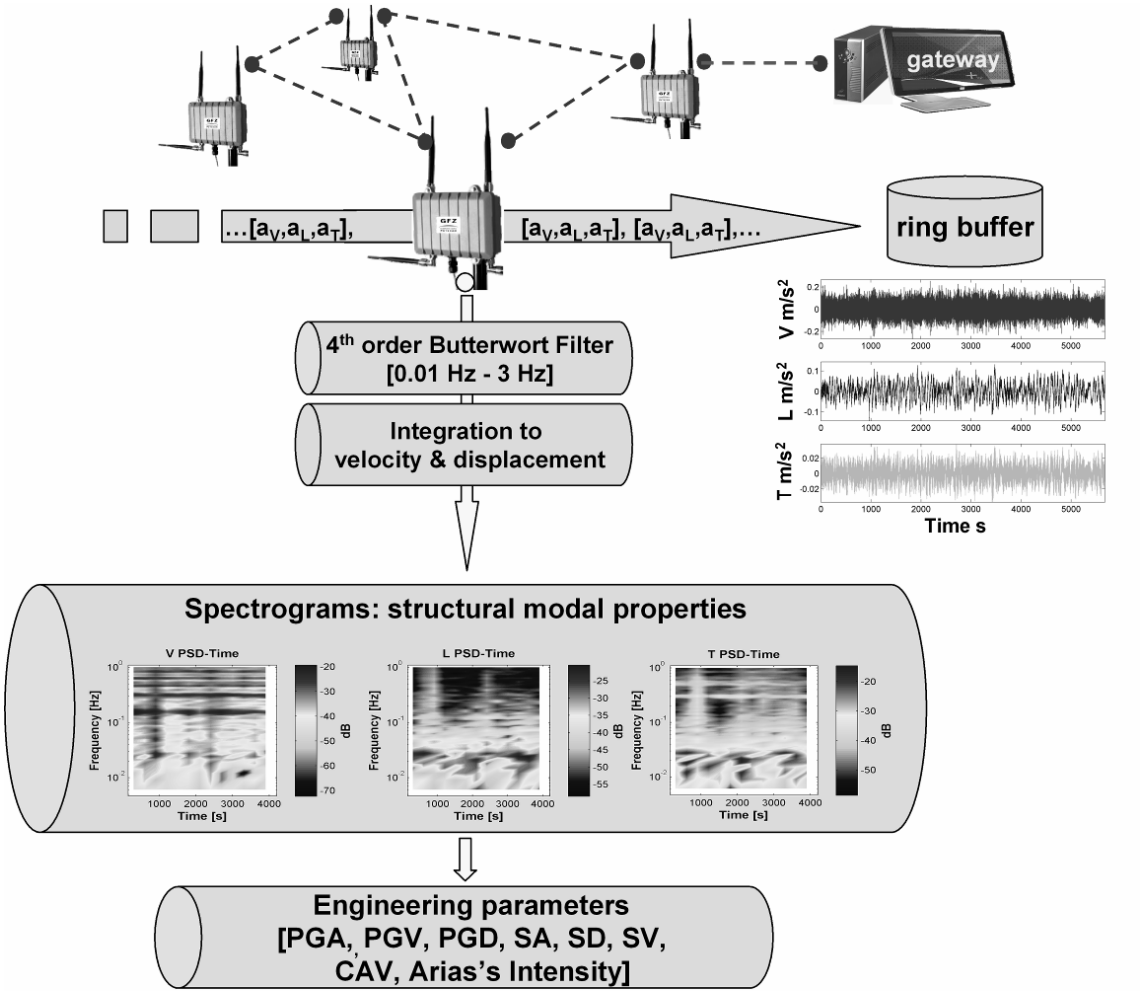

Figure 3.2: The general scheme followed for the seismological processing and analysis that has been incorporated into the wireless sensing units.

On the other hand, since WSUs are being developed for earthquake early warning purposes in the SAFER and EDIM projects, they are designed also to carry out analysis for earthquake detection and characterization (i.e. estimation of several engineering parameters). Of course, these analyses are also useful for earthquake early warning and rapid response systems within buildings and other structures. The sequence of the processing undertaken by the WSU is described in detail in Fleming *et al.* (2009). In brief, the event detection is performed on the vertical ground motion component by a recursive short-term average/long-term average (STA/LTA) trigger algorithm (Schweitzer *et al.*, 2002). The event characterization is done by continuously updating the maximum ground motion parameters (PGA, PGV, and PGD). In addition, other parameters of engineering interest as the cumulative absolute velocity (CAV, Böse, 2006) and the Arias Intensity (Arias, 1970) are calculated. At the end of the main ground motion, a final event-report is delivered by each WSU containing the peak

ground values (PGA, PGV, and PGD) detected as well as the response spectra acceleration, velocity, and displacement for some representative periods (e.g. those of the main modes of vibration estimated by modeling). Finally, this information is delivered by files in a format appropriate for the USGS tool ShakeMap (Wald *et al.*, 2006).

3.4 COMMUNICATION

The communication of information is based on the routing concept. The term routing means the selection within a network of paths along which data can be sent from a source to a sink. In wireless communications, routing activities are made more complicated by the fact that all nodes act contemporarily as sources, sink and routers of data. WSUs are designed to form a self-organizing ad-hoc wireless mesh network (WMN), and rely on the OLSR (Optimized Link State Routing) as routing strategy (see above for the OLSR description). The use of WMN protocols allows a network of WSUs to continuously adapt to changing circumstances (addition or removal of nodes, interference in communications, loss of part of the network following an earthquake etc.) in order to maintain optimal communications.

Structural modal parameters and event-reports (i.e. few bytes of information) and, under request, accelerometric data (i.e. 512-byte Mini-SEED packets) are transferred following the SeedLink protocol up to 54 Mbps in both the 2.4 GHz and 5 GHz unlicensed bands. In the case of a low signal-to-noise ratio in the communication, the WLAN cards driver can automatically decrease the rate of transmission.

3.5 FEATURES OF THE AMBIENT MONITORING TEST PERFORMED ON THE FATIH SULTAN MEHMET SUSPENSION BRIDGE AND STATE OF THE ART

The Fatih Mehmet Sultan Bridge is the second suspension bridge across the Bosporus strait in Istanbul, Turkey (Figure 3.3a), spanning the strait between Hisarüstü (European Side) and Kavacık (Asian Side).

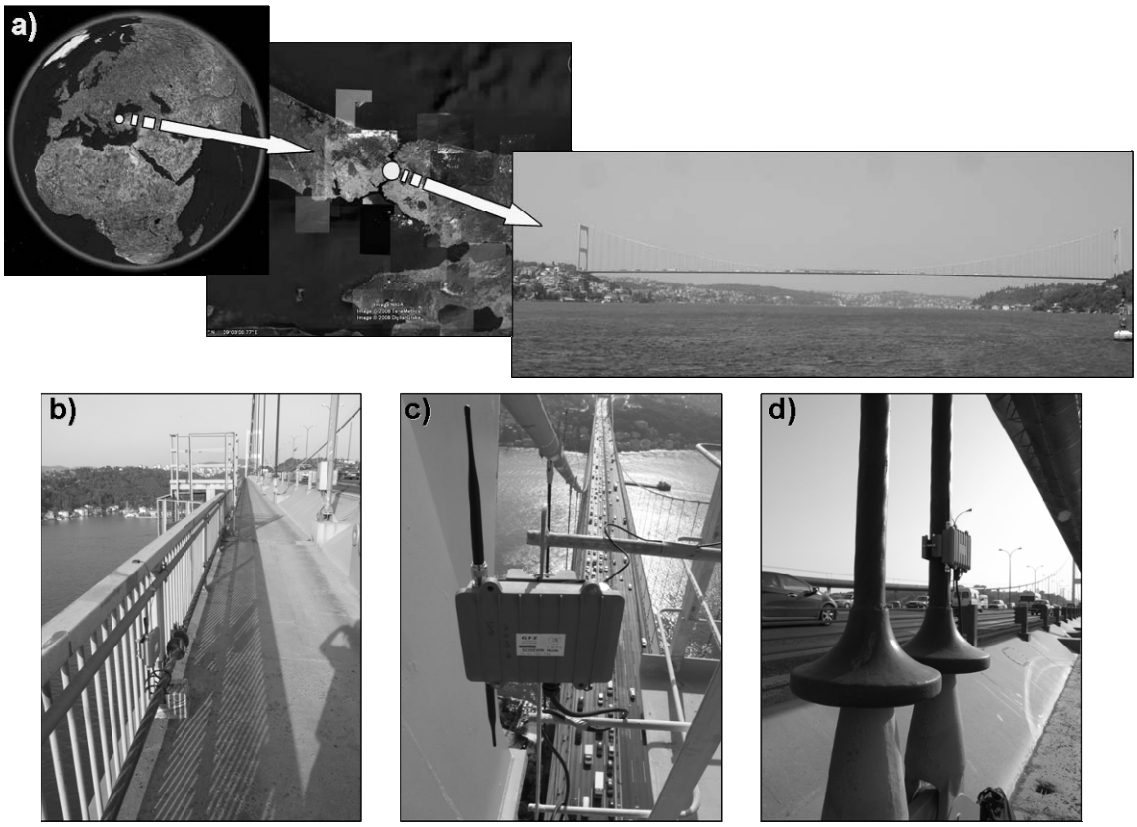

Figure 3.3: (a) Location map of the Fatih Sultan Mehmet Bridge in Istanbul, Turkey. (b), (c), and (d) examples of some types of sensor installation during the test measurements in June 2008.

The Bridge was designed by Freeman Fox & Partners at a cost of USD 130 million as part of a major program involving the construction of a second highway around Istanbul, carrying two four-line highways. From the structural point of view, it is a gravity-anchored suspension bridge with no side spans and with steel pylons and double vertical hangers. It is characterized by a box girder deck, 39·4 m wide overall, and 1090 m long (World rank 11th), and steel towers rising 110 m above ground level (Figure 3.4a). Table 3.2 provides a summary of the structural characteristics of the bridge.

Other details of both the structural characteristics and the mathematical modeling, and estimates of the modes of the bridge can be found in Dumanoglu *et al.* (1986, 1992). The main conclusions of this work can be summarized as follows: (1) even though the bridge is located in a seismic area, wind is likely to be the bigger threat for its stability; (2) the towers are the most vulnerable components, with the largest bending stress related to the lateral and longitudinal excitation; and (3) the strongest asynchronous effects are estimated to occur both for the vertical deck displacement due to longitudinal

anti-phase motion of the towers, and for the bending moments of the towers themselves for longitudinal and vertical excitation.

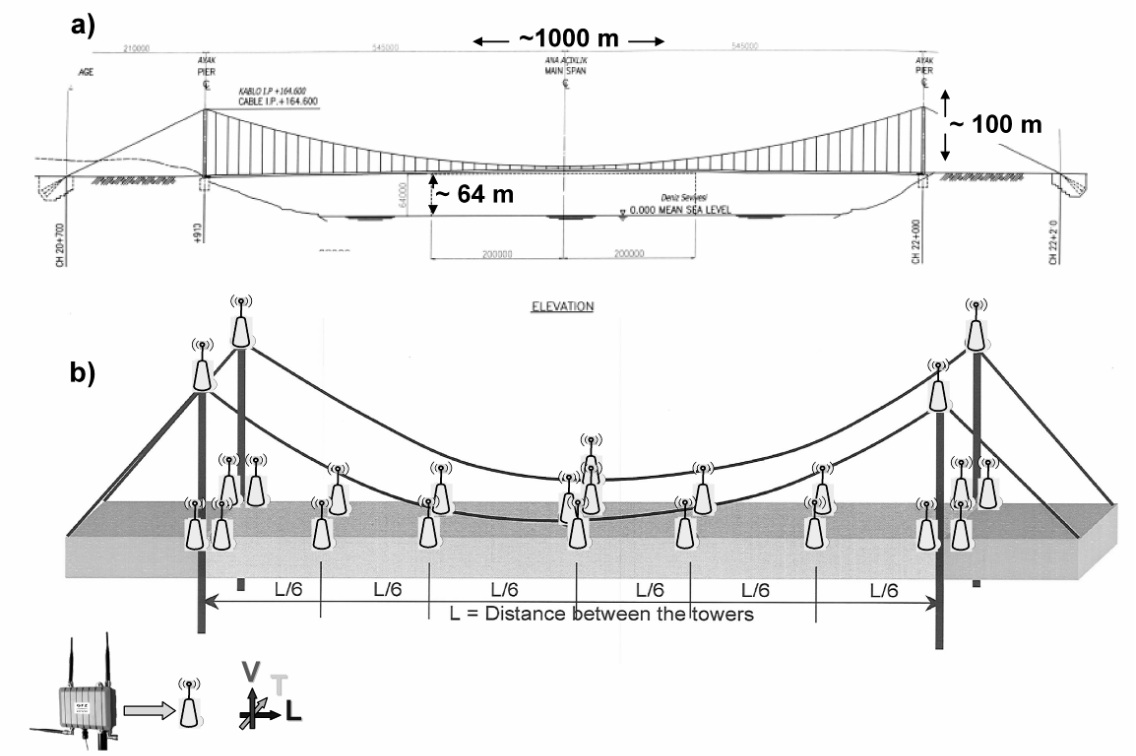

Figure 3.4: (a) General characteristics of the Fatih Sultan Mehmet Bridge (from Dumanoglu et al., 1992). (b) Measurement positions, and motion convention: vertical (V), longitudinal (L), and transversal (T) components.

Among other theoretical studies of the bridge that have been carried out, Apaydin (2002) provided a comprehensive assessment of the response of the Fatih Sultan Mehmet Suspension Bridge under excitation due to spatially varying (asynchronous and/or travelling) ground motion. Moreover, the Japanese Bridge and Structure Institute (JBSI, 2004) performed an earthquake response and performance analysis of the bridge for the General Directorate of State Highways (Turkey) to determine the seismic vulnerability, retrofitting requirements, as well as to gain an understanding of the dynamic seismic behaviour of the bridge. These studies showed that finite element analysis techniques can be used satisfactorily for the analytical assessment of the expected mode shapes, frequencies and the participation factors.

Span	Main Span 1090 m
Deck Width	33.8 m (39.4m total)
Substructure	2 Steel Towers (107m)
	2 Anchorages
	Spread Foundation
Dead Load per Unit Length	216 kN/m
Area per Cable	0.365 m2
Gross x-sectional area	1.26m2
Deck Moment of Inertia	Ixx=1.73 m4
	Iyy=129.2 m4
	Torsional=4.7 m4
Modulus of Elasticity of Cables	205 kN/mm2
Sag	91m + 6.3m
Hanger Geometry	Vertical (Double)
Clearance from the sea level	64m

Table 3.2: Structural characteristics of the Fatih Sultan Mehmet Suspension Bridge.

Erdik and Apaydin (2005) provided some general results on the dynamic characteristics and earthquake response of suspension bridges. Their findings can be summarized as follows: suspension bridges are complex 3-D structures that can exhibit a large number of closely spaced coupled modes of vibration; for suspension bridges exposed to strong earthquake-induced ground motions, significant changes in the initial bridge geometry will result in geometric nonlinearities as the stiffness of the suspension cables and deck system change appreciably with large displacements of the structure; theoretical analysis of the free vibration of suspension bridges indicates that the modes of the structure can be divided into three groups with respect to the dominance of the respective displacements (i.e. in the first group 'Deck Modes' are important, in the second one 'Cable Modes' are important, and in the third group 'Tower Modes' dominate); the deck modes can also be classified as symmetric and asymmetric or as lateral, vertical and torsionally dominant.

Concerning full scale dynamic studies made on the Fatih Sultan Mehmet Suspension Bridge, Brownjohn *et al.* (1992) performed an ambient vibration survey in order to determine experimentally the modal properties of the bridge in terms of its natural frequencies, and to verify the reliability of the eigensolutions obtained from the mathematical models of Dumanoglu *et al.* (1986, 1992). The equipment of Brownjohn *et al.* (1992) for the survey of the bridge consisted of five accelerometers. Therefore, using as reference an accelerometer in the European side of the bridge, 27 single

measurements were carried out at strategic points throughout the deck and a tower, covering a timeframe from the 6th to the 15th of June 1989.

Results of this experimental work indicate that the measured vertical natural frequencies and mode shapes matched fairly well the predicted values from the modeling in the lower frequency range, while an increasing divergence was observed for increasing frequencies. The experimental modal frequencies of vibration provided by Brownjohn *et al.* (1992) (the first five deck vertical, torsional and lateral modes are listed in Table 3.2 as an example), were recently confirmed by Apaydin (2002), and Erdik and Apaydin (2005).

Another study of the Fatih Sultan Mehmet Suspension Bridges was an evaluation of its response to strong wind (Kaya and Harmandar, 2004). This study relied on three accelerometers deployed on the two sides and at the center of the bridge, respectively. The findings in terms of peaks in the spectra were in good agreement with the modal frequencies of vibration, and peak accelerations, velocities and displacements reached respectively the values of 0.1g, 0.1m/s and 0.2m in the horizontal and 0.6g, 0.2m/s and 0.3m in the vertical direction (Kaya and Harmandar, 2004).

Finally, the bridge is also well-equipped by a traditional vibration monitoring system encompassing 12 tri-axial acceleration transducers and a data acquisition unit installed along the Asian half span of the Fatih Sultan Mehmet Suspension Bridge (Apaydin and Erdik, 2001; Apaydin, 2002).

3.6 AMBIENT VIBRATION MEASUREMENTS

This wealth of information makes the Fatih Sultan Mehmet bridge a site particularly suitable for testing the reliability of this innovative WSU instruments. Therefore, on the 27th of June 2008, 24 sensors were used to perform ambient vibration measurements at the bridge. The acquisition scheme (Figure 3.4b) consisted in the installation of 4 reference sensors placed outside the bridge deck, 8 sensors along each side, 2 sensors on the lowest part of the vertical cable at the midpoint of the bridge, and 4 sensors on top of the bridge towers. All the sensors were installed following the same spatial arrangement, in order to detect the bridge vibrations on the vertical (V), the longitudinal (L), and the transversal (T) components. With a crew of 4 workers, both the installation and removal of all station required about 1 hour. Figure (3.3b, c, and d) shows examples of these installations. The test was performed for a few hours, and about 1-½ hours of contemporary recordings at all sensors are available. The sampling rate was fixed to 100

samples/sec, and the energy required by the WSU was provided by 17 Ah lithium-based batteries.

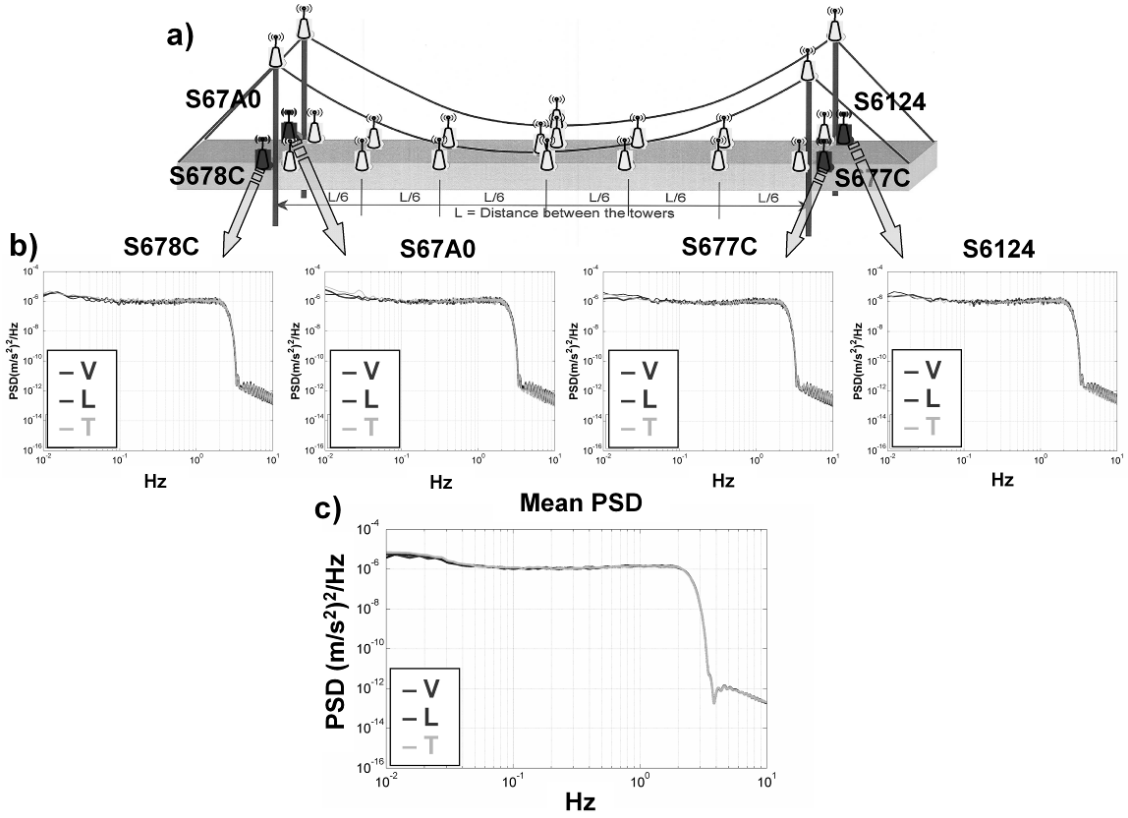

Figure 3.5: (a) Reference measurement positions (red symbols). (b) Power Spectrum Density (PSD) functions for the three components of motion: vertical (V - red), longitudinal (L - blue), and transversal (T - green), respectively. (c) Same as (b), but mean of the PSD functions.

Although each WSU is able to perform its own local signal analysis, the purpose of this work is the evaluation of the WSU performance for structural monitoring. Hence, the results discussed in the following refer to post-survey analysis.

Figure (3.5) shows the Power Spectrum Density (PSD) functions computed for the 3 components of motion at the 4 reference sensors located outside the bridge deck, and their average.

The PSDs were computed using non-consecutive signal windows 200 s wide; this width is suitable for the frequency range of interest and guarantees a sufficient frequency resolution.

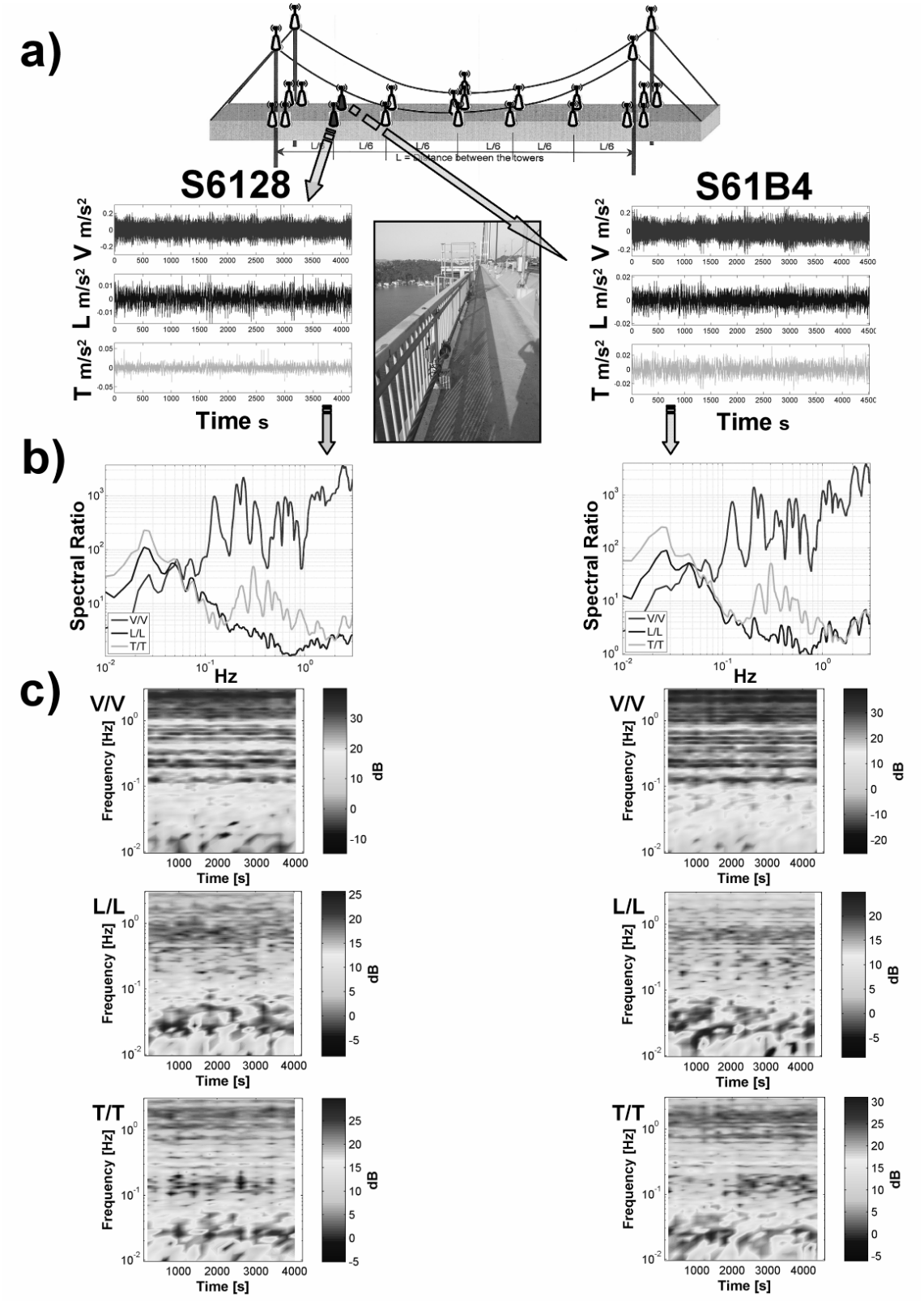

Figure 3.6: Results for two WSUs placed at the bridge's deck. (a) Selected sensors (red symbols), time series, and example of installation. (b) Spectral Ratio (SR) functions for the vertical (red), longitudinal (blue), and transversal (green) components of motion. (c) SR spectrograms for the different components of motion.

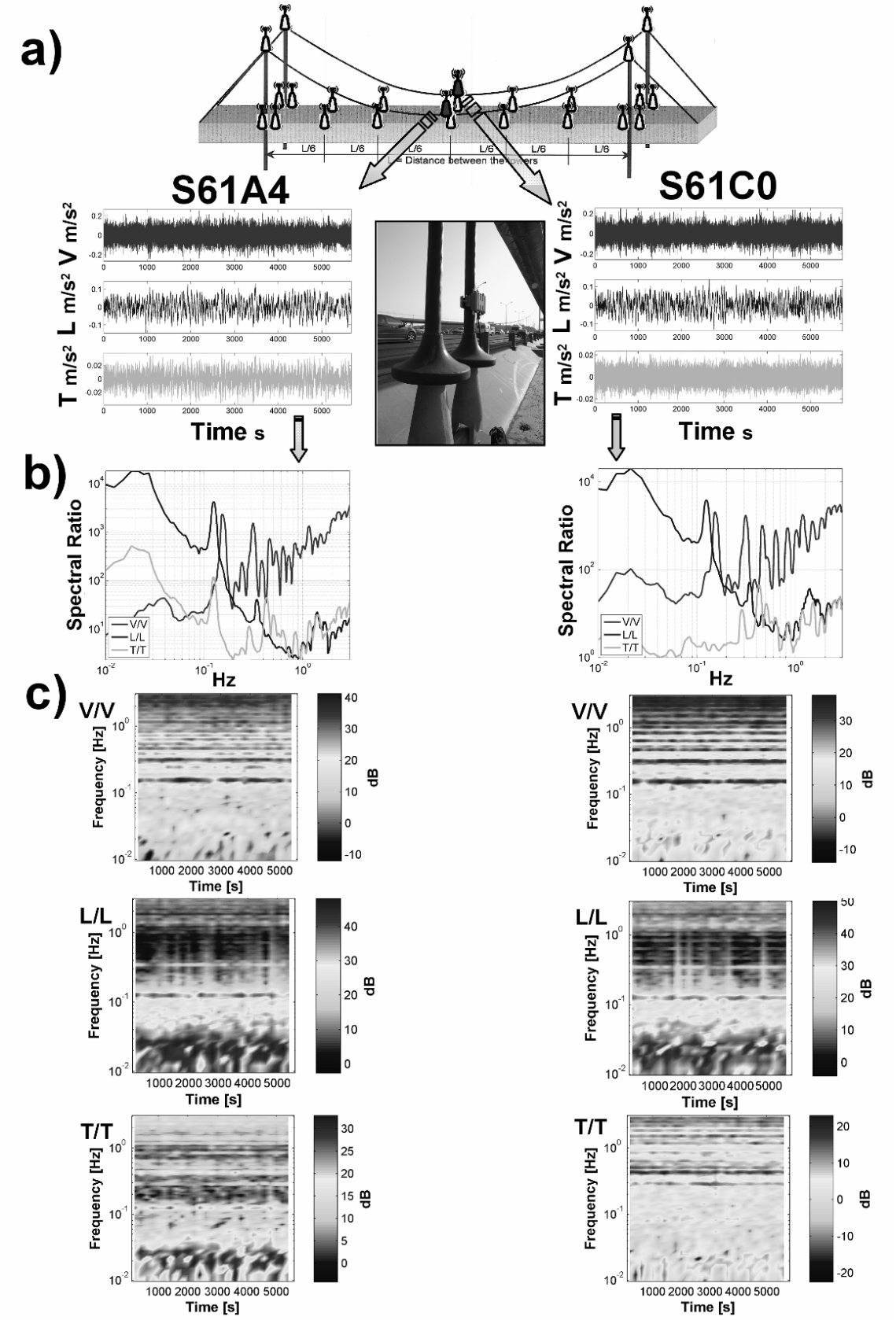

Figure 3.7: Same as Figure 3.6, but for WSUs placed at the lowest part of the vertical cables in the middle of the bridge's deck.

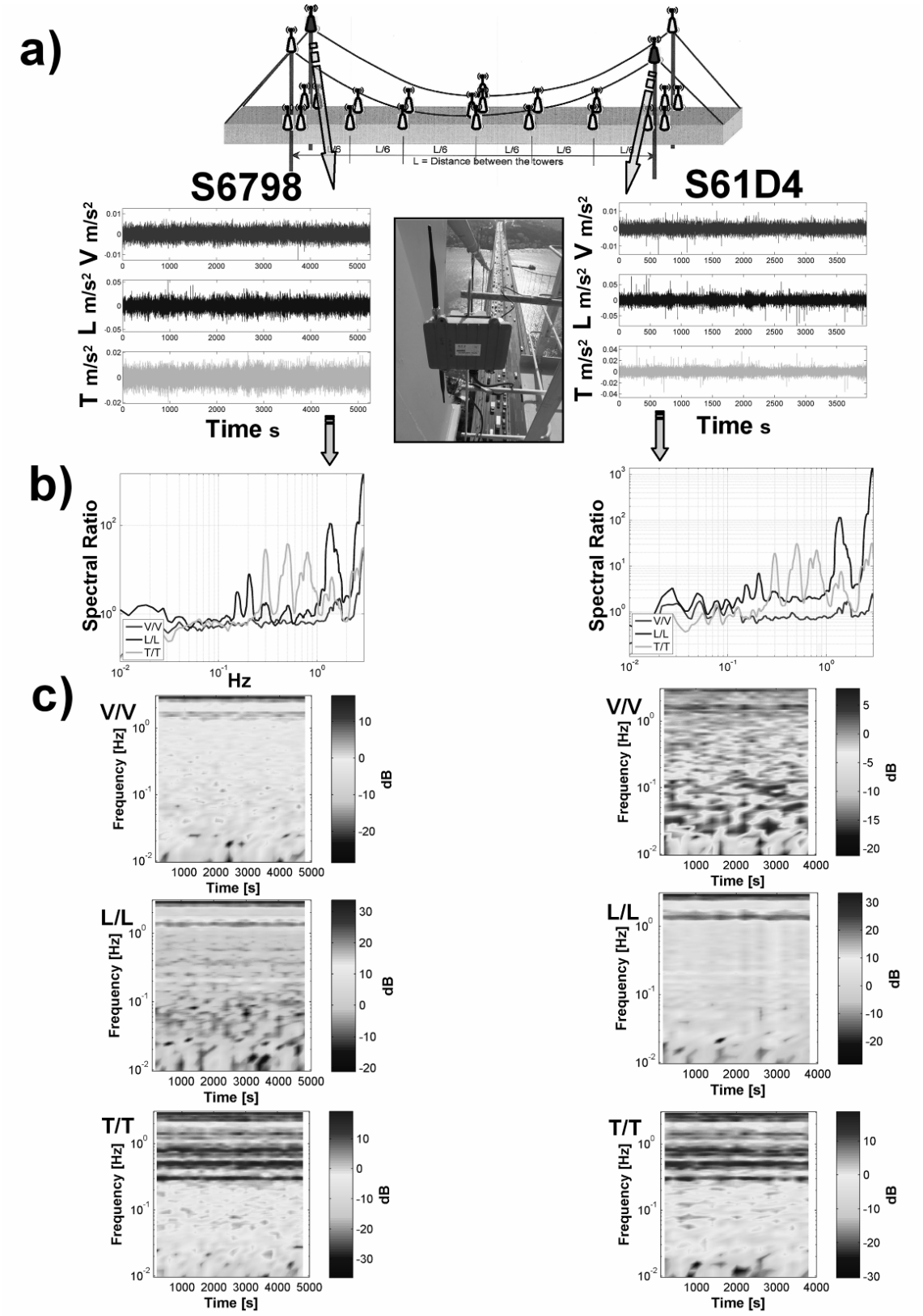

Figure 3.8: Same as Figure 3.6, but for WSUs placed on top of the bridge's towers.

Vertical	[Hz]	Lateral	[Hz]	Torsional	[Hz]
1 asym.	0.125	1	0.77	1 sym.	0.296
2 sym.	0.155	2	0.239	2 asym.	0.352
3 sym.	0.208	3	0.25	3 sym.	0.529
4 asym.	0.244	4	0.287	4 asym.	0.692
5 sym.	0.317	5	0.315	5 sym.	0.867

Table 3.3: First five experimental frequency of the vertical, lateral and torsional, symmetrical and asymmetrical, deck modes, respectively (from Brownjohn et al., 1992).

	V/V peaks [Hz]	T/T peaks [Hz]	L/L peaks [Hz]
A	0.122	0.076	0.204
B	0.152	0.22	0.247
C	0.207	0.302	0.311
D	0.241	0.43	0.387
E	0.314	0.5	0.467

Table 3.4: First five experimental SR peaks selected for the vertical (V/V), transversal (T/T), and longitudinal (L/L) directions.

Before computing the cross-correlations, the linear trend was removed from each window and a 5% cosine-taper was applied at both ends. This scheme of analysis for the computation of PSDs was adopted for all WSUs. The average PSD curves from the reference stations were used for the computation of Spectral Ratio (SR) functions for both the vertical, transversal and longitudinal directions with respect to all the other 20 monitored points inside the bridge.

Figure 3.6, 3.7, and 3.8 provide an overview of SR results for a couple of WSUs installed at some characteristic locations on the bridge (i.e. the deck, the vertical cable, and the towers, respectively). When comparing the average SR curves (Figures 3.6b, 3.7b, and 3.8b) for pairs of sensors installed at different points, it is clear that WSUs provide consistent, robust results, with a clear image of how the diverse parts of the bridge react differently to ambient vibrations. Moreover, SR spectrograms (Figures 3.6c, 3.7c, and 3.8c) show that ambient vibrations have a stationary character and indicate that WSUs provide very stable estimates.

Results for WSUs located on the deck (Figure 3.6, Table 3.4) indicate that the highest amplitude vibrations occur on the vertical component, and the SRs provide

experimental vertical modes of vibration estimates (e.g. 0.122 Hz, 0.207 Hz) that match very well those obtained by Brownjohn *et al.* (1992) as reported in Table 3.3.

In the case of WSUs located at the base of the vertical cable (Figure 3.7), the first mode of vibration for the vertical component is at 0.15 Hz. The SRs show the coincidence in frequency of the first peak in the longitudinal and transversal directions (i.e. 0.125 Hz), although they differ in amplitude by about 2 order of magnitude. Finally, WSUs located on top of the towers (Figure 3.8) indicate that, again in agreement with Brownjohn *et al.* (1992), the first two longitudinal vibration modes are at 0.155 Hz and 0.2 Hz, while the lateral modes are at 0.3 Hz, 0.5 Hz, and 0.8 Hz.

Figure (3.9) compares SR curves computed for WSUs placed at different location on the deck. The first five experimental SR peaks selected for each direction are listed in Table 3.4. It is worth stressing the consistency in frequency of peaks estimated at different points, while, as expected, the amplitudes of the peaks are dependent on the sensor location. In the case of the vertical component (Figure 3.9a), several modes of vibration can be identified, and the amplitude versus frequency path is rather irregular. On the other hand, for both the transversal and longitudinal components (Figure 3.9b, and c, respectively) the location and amplitude of the peaks follow a quite regular path with the increasing of frequencies. Although a detailed analysis of the dynamic behavior of the bridge is beyond the scope of this study, due to the preliminary character of the analysis being carried out at this stage and the limited extension in time of the data-set, the coincidence in frequency of peaks for both the vertical and transversal components of motion at about 0.3 Hz is a strong indication that this is the first torsional deck mode. Finally, the results obtained by the ambient vibration monitoring of the bridge using the new WSUs (e.g. in Table 3.3) are in excellent agreement with those obtained by previous studies (e.g. Brownjohn *et al.*, 1992; Table 3.4; and Apaydin, 2002).

3.7 DISCUSSION

New low-cost wireless sensing unit designed to form dense wireless mesh networks has been presented. The main advantages of this approach are that the analysis and storage of data can be decentralized, while only the most significant information and estimated parameters are spread through the whole network towards dedicated targets.

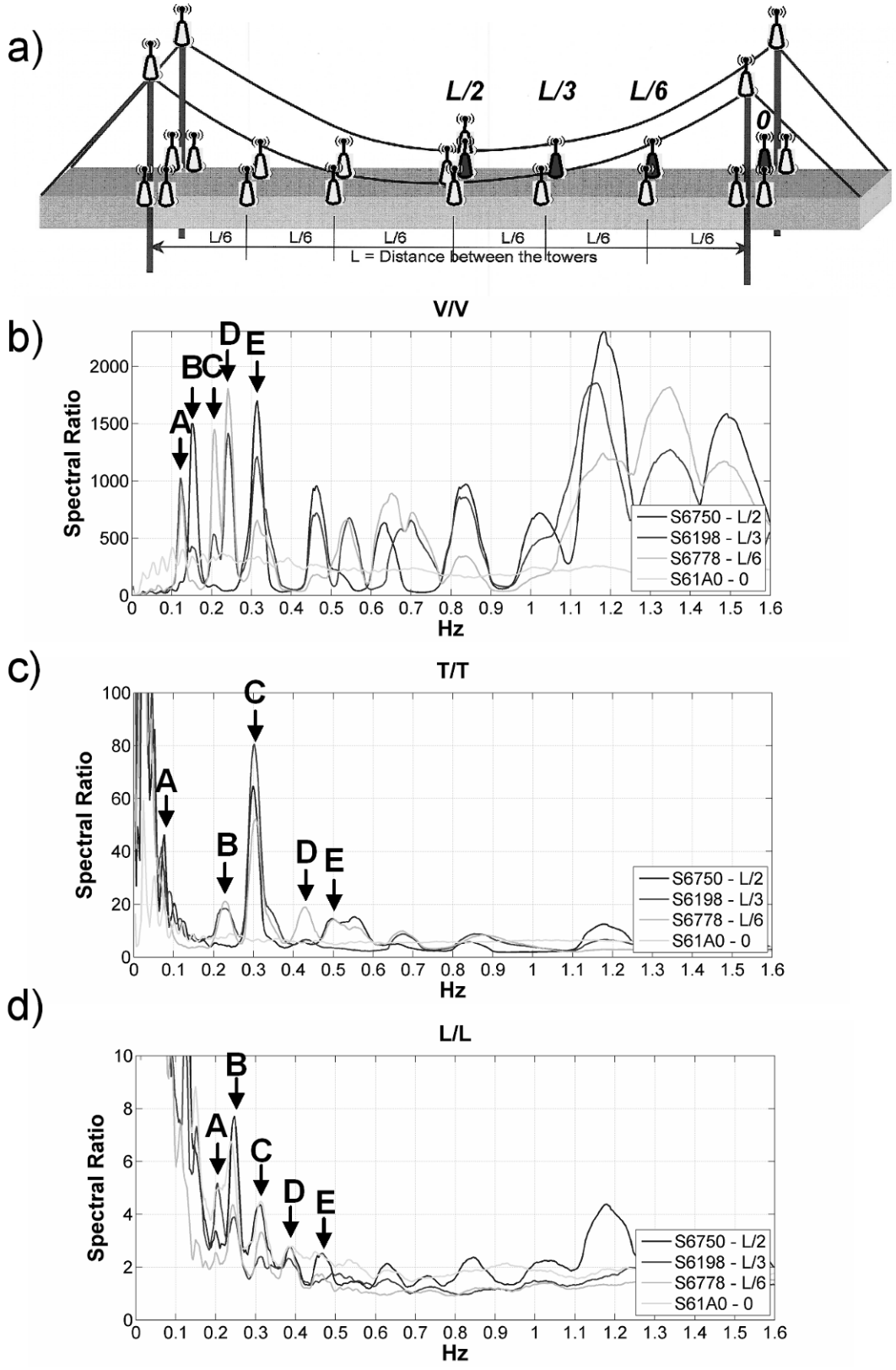

Figure 3.9: SR results for some characteristic points along the bridge's deck. (a) Selected stations (red symbols). (b) Aggregate SR functions for the vertical component. (c) Same as (b) but for the transversal component. (d) Same as (b) but for the longitudinal component. The selected SR peaks for each of the three components of motion (black arrow) are listed on Table 3.3.

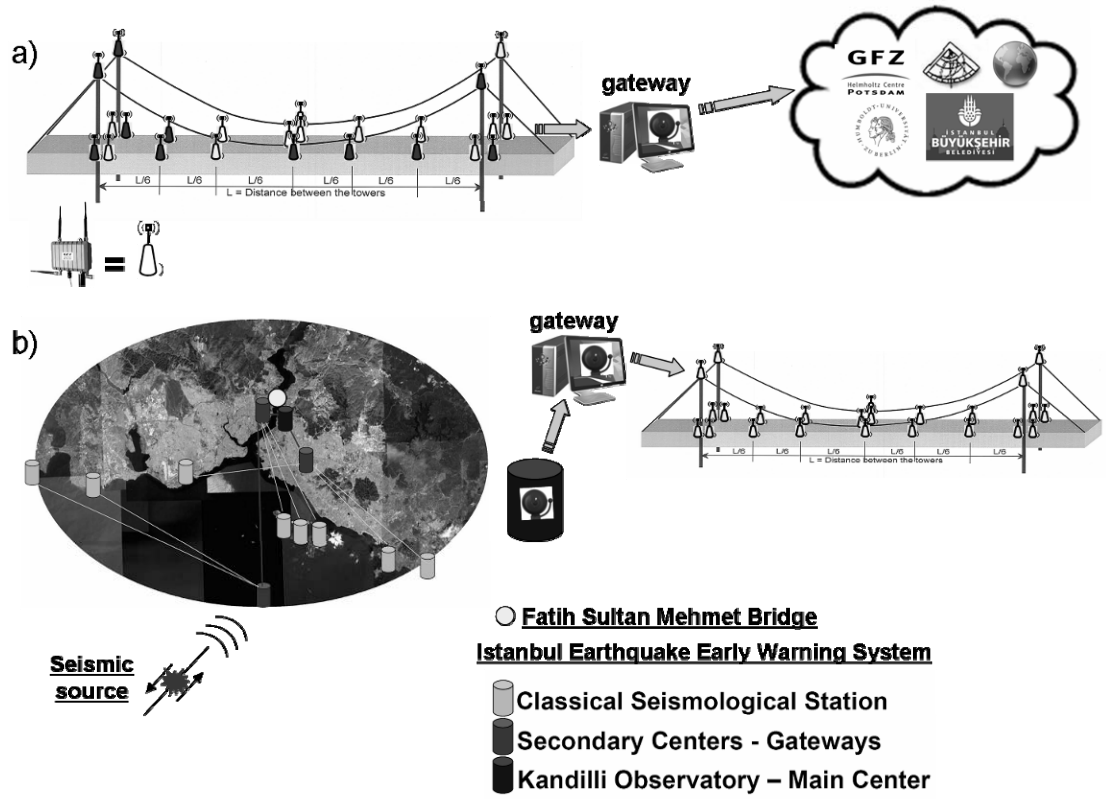

Figure 3.10: The possible double way early warning for the Fatih Sultan Mehmet bridge. (a) The warning can be issued by a gateway from the bridge in the case WSUs detect anomalous bridge behavior. (b) The wireless network can receive earthquake early warnings from the IERREWS operated by KOERI.

While the instrumentation and network communication protocols have been developed within the framework of two earthquake early warning projects, this study has been carried out to show that they can also represent a valuable tool for innovative, dense, wireless structural monitoring systems.

An experiment to determine the suitability of such a system for structural monitoring was conducted, involving ad-hoc ambient vibration recordings performed on the Fatih Sultan Mehmet bridge in Istanbul (Turkey). Results of data analysis indicate an excellent performance of the low-cost WSU, with the data and estimated parameters obtained from instruments placed on similar structural elements of the bridge being highly coherent. Moreover, the main modal properties of the bridge determined from the recordings were found to be consistent with those from the studies of Brownjohn *et al.* (1992) and Apaydin (2002).

The results shown in this work are not meant to provide new understanding about the dynamic behavior of the bridge, a task beyond this work due to the limited extension in time of the experiment, but they do provide a clear indication that WSUs are also

suitable for structural monitoring tasks. Therefore, the current, traditional structural health monitoring system operating on the Fatih Sultan Mehmet Suspension Bridge (Apaydin and Erdik, 2001; Apaydin 2002) could be economically extended by the low-cost WSU instruments. The next step might be the application of a dense wireless network of these instruments for a long-term, full scale, ambient vibration monitoring program of the Fatih Sultan Mehmet Suspension Bridge, which might allow the main modal properties of the bridge to be regularly re-evaluated with great detail. Furthermore, thanks to the availability in the instrument of an additional channel, extra functionality to the WSU network could be explored, allowing, for example, the long-term monitoring of the wind load on the structure.

Finally, the addition of a dense wireless network of WSUs on the Fatih Sultan Mehmet Suspension Bridge would provide an early warning capacity for the bridge itself (Figure 3.10). In fact, the WSU network could be programmed to release alarms through a gateway to some target (e.g. the Disaster Coordination Center of the Istanbul Metropolitan Municipality) in the case that anomalous bridge behaviour were detected. In the meantime, the wireless network could receive warnings from the Istanbul Earthquake Rapid Response Early Warning System (IERREWS) operated by KOERI (Erdik *et al.* 2003c) in the event of an earthquake, and thus be used to coordinate early safety actions (e.g. stopping the traffic access to the bridge).

REFERENCES

Abdel-Ghaffar, A.M., and G. W. Housner (1978). Ambient Vibration Tests of Suspension Bridges, Journal of Engineering Mechanics Division, ASCE, V.104, No.EMS, Proc. Paper 140b5, Oct. 1978, pp. 983-999.

Apaydin, N. and M.Erdik (2001). Structural Vibration Monitoring System for the Bosporus Suspension Bridges in Strong Motion Instrumentation for Civil Engineering Structures (NATO Science Series), Vol. 373, Ed.By. M.Erdik *et al.*, Springer-Verlag New York, LLC

Apaydin, N (2002). Seismic Analysis of Fatih Sultan Mehmet Suspension Bridge, Ph.D Thesis, Department of Earthquake Engineering, Bogazici University, Istanbul, Turkey

Arias, A. (1970). A measure of earthquake intensity, Seismic Design for Nuclear Power Plants, ed. R.J. Hansen, MIT Press, 438-483.

Böse, M. (2006). Earthquake early warning for Istanbul using artificial neural networks, Doctor of Natural Sciences thesis, Faculty of Physics, University of Karlsruhe, Karlsruhe.

Brownjohn, J.M.W., Dumanoglu, A.A., Severn, R.T., and Taylor, C.A. (1987). Ambient vibration measurements of the Humber suspension bridge and comparison with calculated characteristics, Proc. ICE, Pt.2, 83, 561-600.

Brownjohn, J.M.W., Dumanoglu, A.A., and Severn, R.T. (1990). Fatih Bridge Part II: ambient vibration survey, Report UBCE-EE-90-12, University of Bristol, Department of Civil Engineering.

Brownjohn, J.M.W., Dumanoglu, A.A., and Severn, R.T. (1992). Ambient vibration survey of the Fatih Sultan Mehmet (Second Bosporus) Suspension Bridge, Earthquake Engineering and Structural Dynamic, Vol. 21, 907-924.

Dumanoglu, A.A., and Severn, R.T. (1986). Asynchronous seismic analysis of modern suspension bridges part I: Free vibration, Report UBCE-EE-85-2; Part II: Response to travelling vertical ground motion, Report UBCE-EE-86-3; Part III: Response to travelling longitudinal ground motion, Report UBCE-EE-86-4; Part IV: Response to travelling lateral ground motion, Report UBCE-EE-86-5, University of Bristol, Department of Civil Engineering.

Dumanoglu, A.A., Brownjohn J.M.W., and Severn, R.T. (1992). Seismic analysis of the Fatih Sultan Mehmet (Second Bosporus) Suspension Bridge, Earthquake Engineering and Structural Dynamic, Vol. 21, 881-906.

EDIM (2007). Earthquake Disaster Information System for the Marmara Region, Turkey. http://www.cedim.de/EDIM.php. Accessed December 09, 2008.

Erdik, M and E.Uckan (1988). Ambient Vibration survey of the Bogazici Suspension Bridge, Report No: 89-5, Department of Earthquake Engineering, Bogazici University, Istanbul, Turkey

Erdik, M., Aydinoglu, N., Fahjan, Y., Sesetyan, K., Demircioglu, M., Siyahi, B., Durukal, E., Ozbey, C., Biro, Y., Akman, H., & Yuzugullu, O. (2003a). Earthquake Risk Assessment for Istanbul Metropolitan Area, Earthquake Engineering and Engineering Vibration, vol. 2, No. 1, 1-27.

Erdik M, Aydinoglu N, Fahjan Y, Sesetyan K, Demircioglu M, Siyahi B, Durukal E, Ozbey C, Biro Y, Akman H, Yuzugullu O. (2003b). Earthquake Risk Assessment for Istanbul Metropolitan Area. Earthquake Engineering and Engineering Vibration, 2, 1.

Erdik, M., Fahjan, Y., Özel, O., Alcik, H., Mert, A., & Gul, M. (2003c). Istanbul Earthquake Rapid Response and the Early Warning System, Bulletin of Earthquake Engineering, 1, 157-163.

Erdik, M., and Apaydin, N. (2005). Earthquake Response of Suspension Bridges, Vibration Problems ICOVP, Ed. By E. Inan and A. Kiris, Springer, pp.181-195.

Fleming, K., Picozzi, M., Milkereit, C., Kuehnlenz, F., Lichtblau, B., Fischer, J., Zulfikar, C., Ozel, O., and the SAFER and EDIM working groups. The Self-Organising Seismic

Early Warning Information Network (SOSEWIN), accepted to be published by Seismological Research Letters.

Grosse, C. U., Finck, F., Kurz, J. H., and Reinhardt, H. W. (2004). "Monitoring techniques based on wireless AE sensors for large structures in civil engineering", in Proc. EWGAE 2004 symposium in Berlin, BB90, pp 843-856. Accessed December 09, 2008.

Heinloo, A. (2000). SeedLink design notes and configuration tips. http://geofon.gfz-potsdam.de/geofon/seiscomp/seedlink.html. Accessed December 09, 2008.

Holland, A. (2003). Earthquake data recorded by the MEMS accelerometer, Seismological Research Letters, 74(1), 20-26.

Hons, M., Stewart, R., Lawton, D. and Bertram, M. (2008). Field data comparisons of MEMS accelerometers and analog geophones, The Leading Edge, July 2008, 896-902.

Japanese Bridge and Structure Institute – JBSI (2004). Project Reports and Basic Design Documents for the project entitled "Seismic Reinforcement Of Large Scale Bridges In Istanbul", prepared for the General Directorate of State Highways (Turkey)

Kanamori, H., Maechling, P. and Hauksson, E. (1999). Continuous monitoring of ground-motion parameters, Bulletin of the Seismological Society of America, vol. 89(1), 331-316.

Kaya, Y., and Harmandar, E. (2004). Analysis of Wind Induced Vibrations on Bogazici and Fatih Sultan Mehmet suspension Bridges, Internal Report, Department of Earthquake Engineering, Bogazici University, Istanbul, Turkey

Kohler, E. (2006). The click modular router. http://www.read.cs.ucla.edu/click/. Accessed December 09, 2008.

Krüger, M., Grosse, C., and Marrón, P.J. (2005). Wireless structural health monitoring using MEMS, Key Engineering Mat., vol. 293-294, pp 625-634.

Loh, K.J., Lynch, J.P., Wang, Y., Law, K.H., Fraser, M. and Elgamal, A. (2007). Validation of a wireless traffic vibration monitoring system for the Voigt Bridge, Proceedings of the World Forum on Smart Materials and Smart Structures Technology (SMSST07), Chongqing & Nanjing, China, May 22 - 27, 2007. Accessed December 09, 2008.

Lynch, J. P. (2002). Decentralization of Wireless Monitoring and Control Technologies for Smart Civil Structures, Ph.D. Thesis, Department of Civil and Environmental Engineering, Stanford University, Stanford, CA. Accessed December 09, 2008.

Lynch, J. P., Sundararajan, A., Law, K. H., Kiremidjian, A. S., and Carryer, E. (2003). Power-Efficient Wireless Structural Monitoring with Local Data Processing, International Conference on Structural Health Monitoring and Intelligent Infrastructures (SHMII-03), Tokyo, Japan, November 13-15. Accessed December 09, 2008.

Lynch, J.P., Wang, Y., Loh, K.J., Yi, J.-H. and Yun, C.-B. (2006). Performance monitoring of the Geumdang Bridge using a dense network of high-resolution wireless sensors, Smart Materials and Structures, 15(6): 1561-1575. Accessed December 09, 2008.

MadWifi (2007). Multimode Atheros driver for WiFi on Linux. http://madwifi.org. Accessed December 09, 2008.

MikroTik (2008). Routerboard R52 IEEE 802.11a/b/g Wireless Mini-PCI Combo Cards. http://www.mikrotik.com/pdf/R52.pdf. Accessed December 09, 2008.

Milkereit, C., Zünbül, S., Karakisa, S., Iravul, Y., Zschau, J., Baumbach, M., Grosser, H., Günther, E., Umutlu, N., Kuru, T., Erkul, E., Klinge, K., Ibs von Seht, M., Karahan, A. (2000). Preliminary aftershock analysis of the Mw=7.4 Izmit and Mw=7.1 Düzce earthquake in Western Turkey - In: Kozaci, Ö.; Barka, A. (Eds.),The 1999 Izmit and Düzce Earthquakes: preliminary results, Istanbul Technical University, 179-187.

OLSR project (2004). http://www.olsr.org/docs/README-Link-Quality.html. Accessed December 09, 2008.

OpenWRT (2007). http://www.openwrt.org. Accessed December 09, 2008.

PC Engines (2008). WRAP.2E boards. http://www.pcengines.ch/wrap2e3.htm. Accessed December 09, 2008.

Petrovski, J., Paskalov, T., Stojkovich, A., Jurokovski, D. (1974). Vibration Studies of Istanbul Bogazici Suspension Bridge, Report OIK 74-7, Institute of Earthquake Engineering and Engineering Seismology, IZIIS, Skopje, Yugoslavia.

Press, W. H., Teukolsky, S.A., Vetterlin, W.T., and Flannery, B.P. (1992). Numerical Recepies in C: The Art of Scientific Computing, Cambridge: Cambridge University Press.

Safak, E., and Hudnut, K. (2006). Real-time structural monitoring and damage detection by acceleration and GPS sensors, 8th US National Conference on Earthquake Engineering, San Francisco, California.

SAFER, (2006). Test site Istanbul, Turkey. http://www.saferproject.net. Accessed December 09, 2008.

Schweitzer, J., Fyen, J. and Mykkeltveit, S. (2002). Seismic Arrays, Chapter 9, IASPEI New Manual of Seismological Practice, ed. P. Bormann, GeoForschungsZentrum Potsdam.

Straser, E.G., and Kiremidjian, A.S. (1996). A Modular, Visual Approach to Damage Monitoring for Civil Structures, Proc. 2nd International Workshop on Structural Control, Hong Kong.

Straser, E.G., and Kiremidjian, A.S. (1998). A Modular, Wireless Damage Monitoring System for Structures, Report No 128, John A. Blume Earthquake Engineering Center, Stanford University, Stanford, CA.

Tezcan, S., Ipek, M., Petrovski, J., and Paskalov T. (1975). Forced Vibration Survey of Istanbul Bogazici Bridge, Proc. 5th ECEE, Vo1.2, Istanbul, Turkey.

Tibi, R., Bock, G., Xia, Y., Baumbach, M., Grosser, H., Milkereit, C., Karakisa, S., Zünbül, S., Kind, R., Zschau, J. (2001). Rupture processes of the 1999 August 17 Izmit and November 12, Düzce (Turkey) earthquakes, Geophysical Journal International, 144, 2, F1-F7.

Torvalds, L. (2007). The Linux kernel. http://www.kernel.org. Accessed December 09, 2008.

Wald, D.J, Worden, B.C., Quitoriano, V., and Pankow, K.L. (2006). ShakeMap Manual; Technical Manual, Users Guide, And Software Guide; http://pubs.usgs.gov/tm/2005/12A01/pdf/508TM12-A1.pdf

Wang, Y., Loh, K.J., Lynch, J.P., Fraser, M., Law, K.H. and Elgamal, A. (2006). "Vibration monitoring of the Voigt Bridge using wired and wireless monitoring systems," Proceedings of the 4th China-Japan-US Symposium on Structural Control and Monitoring, Hangzhou, China, October 16 - 17, 2006. Accessed December 09, 2008.

CHAPTER 4

APPLICATION OF NEW WIRELESS SENSOR UNITS FOR SYSTEM IDENTIFICATION: THE CASE OF NAVELLI (AQ)

The rapid improvement in telemetry and computer technology is literally driving a revolution in earthquake engineering, and, in particular, in the monitoring of civil built infrastructures. Monitoring buildings in earthquake-prone areas is a task of major importance both to ensure their structural integrity, and to obtain an insight into their responses in the event of an earthquake and in order to mitigate urban earthquake risk by new, effective seismic design provisions.

This revolution started in the late 90s (Straser and Kiremidjian, 1998), when the earliest applications of wireless communication technology were connected together with embedded pc and sensors for structural monitoring purposes. These earlier applications first showed that real-time processing of data can be performed locally, and that wireless monitoring systems are feasible, reliable and cost-effective. Over the last few years, prototype structural wireless monitoring systems have been validated by tests performed on bridges and other structures (Lynch *et al.*, 2006), where they have been found to be a highly cost-competitive, completely autonomous and very reliable alternative to traditional wired systems.

At the present time, research efforts in seismic early warning and the monitoring of strategic infrastructures has mainly concentrated on the development of self-organizing wireless mesh information networks made up of low cost sensors (Fleming *et al.*, 2009; Picozzi *et al.*, 2009). This innovative system employs advances in various technologies to incorporate off-the-shelf sensor, processing and communications components into low-cost accelerometric seismic sensing units that are linked by advanced, robust and rapid communication routing and network organizational protocols appropriate for wireless mesh networks. The reduced cost of the instruments (less than one tenth of a standard instrument) and the possibility of creating dense, self-organizing and decentralized seismic monitoring networks are key aspects that are changing the approaches previously followed for structural engineering monitoring. In particular, the decentralized, self-organizing character guarantees the functionality of the network during a disastrous event, even when some of the sensing units are damaged. These novel accelerometric stations are easy to install (and therefore very suitable for rapid deployment during emergencies) and are able to collect, store and perform preliminary analysis of data. Furthermore, at the same time the stations also create a wireless mesh

network by which raw data and computed parameters can be communicated to a user's laptop connected to any node that belongs to the network. Wireless technology has been found to be particularly useful in such post-event operational conditions, making it possible for the operators to download the aftershock waveform data remotely without visiting the actual site, thus, allowing the safe retrieval of data from damaged buildings. On the other hand, considering the scenario of buildings monitored by wireless instruments, the system itself might be exploited to provide early warning of aftershocks to rescue teams operating within or nearby to the structure, similar to what was provided to workers clearing a collapsed freeway following the Mw 7.1 17.10.1989 Loma Prieta earthquake (Bakun *et al.*, 1994).

Immediately after the recent moment magnitude (Mw) 6.3 Central Italy Earthquake of the 6th of April 2009, where at least 294 people are known to have died, the German Earthquake Task Force has been involved in the installation of a temporary seismological network to support their Italian colleagues. In particular, under the request and coordination of the Department of Civil Protection (DPC), wireless accelerometric sensing units (4) have been installed within selected strategic infrastructures, both damaged and undamaged, for the recording of aftershocks and the real-time determination of characteristic building parameters (see the Figure 4.1).

Taking advantage of the real time accessibility of data soon after each aftershock, it was possible to monitor the behavior of the building during the aftershock sequence by performing interferometric analysis, which allows a rapid estimation of the velocity of shear waves, their attenuation and other changes within the buildings. Furthermore, the continuous spectral analysis of the shaking allows the main modal properties of the building to be regularly re-evaluated in great detail (see the figure). Interestingly, the variation of the fundamental resonance of the building during the largest amplitude arrivals of the strongest aftershock recordings has been observed under almost real-time conditions. Even more importantly, the system has allowed the collection of large data set of more than fifty aftershocks with Mw higher than 3 (including the third strongest aftershock, Mw 5.4, of the sequence). The availability of such a data set represents for structural engineers a valuable, and probably unique, new source of insights about the effective structural behavior of a building during earthquake shaking.

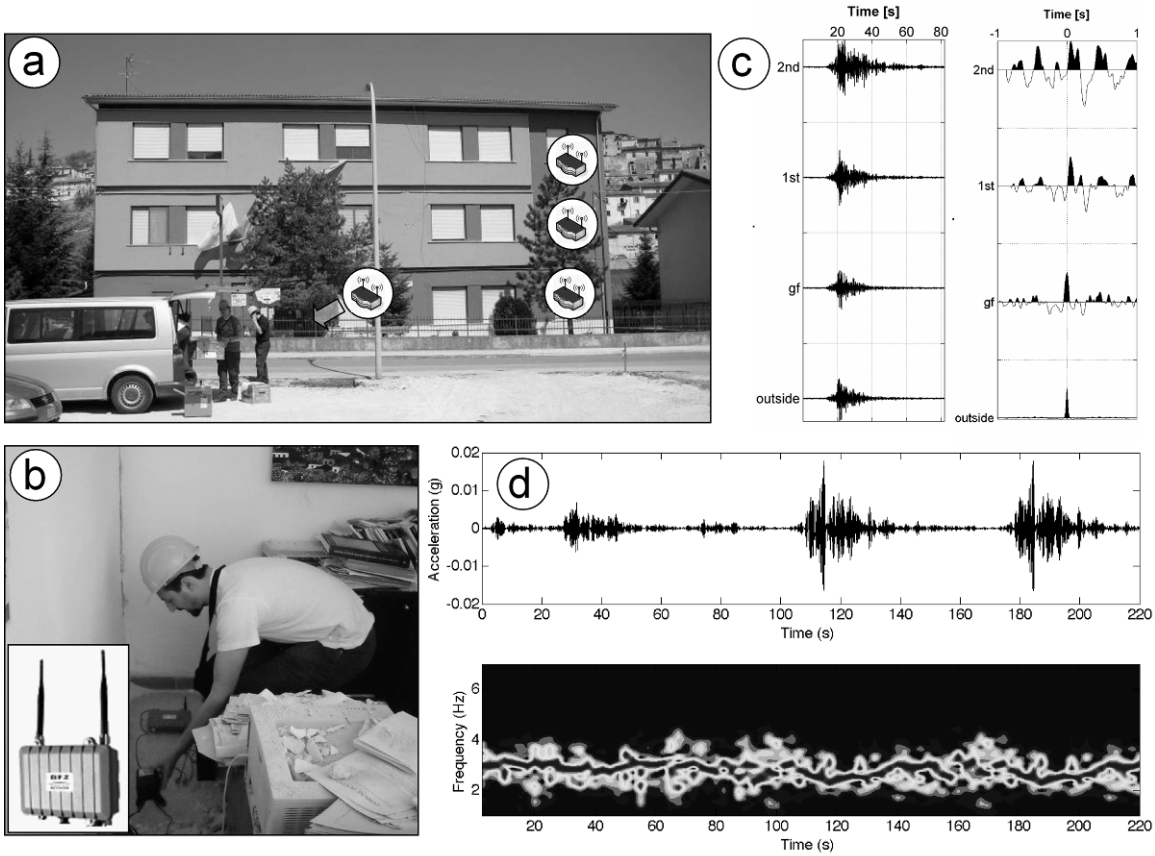

Figure 4.1: Real-time monitoring of Navelli's municipality center (L'Aquila, Italy). (a and b) Since the April, 8th, 2009, three wireless accelerometric stations have been installed at the different floors of the Navelli municipality building, with one station deployed outside it, all recording the sequence of aftershocks following the Mw 6.3 Central Italy Earthquake April 6, 2009. (c and d) During the last few weeks, the structure has experienced an increasing amount of damage, with access to the structure no longer considered possible. Nevertheless, the wireless accelerometers are still operating, hence the earthquake data can still be safely downloaded from outside the building. The deconvolution of accelerometric recordings within the building with a reference one (in this case the station located outside) allows the monitoring of the transfer function of the structure The continuous spectral analysis of data (d) allows a nearly real-time monitoring of the building's modal property variations and of the level of damage during the occurrence of aftershocks. Note the clear decrease between 100 and 140 seconds, as well as 170 and 210 seconds, of the fundamental resonance frequency of the building during the largest amplitude arrivals of the strongest aftershock recordings.

The current Task Force mission in Italy is showing to the engineering community that wireless sensing instruments represent a valuable, innovative tool for the structural monitoring of strategic structure, a fundamental task, especially after severe earthquakes, when the retrieval of critical data for the rapid assessment of possible damage and structural degradation in structures is urgently needed.

Considering the relative low cost of these novel instruments, a modest investment would allow, for cities located in areas prone to seismic risk, the setting up of modern, dense, wireless seismic monitoring systems for strategic infrastructures. Moreover, the

experience gained recently in Italy has also shown that these innovative system could provide an early warning capacity for the structure itself, contributing to the mitigation of urban earthquake risk and to desirable benefits in terms of losses avoided in the future.

REFERENCES

Straser, E.G., and Kiremidjian, A.S. (1998). A Modular, Wireless Damage Monitoring System for Structures, Report No 128, John A. Blume Earthquake Engineering Center, Stanford University, Stanford, CA.

Lynch, J.P., Wang, Y., Loh, K.J., Yi, J.-H. and Yun, C.-B. (2006). Performance monitoring of the Geumdang Bridge using a dense network of high-resolution wireless sensors, Smart Materials and Structures, 15(6): 1561-1575. Accessed December 09, 2008.

Fleming, K., Picozzi, M., Milkereit, C., Kuehnlenz, F., Lichtblau, B., Fischer, J., Zulfikar, C., Ozel, O., and the SAFER and EDIM working groups. The Self-Organising Seismic Early Warning Information Network (SOSEWIN). Accepted to be published from Seismological Research Letters.

Picozzi, M., Milkereit, C., Zulfikar, C., Fleming, K., Ditommaso, R., Erdik, M., Zschau, J., Fischer, J., Safak, E., Özel, O., and Apaydin N., (2009). Wireless technologies for the monitoring of strategic civil infrastructures: an ambient vibration test on the Fatih Sultan Mehmet Suspension Bridge in Istanbul, Turkey. Bulletin of Earthquake Engineering. DOI: 10.1007/s10518-009-9132-7.

Bakun, W., Fischer, F., Jensen, E., and VanSchaack, J. (1994) Early warning system for aftershocks, Bulletin of the Seismological Society of America, vol. 84(2), 359-365.

CHAPTER 5

A FAST METHOD FOR STRUCTURAL HEALTH MONITORING

The increasing demand for a widespread use of health monitoring for strategic buildings in seismic areas has emphasized the need to realize in-depth scientific studies, in order to verify the feasibility of economic and fast methods to detect anomalous vibrations, to perform post earthquake warning and monitoring, damage assessment and first damage scenarios. Generally, an effective system for structural health monitoring requires an appropriate number of sensors, suitably located in the structures, and complex elaborations of large amounts of data. The simplified method presented in this chapter is based on a statistical approach that uses the most significant data recorded on the top floor of the building, with the purpose of extracting information on the maximum inter-story drift, used as damage indicator. The parameters considered in the method are (i) maximum top acceleration, (ii) the first modal frequency variations and (iii) the equivalent structural viscous damping variation. A vast amount of experimental data relevant to several tests carried out on scaled R/C models and numerical non linear dynamic analyses have been used to verify the feasibility of this approach.

5.1 INTRODUCTION

The assessment of an increasing number of old structures and infrastructures requires a huge effort, especially if the purpose is to provide a faithful evaluation of seismic risk. The current practice of periodic visual inspections for safety evaluation appears more and more inadequate.

A specific task of the Italian RELUIS research project, funded by the Department of Italian Civil Protection (DPC), deals with devising and implementing a fast procedure to get useful information about the damage evolution in a large number of strategic buildings during and after seismic events, using the records of just few sensors located on the structure.

The feasibility and the cost optimization are the most important goals for the simplified monitoring system in order to favour the widespread use of such systems.

During the past two decades, a significant amount of researches have been carried out in the field of Non-destructive Damage Evaluation (NDE) methods using the changes in the dynamic response of a structure (Picozzi *et al.*, 2009; Ditommaso *et al.*, 2009). NDE methods can be classified into four levels [Stubbs *et al.*, 2000], according to the specificity of the information provided by a given approach [Rytter 1993]. (i) Level I

methods, i.e. those methods that only identify if damage has occurred. (ii) Level II methods, i.e. those methods that identify if damage has occurred and simultaneously determine the location of damage. (iii) Level III methods, i.e. those methods that identify if damage has occurred, determine the location of damage as well as estimate the severity of damage. (iv) Level IV methods, i.e. those methods that identify if damage has occurred, determine the location of damage, estimate the severity of damage and evaluate the impact of damage on the structure. Each level of damage identification described above requires a gradually increasing amount of data and more complex algorithms. Consequently, their set-up and effectiveness often require increasing costs, with higher error probability.

The objective of this section is to set-up a simplified practical method of Level I, based on a statistical approach, to check continuously the safety and reliability of strategic buildings. The method detects the evolution of the damage by comparing the dynamic response of the building before, during and after the earthquake. The response is evaluated considering the following approach: i) structural dynamic parameters (maximum top acceleration, first modal frequency variations and equivalent structural viscous damping variation) are evaluated just from top floor records; ii) a non linear correlation between all dynamic parameters and the maximum inter-storey drift, considered as damage index, is defined. The data of two experimental applications and many numerical simulations are provided to verify the effectiveness of the method.

5.2 METHODOLOGY

Level I methods are generally based on the variation of the main vibration frequencies or the variation of equivalent viscous damping. Such methods are often convenient because they are simple, robust and use a reduced number of sensors installed within the structure, although they can lead to wrong evaluations. In fact, the variation of vibration frequencies is not necessarily representative of the damage evolution, but it can also be determined by the variation of the temperature or the configuration of masses and stiffness, especially for deformable structures as reinforced concrete or steel frames.

The proposed simplified fast method for structural health monitoring of strategic buildings starts from a limited number of records collected on top floor (velocity or acceleration) and overcomes some limitations of the Level I methods. Indeed, the method considers some parameters evaluated by the recorded signals: (i) maximum absolute top acceleration (MATA); (ii) variations of the fundamental frequency (iii)

variation of the equivalent viscous damping, and provides a combination of these parameters to estimate the maximum inter-storey drift by means of nonlinear correlation analysis. All signals are filtered with band-pass filter 0.1-20 Hz. Finally, the maximum value of the estimated drift along the building height can be assumed as a correction factor of the Damage Index determined by classic first levels methods.

The MATA represents the first instrumental parameter considered in this method. It can be evaluated directly by the filtered signal (acceleration), or by a derivation of filtered signal in velocity, recorded on the top floor of the building. An appropriate arrangement of recording sensors on the structure permits to reconstruct all displacement and rotation components of the floor.

The other two instrumental parameters considered in the method are i) the percent variations (Δf_1) between the fundamental frequency of the building before the seismic event f_{init} and the minimum one f_{min}, corresponding to the maximum non linear behavior of the building and ii) the percent variations (Δf_2) between initial and final frequency (f_{fin}), as given by equations 1 and 2.

$$\Delta f_1 = (f_{init} - f_{\min}) / f_{init} \qquad (1)$$

$$\Delta f_2 = (f_{init} - f_{fin}) / f_{init} \qquad (2)$$

All frequencies can be evaluated by a Short Time Fourier Transform (STFT) [Gabor, 1946] applied on the whole signal, as shown in Figure 5.1, that refers to an earthquake recorded on a real building. This particular analysis allows to describe the variation in the time of the main frequencies of the structure.

The last instrumental parameter considered in the method is the variation of equivalent structural viscous damping $\Delta\xi$ related to the first structural mode. Information about damping can enrich the quality and quantity of the knowledge on the global damage, particularly if the damping is associated to the other parameters above described. For a non stationary signal the damping can be estimated using the *only output* non-parametric technique elaborated by Mucciarelli and Gallipoli, (2007). It measures the viscous equivalent damping of the signal recorded using a semi-probabilistic approach. The damping is estimated by logarithmic decrement method on a minimum of three consecutive decreasing peaks separated by the same period T, as shown in Figure 5.2a. The period T is assumed considering a fixed tolerance ε as function of T.

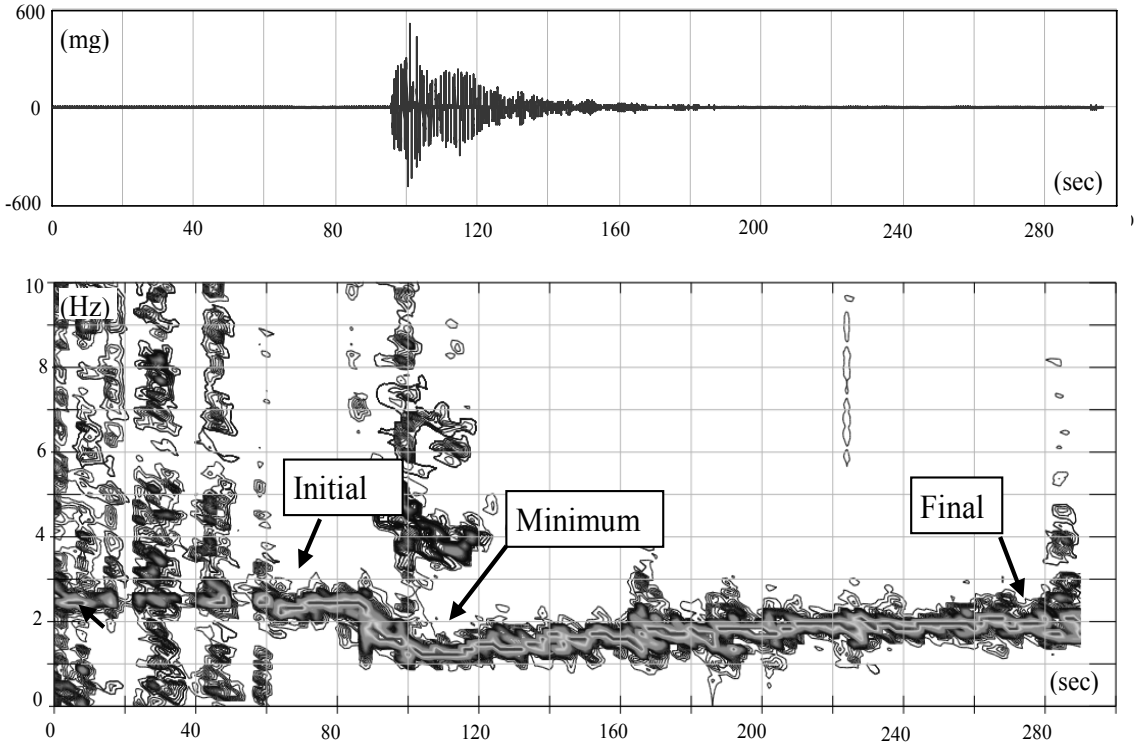

Figure 5.1: Example of application of STFT applied on a non-stationary signal

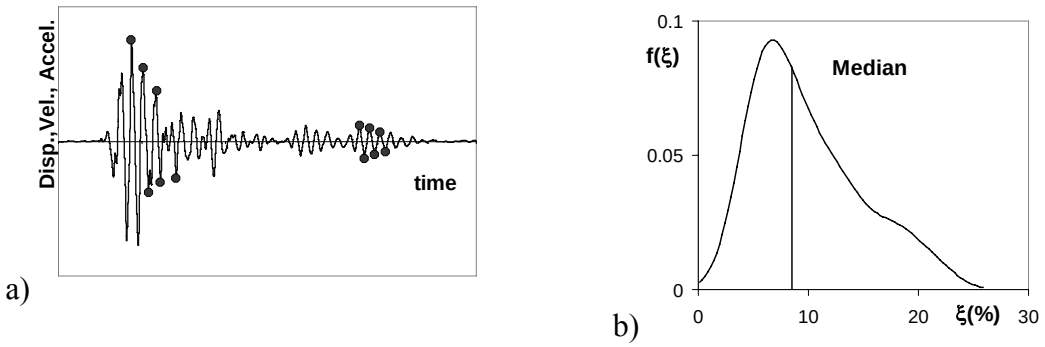

Figure 5.2: (a) Application of logaritmic decrement method on a recorded signal. (b) Statistical distribution of values.

The routine output provides a vector $\boldsymbol{\xi} = (\xi 1, \xi 2, ..., \xi n)$, where ξi is the value obtained by two consecutive decreasing peaks. Then, the lognormal distribution of the vector $\boldsymbol{\xi}$ is evaluated in order to get a median value of distribution for the whole signal, as shown in Figure 5.2b. A check on the effectiveness of the result is, then, carried out by comparing the fit curve between theoretical and empirical cumulative distribution function, through the Kolmogorov-Smirnov test [Piccolo, 1998]. The variation $\Delta\xi$ between the equivalent viscous damping evaluated on the signal before and after the earthquake is assumed as reference parameter in the method.

5.3 REGRESSION ANALYSIS FOR STRUCTURAL CONSTANTS EVALUATION

In order to verify the existence of a relationship between the selected parameters and the maximum inter-storey drift, several correlation analyses were performed considering: (i) the outcomes of experimental shaking table tests carried out by the University of Basilicata within the research projects TREMA and POP [Dolce *et al.*, 2005 and 2006]; (ii) numerical non linear dynamic analysis carried out considering different natural accelerograms compatible with Italian OPCM 3431, selected in the European Strong Motion Database, and different structure configurations. The flow-chart shown in Figure 5.3 explains the proposed approach.

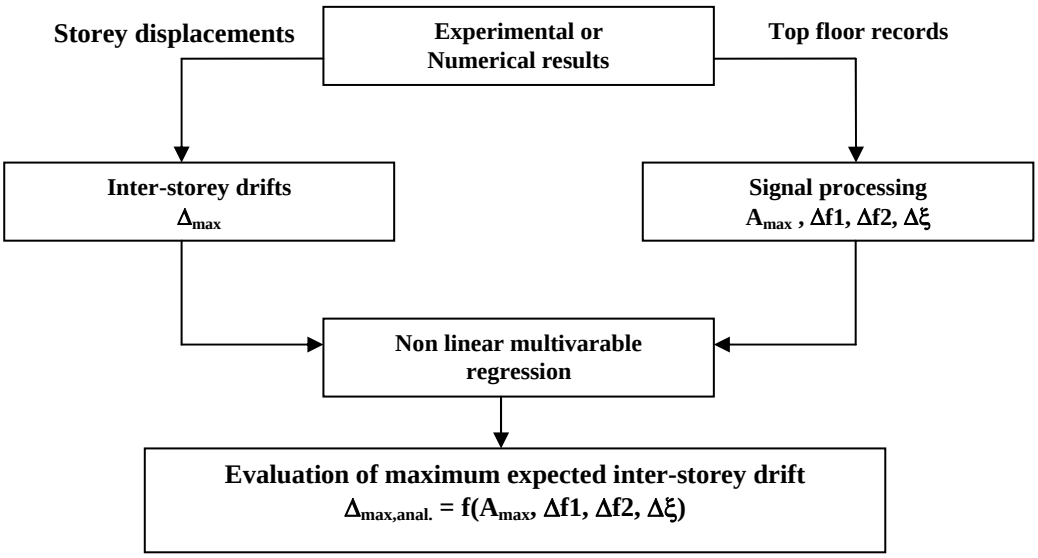

Figure 5.3: Scheme of approach used in the method.

Considering the output of each experimental or numerical test, a matrix containing the maximum inter-storey drift along the height of the model (dependent parameter) and the four instrumental parameters above defined (independent parameters) is built (eq. 3) in order to perform the correlation and regression analyses. Each row refers to a single test or numerical analysis.

$$\begin{vmatrix} \Delta_{\max 1} & a_{\max 1} & \Delta f_{11} & \Delta f_{21} & \Delta\xi_1 \\ \Delta_{\max 2} & a_{\max 2} & \Delta f_{12} & \Delta f_{22} & \Delta\xi_2 \\ .... & .... & .... & .... & .... \\ \Delta_{\max n} & a_{\max n} & \Delta f_{1n} & \Delta f_{2n} & \Delta\xi_n \end{vmatrix} \qquad (3)$$

In case of structural damage the global non linear behavior of the building makes the linear approach ineffective and a non linear multivariable regression becomes necessary to describe the relation between the considered parameters and the maximum inter-story drift.

For this study a non linear relation for each structure characterized by a second-degree polynomial, with eight coefficients, can be sufficient to describe efficiently the correlation between drift and other parameters, as shown in the following paragraphs.

$$\begin{pmatrix} \Delta_1 \\ \Delta_2 \\ . \\ . \\ . \\ \Delta_n \end{pmatrix} = \begin{pmatrix} a^2_{\max 1} & a_{\max 1}\,\Delta f^2_{11} & \Delta f_{11} & \Delta f^2_{21} & \Delta f_{21}\,\Delta\xi^2_1 & \Delta\xi_1 \\ a^2_{\max 2} & a_{\max 2}\,\Delta f^2_{12} & \Delta f_{12} & \Delta f^2_{22} & \Delta f_{22}\,\Delta\xi^2_2 & \Delta\xi_2 \\ . & . & . & . & . & . \\ . & . & . & . & . & . \\ . & . & . & . & . & . \\ a^2_{\max n} & a_{\max n}\,\Delta f^2_{1n} & \Delta f_{1n} & \Delta f^2_{2n} & \Delta f_{2n}\,\Delta\xi^2_n & \Delta\xi_n \end{pmatrix} \cdot \begin{pmatrix} c_1 \\ c_2 \\ c_3 \\ c_4 \\ c_5 \\ c_6 \\ c_7 \\ c_8 \end{pmatrix} \qquad (4)$$

The constants $c_1, c_2..., c_8$ are the regression factors determined by solving the equation system for each single structure, starting from experimental or numerical data. They constitute the characteristic factors of the structure obtained considering all set of results.

Finally, the analytical expression to evaluate the maximum expected drift along the height of the building can be written as:

$$\Delta_{an} = c_1 \cdot a^2_{\max} + c_2 \cdot a_{\max} + c_3 \cdot \Delta f_1^{\,2} + \\ + c_4 \cdot \Delta f_1 + c_5 \cdot \Delta f_2^{\,2} + c_6 \cdot \Delta f_2 + c_7 \cdot \Delta\xi^2 + c_8 \cdot \Delta\xi \qquad (5)$$

The contribution of the weight of each single instrumental parameter on the maximum analytical inter-storey drift is estimated by the following expression:

$$W_i = \frac{|F_i|}{\sum_i |F_i|} \qquad (6)$$

5.4 EXPERIMENTAL TESTS

The results of two extensive experimental programs of dynamic tests carried out on two similar 1/4 scaled 3-D R/C models, derived from a prototype building designed for gravity loads only, have been considered. The first 4-storey model was tested at the Structural Laboratory of the University of Basilicata in Potenza, within the POP project [Dolce *et al.*, 2005] (Figure 5.4), through mono-axial shaking table test.

The second model was a 3-storey specimen, with infill panels, tested on the 4x4m 6-DOF shaking table facility of ENEA Casaccia, (Rome) within the TREMA project [Dolce *et al.*, 2006] (Figure 5.4).

The correlation analyses presented here were carried out considering, for the POP model, the structural response to both natural and artificial mono-directional earthquakes, while natural bi-directional earthquake response was considered for the TREMA model.

The natural seismic input used in both projects was the Colfiorito record of the Italian 1997 Umbria-Marche earthquake, while the artificial seismic input considered was derived from the response spectrum provided by Eurocode 8 for soil type B. Both acceleration profiles were scaled down in time by a factor *Sc*:

$$Sc = \frac{1}{\sqrt{\text{Scale Factor}}}$$

for consistency with the scale of the model. In the POP Project, for the tests in the fixed-base configuration here considered, the effective peak acceleration of the table was progressively increased from 0.05g up to 0.35g. All floors displacement were measured through Temposonic digital transducers, fixed to an external steel reference frame. The floor accelerations were acquired through a system of horizontal servo accelerometers. In the tests for the TREMA project, the effective peak acceleration of the table was progressively increased from 0.04g up to 0.23g. In this case, the top floor the accelerations were acquired through 3 horizontal servo accelerometers and their measures were recomposed in the centre of mass. Figures 5.5 and 5.6 show the maximum experimental inter-storey drifts obtained for both POP and TREMA experimental tests vs each considered instrumental parameters. The maximum inter-storey drift Δ_{max} is nonlinearly dependent from the maximum top acceleration *Amax*, as shown by Figures 5.5 and 5.6, and with a low dispersion factor of the experimental points. Indeed, other parameters Δf_1, Δf_2 and $\Delta\xi$ (Figs. 5.5 and 5.6) show a non linear dependence on the maximum inter-storey drift Δmax, more evident for $\Delta\xi$ and Δf_2, and

a dispersion degree considerably larger than *Amax*. It is interesting to notice that both frequency variations Δf_1 and damping variation $\Delta\xi$ assume values different from zero for Δ_{max} greater than about 0.4-0.5%. This value represents the threshold of structural damaging.

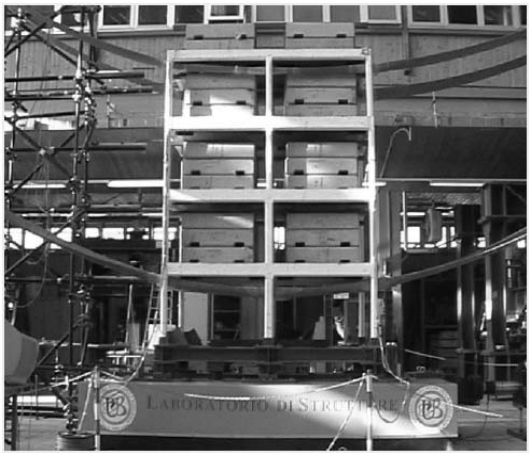

POP Model

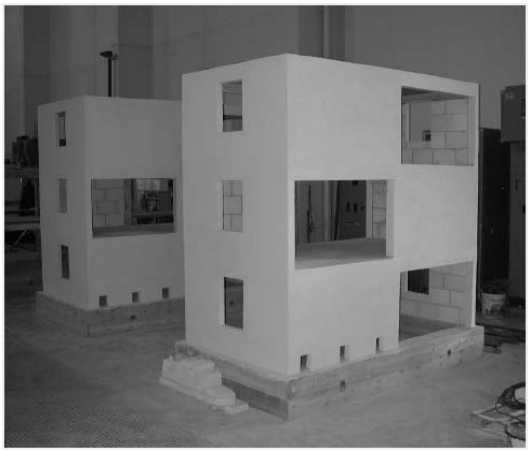

TREMA Model

Figure 5.4: Pictures of POP and TREMA Models

The analytical inter-story drift evaluated by the nonlinear regression analysis, as summarized by equation 5, was compared to the experimental results and shown in Figures 5.9 and 5.10. Then, starting from all experimental data relative to examined structures a single vector of characteristic parameters ($c_1,\ldots,c_8$) was determined for each specimen. Figure 5.9 shows the experimental vs analytical maximum inter-storey drifts for POP model. In this case, the correlation factor between the two parameters ($R^2 \approx 1$) proves the good estimation of maximum drift provided by the proposed formulation as a function of all considered parameters.

In Figure 5.7 the weight of each single instrumental parameter used by non linear regression to estimate the inter-storey drift are reported. Maximum top acceleration Amax provides the most important contribution to Δmax, especially for low intensity earthquake. In this case and for the POP model the frequency variation $\Delta f1$ accounts for 20÷25%. For increasing seismic intensity, and therefore for damage cumulating, the contribution of the two previously considered parameters decreases, while Δf_2 and $\Delta\xi$ play a more significant role.

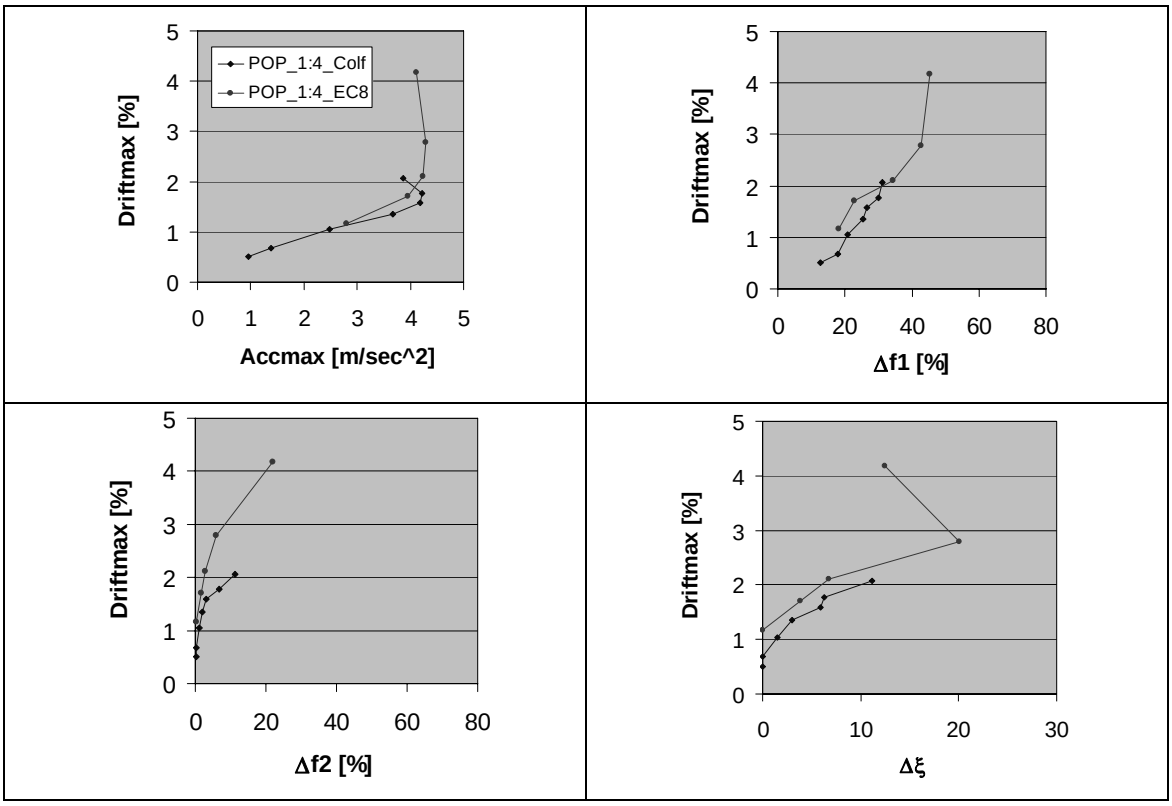

Figure 5.5: POP. Correlation among maximum inter-story drift and instrumental parameters.

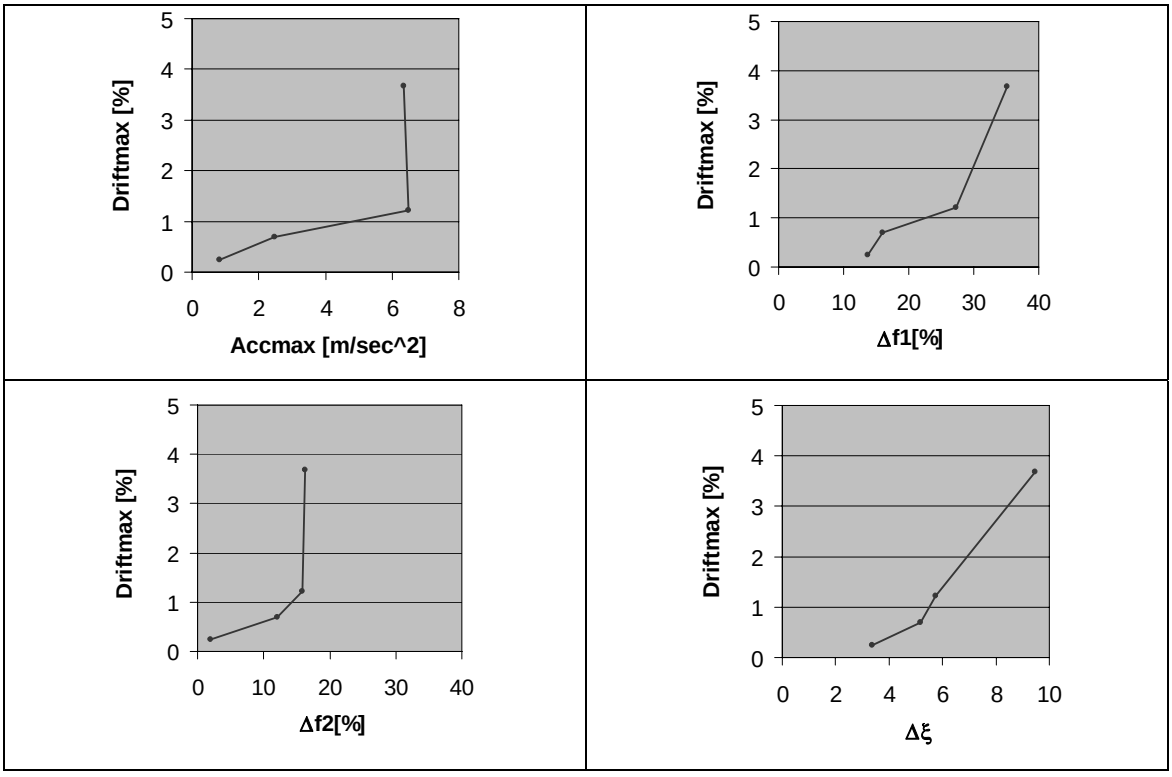

Figure 5.6: TREMA. Correlation among maximum inter-story drift and instrumental parameters.

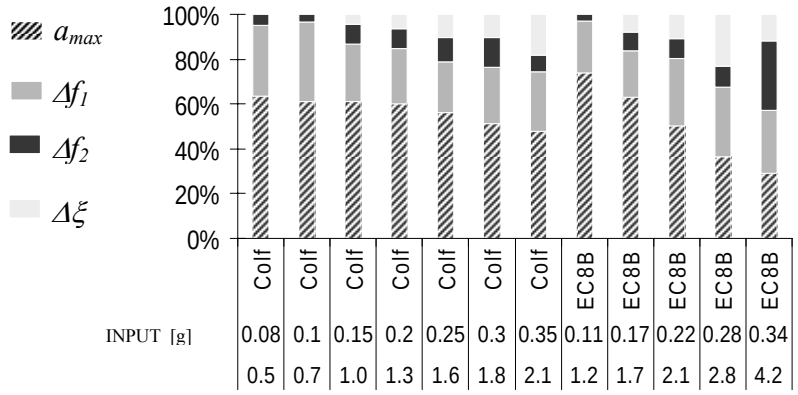

Figure 5.7: POP Model: weight contribute for each instrumental parameter vs experimental test.

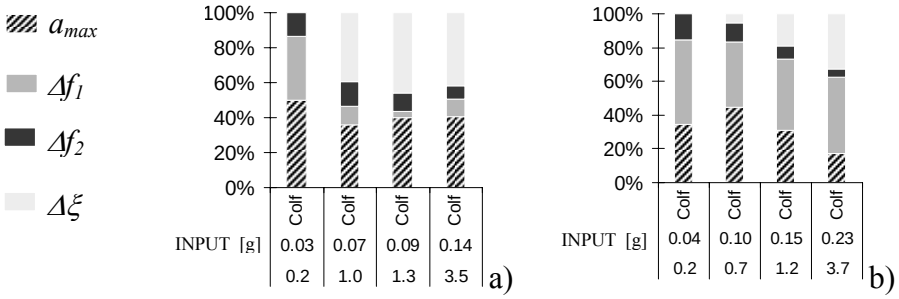

Figure 5.8: TREMA Model: contribute for each instrumental parameter vs experimental test for both X and Y directions.

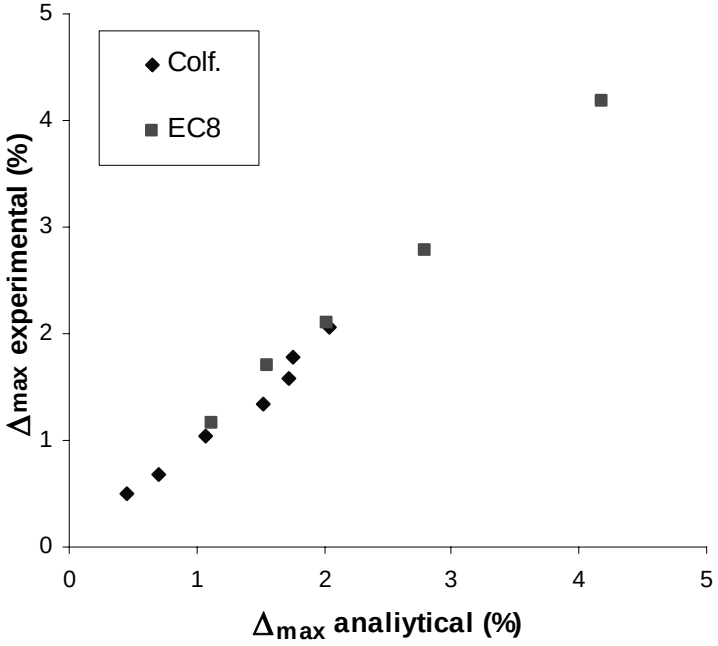

Figure 5.9: POP Model: experimental vs analytical maximum inter-story drift

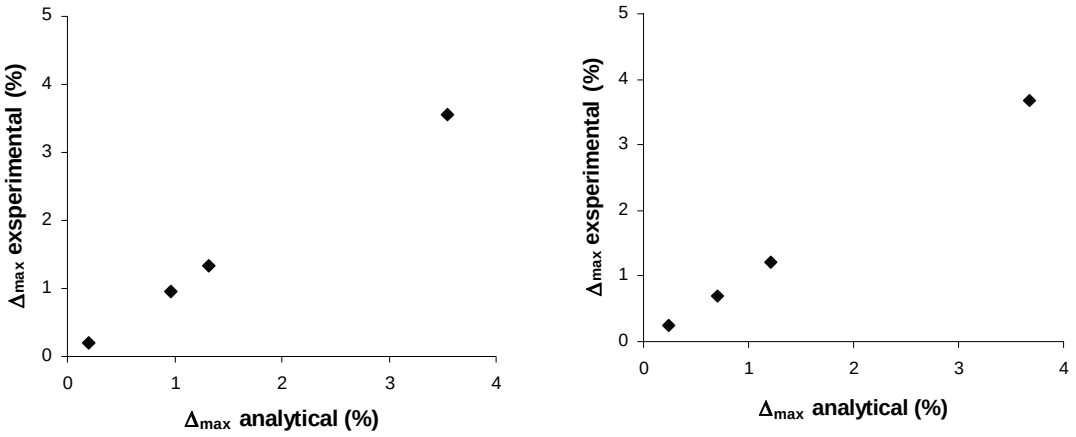

Figure 5.10: TREMA model: experimental vs analytical maximum inter-story drift for both X and Y direction

A different trend was observed for TREMA out-comes, probably because of the presence of masonry infill and of damage suffered by model in previous tests. In all cases the analytical formulation was able to evaluate correctly the maximum inter-storey drift.

5.5 NUMERICAL SIMULATIONS

A parametric numerical study was planned in order to understand the influence of the seismic input and of the most significant geometrical, mechanical and regularity parameters on the weight of the each instrumental parameters for the damage detection. A huge amount of numerical data have been processed. The first results here analyzed have been obtained by considering a non linear numerical model of a R/C regular building, five floor, four frames along the longitudinal direction (X) and three frames in the transverse direction (Y), having a rectangular plan, 15mx12m. The considered structure has been designed following the criteria of the Italian seismic code [OPCM 3431/2005] for high ductility class (CDA), high seismic intensity (PGA 0.35g) and for soil type A. The height of each storey is 3m, for a total height of the building equal to 15m. A software based on non linear finite element (SAP2000 non-linear) [*Wilson 2002*] has been used to model the 3-D structure. Beams and columns have been modelled as frame elements, assuming 20 MPa as cylindrical strength of concrete, and 430 MPa as yield strength of steel. In order to simulate a structural non linear behaviour during a strong ground motion, link elements and plastic hinges have been added at the

end of beam and column elements respectively. Link elements have a Takeda hysteretic behaviour, while plastic hinges have an axial load-dependent one.

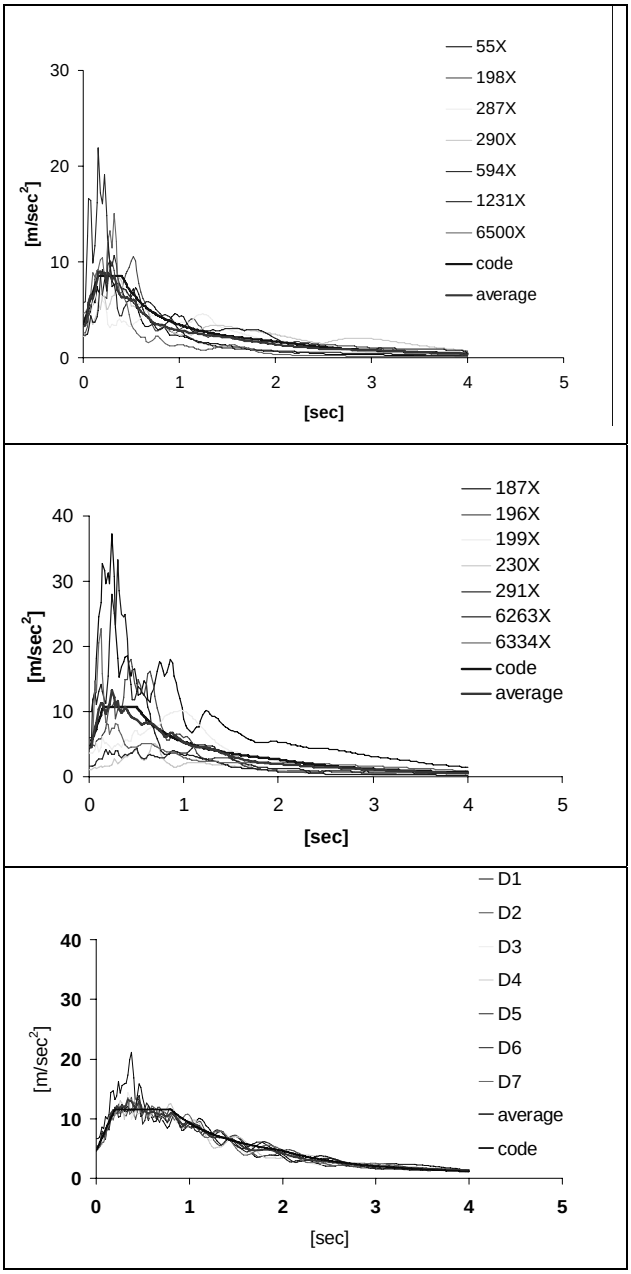

Figure 5.11: Response spectra of the numerical seismic input

A total of 168 non-linear bi-directional dynamic analyses have been carried out using, for each category of seismic zones (from a_g=0.05g up to 0.35g) and for soil type A and B,C,E (S=1, 1.25), seven different pairs of natural accelerograms, selected in the European Strong Motion Database, compatibles with the Italian OPCM 3431/05. For soft soil, D type, seven artificial accelerograms pairs, having the spectrum compatible

with the Italian seismic code, have been considered. Figure 5.11 shows the response spectra of each group of seismic inputs.

Figure 5.12 shows the maximum numerical inter-storey drifts vs all the considered parameters. These parameters were evaluated by the displacement and acceleration histories of the master joint at each floor and for all considered earthquakes. The maximum inter-storey drift Δ_{max}, depicted in Fig. 5.12, is still linear dependent from maximum top acceleration A_{max}, where the linear correlation coefficients between maximum drift and each parameter are provided.

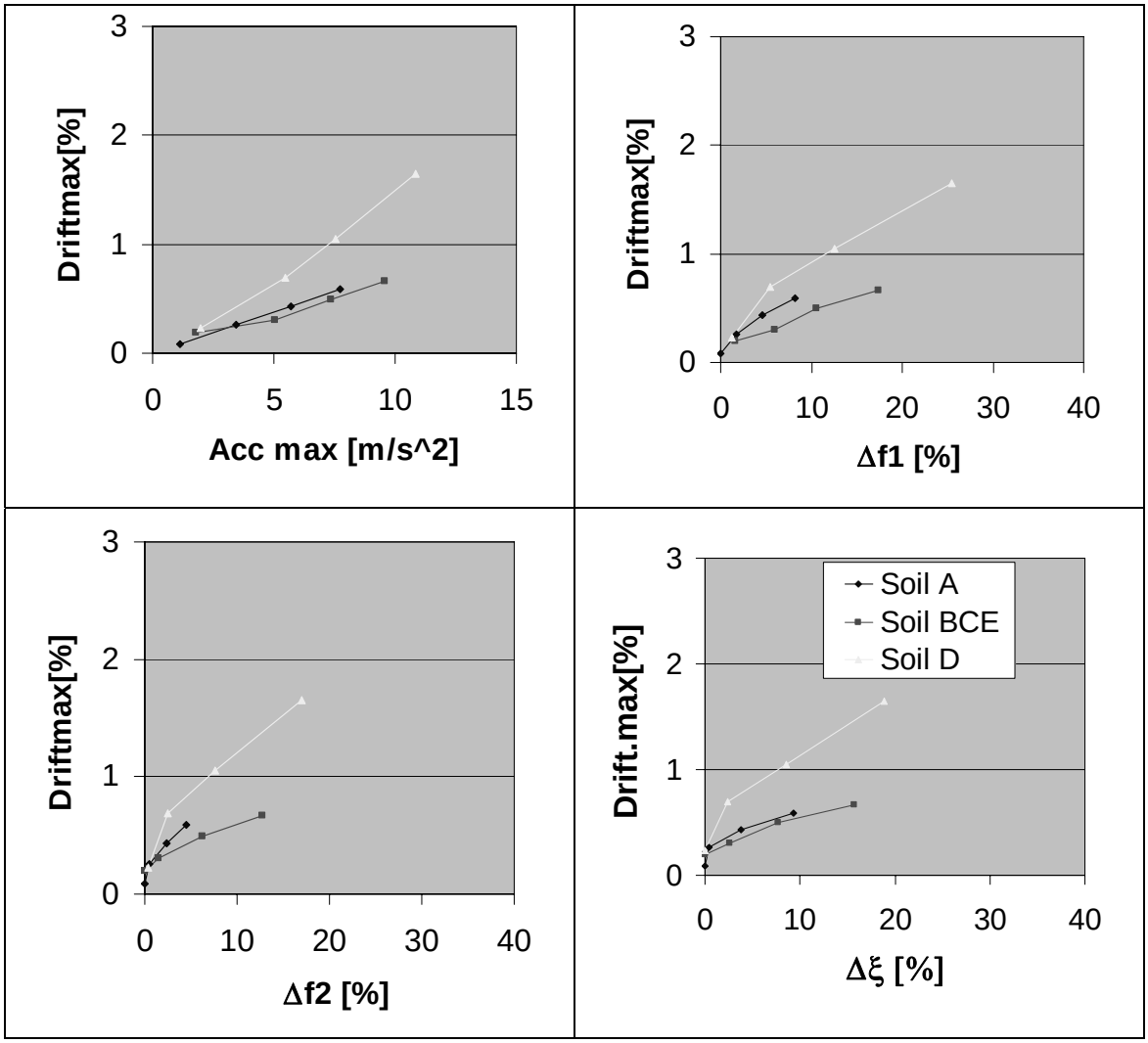

Figure 5.12: Correlation among maximum inter-story drift and instrumental parameters.

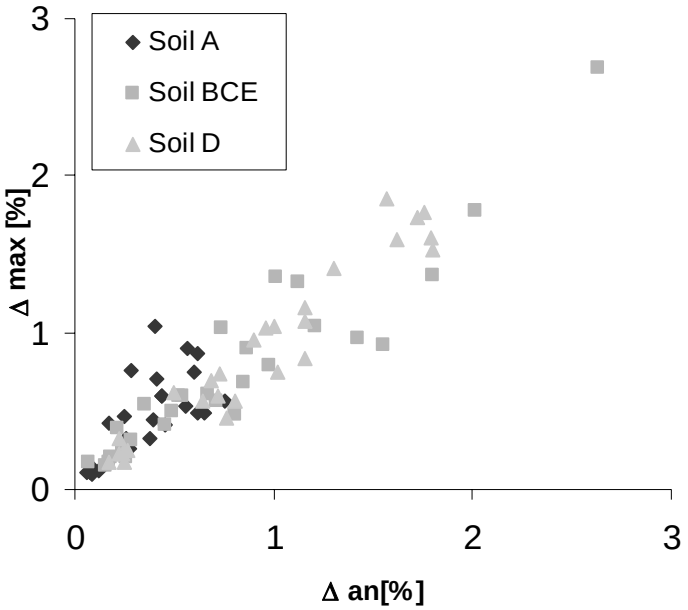

Figure 5.13: Experimental vs analytical maximum inter-story drift for soil A-BCE-D.

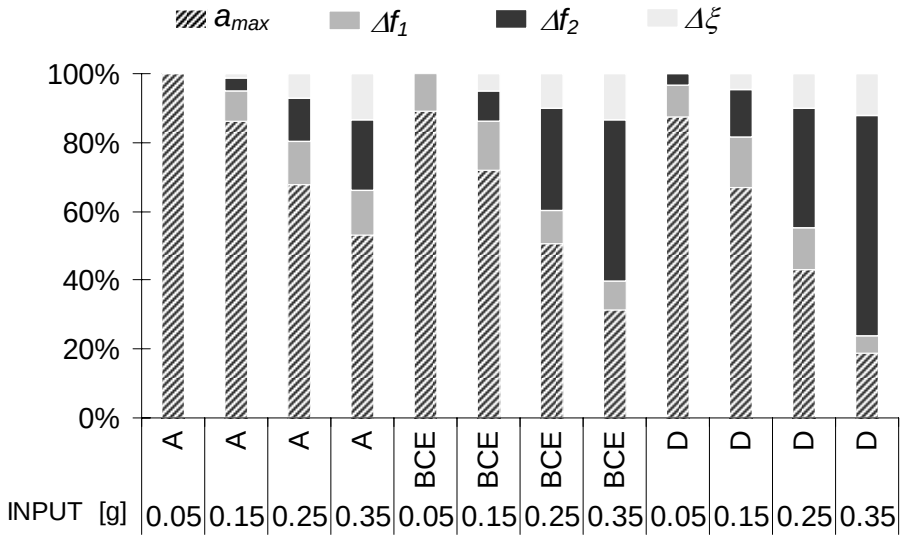

Figure 5.14: Weight contribute for each instrumental parameter vs experimental test.

Furthermore, in the diagram of Figure 5.12 a clear low dispersion of the results can be observed. Other parameters Δf_1, Δf_2 and $\Delta\xi$ (Figg. 5.12b, c and d) show a dispersion of results greater than A_{max}, while frequency variation Δf_2 and damping variation $\Delta\xi$ confirm the same trend observed for experimental correlation analyses, in particular, that a drift of about 5% represents a damage threshold for R/C buildings.

Damage Index	Damage Level	Building Appearance	Reparability
>1.0	Collapse	Local or global collapse of building	No
0.4-1.0	Heavy	Extensive Cracks of concrete and buckled bars	Hardly Repairable
< 0.4	Moderate	Extensive Cracks; expulsion of concrete from critic zones of elements	Repairable
---	Low	Few cracks distributed on building; expulsion of cover concrete from columns	Easily Repairable
---	Weak	Few Cracks	Total

Table 5.1: Correlation between damage index and damage level [Park and Ang, 1985 and 1987].

For numerical model a regression analysis, considering the results of all numerical simulations, has been made. Therefore, a single vector (c_1,…,c_8) of constitutive constant of the considered structure has been carried out. In Figure 5.13 the maximum numerical and analytical inter-storey drifts are compared. As for experimental tests, also in this case the analytical procedure (eq. 5) provides a good estimation of the drift values, as testified by a correlation vector $R^2 \approx 1$. Using this procedure the vector (c_1,…,c_8) is independent from input and soil type.

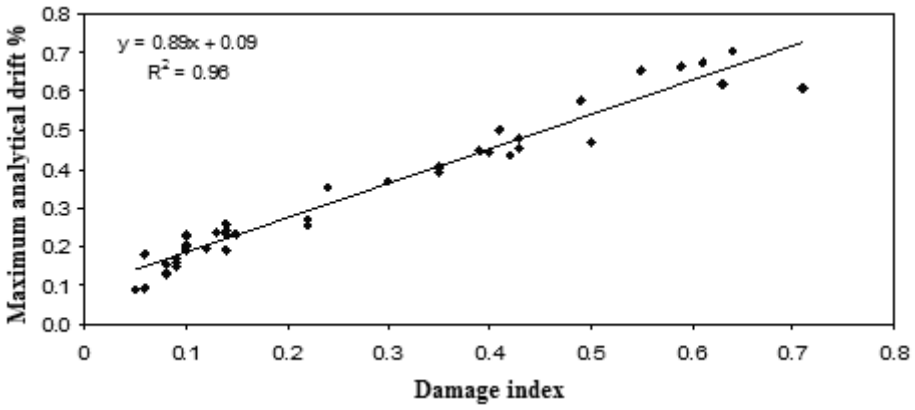

Figure 5.15: Correlation between analytical maximum drift and damage index evaluated by Park and Ang procedure.

In Figure 5.14 the weight of each single parameter on the analytical evaluation of the maximum drift with equation 5 are reported. The non linear analyses confirmed the trend observed with experimental results. For low values of PGA and for all soils the maximum top acceleration A_{max} provides the more consisting contribution on Δmax,

while for PGA increasing the frequency variation Δf_2 and $\Delta\xi$ become more important; while Δf_2 maintains the same relevance.

In order to validate the proposed method, the results obtained from our procedure were compared with the results obtained using another damage index: Park and Ang damage index [Park and Ang, 1985 and 1987].

As shown in Figure 5.15 there is a good correlation between Park Index and analytical maximum drift obtained with the proposed procedure.

5.6 DISCUSSION

The damage assessment methodology proposed in this paper can detects and quantify the damage suffered by a R/C building using only few instrumental parameters measured on the top of the monitored structure (Level I methods). The damage is expressed in terms of maximum inter-story drift (damage indicator) evaluated through a non linear regression analysis, starting from parameters above defined.

Several outcomes obtained from experimental and numerical tests allowed to calibrate and verify the methodological approach.

This approach can be useful especially for high excitation level and, considering its low cost, it should favour the possibility to increase the number of monitoring strategic structures.

The first analyses of the results show that, for regular buildings the only case investigated up to now, the maximum value of the top floor acceleration is the most strictly related parameter to the maximum inter-storey drift along the building height. The other parameters become important for high PGA values, when a strong non linear behavior is activated.

In order to estimate the influence of soil on the dynamic response of the structure, further studies are necessary to estimate the influence of frequency variation of soil during the strong motion.

ACKNOWLEDGEMENTS

This study was developed within the project DPC-RELUIS 2005-2008 (Research Line 9) funded by the Department of Italian Civil Protection.

REFERENCES

Ditommaso R., Parolai S., Mucciarelli M., Eggert S., Sobiesiak M. and J. Zschau (2009). Monitoring the response and the back-radiated energy of a building subjected to ambient vibration and impulsive action: the Falkenhof Tower (Potsdam, Germany). Bulletin of Earthquake Engineering. DOI: 10.1007/s10518-009-9151-4.

S.W. Doebling, C.R. Farrar, M.B. Prime, (1998), A summary review of vibration-based damage identification methods. The Shock and Vibration Digest.

Dolce M., Cardone D., Di Cesare A., Moroni C., Nicoletti M., Ponzo F.C., Nigro D. (2005). Dynamic Tests on a 1:4 Scaled R/C Existing Building: Comparison Of Several Isolation Systems. 9th Assisi, Kobe,Japan.

Dolce M., Cardone D., Moroni C., Nigro D., Ponzo F.C., Di Cesare A., Ventura G., De Canio G., Ranieri N., Goretti A., Marnetto R. (2006). Experimental Performance of Exist-ing R/C Building Seismically Upgraded with New Added Viscous Damping Rubber Isolators. 4th World Conference on Structural Control and Monitoring, July, San Diego, USA.

Dolce M., Ponzo F.C., Masi A., Mucciarelli M., Gallipoli M., Di Cesare A., Tetta M., Vona M., (in press), Identification of the structural model and analysis of the global seismic behaviour of the IACP Bonefro building, The BobCode Project, BEE Special Issue.

Rytter A. (1993). Vibrational based inspection of Civil Engineering Structures. Ph.D. Thesis, University of Aalborg, Denmark.

Gabor D. (1946). Theory of communication. IEE Journal 93, 429-457. London, U.K.

Mucciarelli M., Gallipoli M. R., 2007. Damping estimate for simple buildings through non-parametric analysis of a sin-gle ambient vibration recording. Ann. Geoph., 50, 259-266.

Ordinanza del Presidente del Consiglio dei Ministri No. 3431/2005. Ulteriori modifiche ed integrazioni all'Ordinanza del PCM n. 3274 del 20.03.2003, Roma, 3 Maggio 2005.

Stubbs N., Perk S., Sikorsky C., Choi S. (2000). A global non-distructive damage assesment methodology for civil engi-neering structures. International Journal of System Science, 2000.

Wilson E.L. (2002). Three dimensional static and dynamic analysis of structures. CSI - Computer and Structures, Inc, Berkeley California USA, January.

Park YJ e Ang AH-S (1985). Mechanistic seismic damage model for reinforced concrete. Journal of the Structural Engineering, 1985: 111(4): 722-739,1985.

Park YJ, Ang AH-S e Wen YK (1987). Damage-limiting aseismic design of buildings. Earthquake Spectra 1987: 3(1):1-26.

Piccolo D. (1998). Statistica. Società editrice Il Mulino, Bologna. Italy.

Picozzi M., Milkereit C., Zulfikar C., Fleming K., Ditommaso R., Erdik M., Zschau J., Fischer J., Safak E., Özel O., Apaydin N. (2009). Wireless technologies for the monitoring of strategic civil infrastructures: an ambient vibration test on the Fatih Sultan Mehmet Suspension Bridge in Istanbul, Turkey. Bulletin of Earthquake Engineering. DOI: 10.1007/s10518-009-9132-7

CHAPTER 6

JET-PACS PROJECT: EXPERIMENTAL MODEL AND DYNAMIC IDENTIFICATION TESTS

An extensive experimental dynamic testing programme named Jet-Pacs is being carried out at the Structural Laboratory at the University of Basilicata. The Jet-Pacs Project has been developed within the RELUIS 2005-08 project (Research Line 7: Technologies for base isolation and structures and infrastructures control), involving partners from different Italian universities. With regards to dissipating bracing systems, the main objectives of the programme are: (i) to increase user awareness of specific aspects of the currently available techniques, (ii) to carry out a performance assessment of the different techniques, and (iii) to simplify and to suggest a design standardisation procedure.

Shaking table tests are carried out on a 1:1.5 scaled structural model derived from a prototype building, namely a 2-storey, 1-bay, three-dimensional steel frame.

Both passive and semi-active bracing systems are used, featuring the following energy dissipating materials and principles: (i) viscous fluids; (ii) viscoelastic materials; (iii) magnetorheological fluids; (iv) visco-re-centring elements and (v) hysteretic components. The structural model is subjected to three different sets of natural and artificial earthquake records, compatible with the Italian seismic code response spectra for A, B and D soil types. The seismic intensity is progressively increased until the design performance criterion is achieved.

In this section, model dynamic identification test results are presented and key features of the experimental shaking table testing programme are outlined.

6.1 INTRODUCTION

Traditional retrofitting techniques for framed structures are based on widespread strengthening of the structure and alternatively on the introduction of additional, very stiff, structural members. In recent times, innovative strategies for the passive and semi-active control of structures have been studied and experimented, such as those based on the insertion of energy dissipating braces in the frame. However, widespread application of these techniques has not yet been achieved, mainly due to the lack of extensive experimental information allowing for the adoption of less conservative design rules. These techniques have shown their effectiveness in reducing seismic effects on existing

frames, but extensive experimental investigations are required to provide reliable analysis and design data.

Unfortunately, the increasing number of numerical and experimental studies on a large number of dissipating devices [Dolce *et al.*, 2005] and the analysis of real life applications [9ISIED 2005] have not yielded an improvement in related codes and guidelines, in much the same way as for other innovative techniques (e.g. seismic base isolation techniques). In Europe, new seismic codes only implicitly allow for the use of such devices [CEN 2004, DM 14.01.2008], while very few codes worldwide provide for simplified design criteria [FEMA 356, 2000].

Various experimental methods are available for the seismic response assessment of structures equipped with dissipating devices. Shaking table tests are, in principle, the most reliable experimental method for this purpose [Dolce *et al.*, 2001].

An extensive dynamic experimental testing programme, named JetPacs (Joint Experimental Testing on Passive and semiActive Control Systems), is scheduled to be carried out at the Structural Laboratory of the University of Basilicata. The Jet-Pacs Project has been developed within the RELUIS 2005-08 project (Research Line 7), involving several partners from different Italian Universities.

This section provides an overview of the experimental model set up and focuses specifically on presenting the detailed aspects of the experimental model, seismic inputs, test apparatus and sensor set up, energy dissipating devices and dynamic characteristics of the experimental model.

6.2 EXPERIMENTAL MODEL, TEST APPARATUS AND SENSOR SET UP

The 2/3-scale model used for dynamic testing has been obtained from a steel building prototype. Figure 6.1 shows the general layout of the experimental model. The test structure is a 2-storey, single bay steel frame featuring a 4m span in the test direction. The inter-storey height is 2m and a 100mm thick steel-concrete slab (4.2m by 3.2m in plan) is connected to the primary beams. Primary and secondary beams have equal structural sections (IPE 180) for all storeys and the columns have constant cross section (HEB 140) along the height.

Additional masses have been placed on each slab in order to account for non structural dead loads and an adequate amount of live loading (30%), as well as the mass-similitude scaling contribution. Additional steel beams (HE220B) at the base of the experimental model are added to obtain the connection with the shaking table system, as

described later in the section. Dead and live loading values considered in the prototype design are typical for a residential housing type of structure. The experimental model is constructed utilizing Fe360 grade steel having the following characteristics: Young's modulus, $E = 206000N/mm^2$ and yield strength, $f_y = 235N/mm^2$.

The theoretical weight of the experimental model ($W_m = 98.08kN$) is obtained from the prototype model weight ($W_p = 180.88kN$) by assuming the length scaling (S_L) and material scaling (S_E) factors equal to 2/3 and 1, respectively. The actual total weight of the JetPacs experimental model (W_m) has also been estimated utilizing dynamic identification tests carried out at the Structural Laboratory of University of Basilicata, as described below. An additional weight of about 26kN is required to obtain the total model scaling weight contribution. The additional weight due to dead loads and to part of the equivalent mass-similitude scaling contribution is obtained by producing floor slabs with increased thickness. The remaining part of the equivalent weight and live loading (30% DL) is applied at each storey by means of 8 additional concrete masses having the characteristics (coordinates and weight) reported in Table 6.1 and shown in Figure 6.2, for both symmetrical and eccentric (5% of the bay span in the Y direction) mass configurations.

The test apparatus at the University of Basilicata Structural Laboratory includes a single degree of freedom shaking table driven by an MTS dynamic actuator, with ±500kN maximum load capacity and ±250mm stroke, fixed to a (6m high by 10m wide) reaction wall and to the base of the test model by means of cylindrical joints, as shown in Figure 6.3 [Cardone *et al.*, 2005]. The actuator is operated by three MTS SilentfloTM 505-180 hydraulic pumps, each capable of a 600litres/min flow rate.

The shaking table consists of a four profile rail guide system (SKF- Model: LLR HC 65 LA T1), with two carriages for each guide, located under each column of the experimental model, as shown in Figure 6.3a. A friction factor of less than 1‰ ensures accurate linear movement in the test direction.

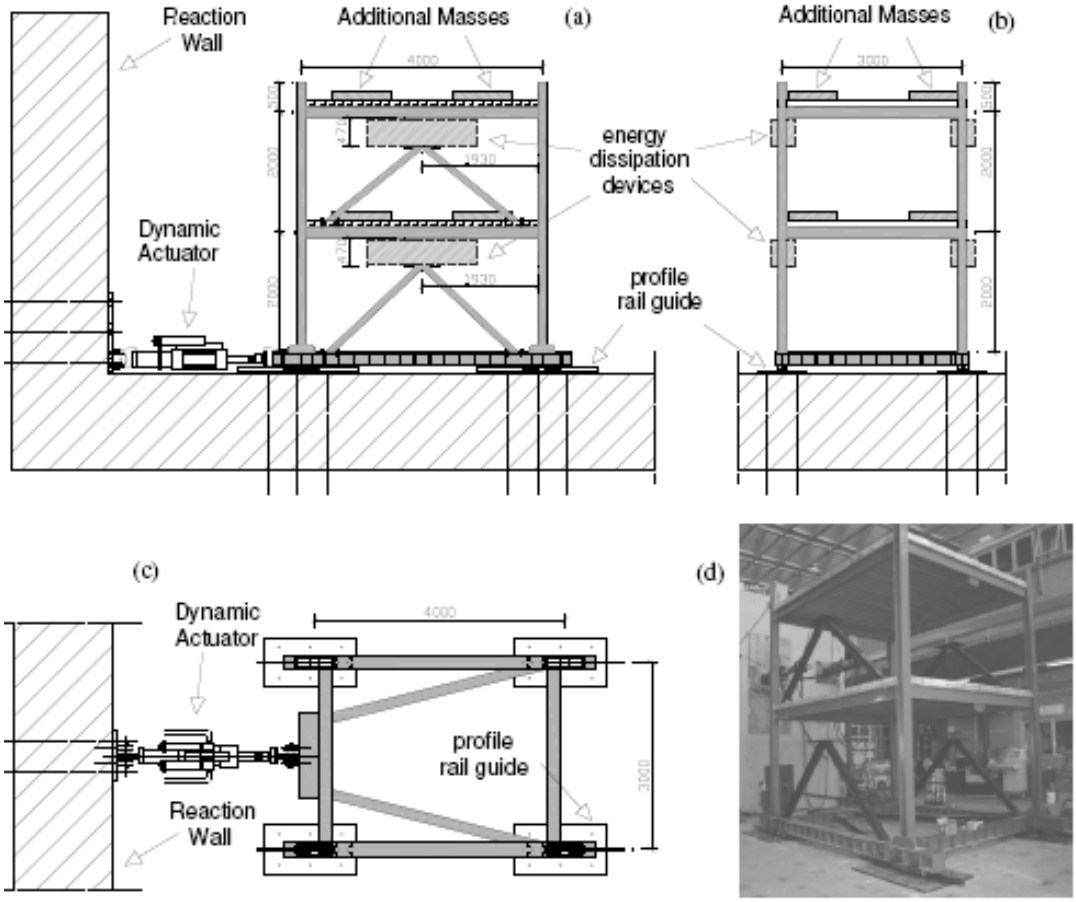

Figure 8.1: Structural model selected for the tests (a) Frame (Test) X Direction; (b) Frame Y Direction; (c) Shaking table plan; (d) 3D view of the test rig.

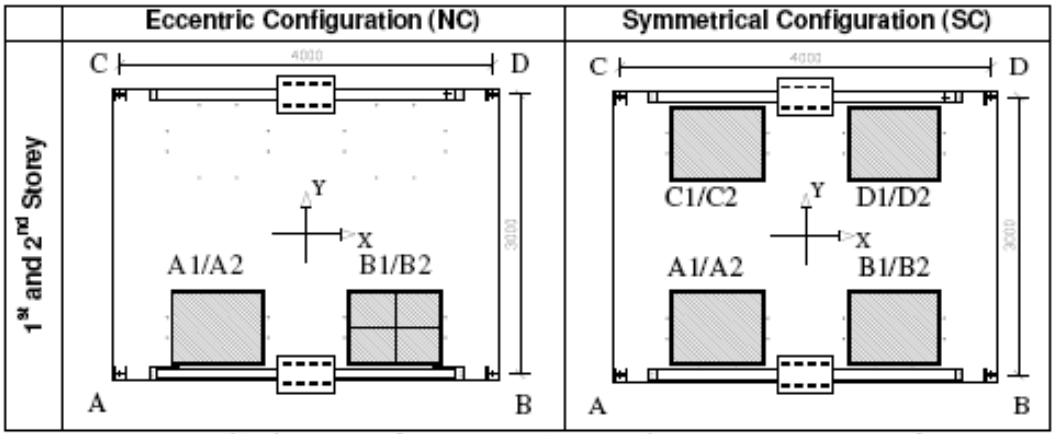

Figure 6.2: Concrete block positions for symmetrical (SC) and eccentric (NC) mass configurations

The rigid diaphragm at the base level is achieved by an adequately braced steel girder (HEM 300), as shown in Figure 6.3b. The model is a 2 degrees of freedom system in the test direction, corresponding to the 2 horizontal floors displacements, where most of the structural mass is concentrated.

Storey	Position ID	Coordinates (m)		Weight (kN)	Eccentric Configuration
		X Dir.	Y Dir.		
1	A1	-0.95	-1.00	3.32	Yes
	B1	0.95	-1.00	3.34	Yes
	C1	-0.95	1.00	3.30	No
	D1	0.95	1.00	3.30	No
2	A2	-0.95	-1.00	3.30	Yes
	B2	0.95	-1.00	3.34	Yes
	C2	-0.95	1.00	3.32	No
	D2	0.95	1.00	3.24	No

Table 6.1: Concrete block positions and weights for symmetrical and eccentric mass configurations

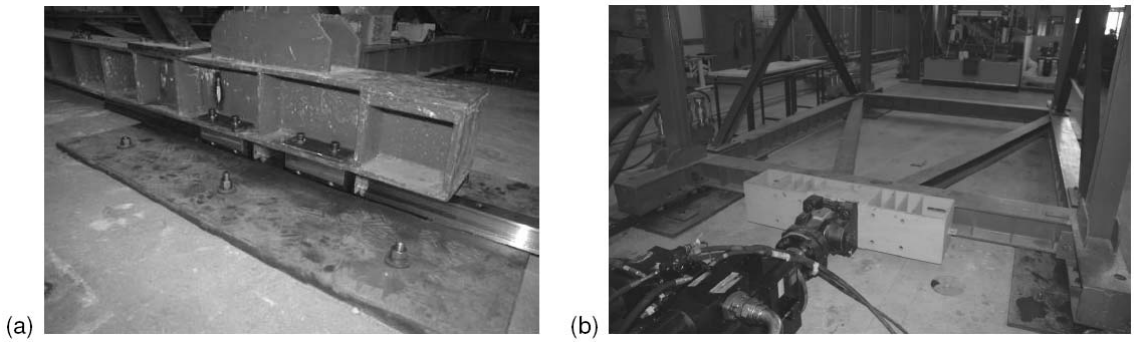

Figure 6.3: Shaking table rig: (a) SKF profile rail guide; (b) Model base.

The actuator applied force is measured by a piezoresistive load cell mounted at the actuator end. A total of 26 acquisition channels are employed to record the structural response. The horizontal displacements of each floor are measured by 4 Temposonic ±250mm digital transducers (2μm resolution) fixed to an external steel reference frame. Floor accelerations are recorded using a total of 8 horizontal servo-accelerometers (4 in the X-direction and 4 in the Y-direction, FGP, ±2g, model FA101-A2) and 1 vertical servo-accelerometer (±0.1g Columbia, model SA-107LN). The table-model base accelerations are recorded by 4 horizontal servo-accelerometers (2 in the X-direction and 2 in the Y-direction, ± 1g Columbia model SA-107LN) and the corresponding displacements by 1 Temposonic digital transducer, also fixed to the external steel reference frame. The remaining 8 input channels are used to measure forces of the energy dissipating devices by a total of 4 piezoresistive load cells (AEP, Mod. TC4: 10kN cells, 25kN cells and 50kN cells) mounted at the end of each device and their relative displacement by means of 4 Penny & Giles LP displacement transducers (±50mm, type HLP190/SA). Additional displacement transducers are added during

dynamic testing of the model equipped with semi-active energy dissipation devices designed in-house by the Research Units.

6.3 SEISMIC INPUTS

During testing, response of the structural model subjected to both natural and artificial earthquakes is assessed. In particular, the model is subjected to three different sets of earthquake records, each compatible with the response spectra of the Italian and European seismic code for A, B and D soil types. Specifically, the following seismic inputs are used:

i. a set of natural records obtained from the RELUIS web site (http://www.reluis.it) for plane analyses, compatible with the response spectrum provided by Eurocode 8 for soil type A, Seismic Zone 1 (Figure 6.3a);
ii. a set of natural records obtained from RELUIS web site (http://www.reluis.it) for plane analyses, compatible with the response spectrum provided by Eurocode 8 for soil type B, Seismic Zone 1 (Figure 6.3b);
iii. a set of artificial acceleration profile type Spectrum-compatible waveforms with the response spectrum provided by OPCM 3431 for soil type D, Seismic Zone 1 (Figure 6.3c).

Natural record acceleration values are scaled by using the Scaling Factor (SF) suggested by RELUIS. To ensure consistency with the scale of the model, all acceleration profiles are then scaled down in time by the factor $(1.5)^{1/2}$. During testing of the model equipped with energy dissipation systems, the seismic intensity is progressively increased from the initial value of 0.05g up to the attainment of the design performance criteria corresponding to a moderate and a high intensity earthquake [Ponzo *et al.*, 2008a and 2008b].

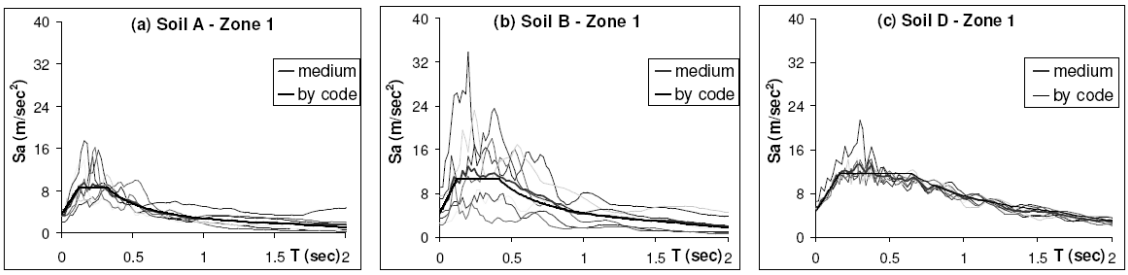

Figure 6.4: Elastic response spectra of sets of natural accelerograms for Seismic Zone 1 and (a) soil type A; (b) soil type B and (c) soil type D; time scaled by t/√1.5.

6.4 ENERGY DISSIPATING DEVICES

The Jet-Pacs Project has been supported by several partners from different Italian Universities which in turn have developed in-house a number of energy dissipation devices based on different materials and/or principles. During testing, a total of six different passive or semi-active energy dissipating devices based on currently available technologies (i.e. viscous and hysteretic damping) or innovative systems (i.e. shape memory alloy wires, magnetorheological fluids) are used, as summarised in Table 6.2. Below, a brief description of each device is given:

- the dampers provided by the research unit of the University of Naples are four nonlinear viscous fluid dampers manufactured by the Italian company FIP Industriale and characterized by a maximum nominal force of 50 kN and a constitutive law F=cv^a, where c=60 kN (sec/m) and a=0.15. The very low value of the velocity exponent allows a much higher energy dissipation capacity, compared to traditional linear viscous dampers;

- a highly non-linear fluid-viscous damper, manufactured by Jarret SL, France, is used by University of Udine. Its distinguishing mechanical characteristics are: total self-centering capacity, ensured by the pressurization of the inner casing; flow of the silicone fluid through a very narrow annular space between piston head and inner casing, which provides the highest normalized damping capacity of this type of dissipater within the class of viscous devices;

- two full-scale prototype semi-active magnetorheological (MR) dampers have been designed and manufactured by the German company Maurer Söhne for Parthenope University of Naples. The overall dimensions of the devices are 675mm (length) x 100mm (external diameter) and their mass is about 16 kg each.

A maximum force of 30 kN can be developed along its longitudinal axis, whereas the presence of special spherical pin joints at both ends prevents the rise of shear bending and torsional moment in the piston rod. The dampers have a stroke of ± 25 mm, and the external diameters of the piston head and of the piston rod are 100 mm and 64 mm, respectively. A magnetic circuit composed by three coils, each of them with a resistance R = 1.11 _ and an inductivity L = 92 mH, can generate the magnetic field in the device. The current in this circuit, in the range of i = 0÷3 A, is provided by a power supply commanded by a voltage input signal;

- the University of L'Aquila uses, as energy-dissipating devices, two magnetorheological dampers (Lord RD1005-3) positioned at the first floor. The

hysteretic properties of the magnetorheological fluids are modified by external magnetic fields induced by a pair of potential differences, namely the control inputs. The two independent command signals are determined on the basis of a clipped-optimal control in which a LQG control is designed to use the four acceleration measures at each floor. Different levels of control activities are considered [Gattulli *et al.*, 2008];

- the University of Basilicata tests a visco-re-centring device obtained by coupling two viscous fluid velocity-dependent energy-dissipating devices with a shape memory alloy (SMA) re-centring element [Ponzo *et al.*, 2008b]. The University of Basilicata, in cooperation with the University of Calabria, examines the seismic behaviour of elasto-plastic devices based on the hysteretic properties of steel plates capable of providing the necessary additional horizontal strength, stiffness and energy dissipation capacity whilst limiting interstorey drifts [Ponzo *et al.*, 2008a];

- the Polytechnic of Bari considers an hysteretic device obtained by considering an aluminum shear panel made up of a central aluminum plate and two lateral steel plates with 12 rectangular openings. The aluminium plate emerges in the steel openings to avoid slip phenomena. The steel plates provide the necessary stiffness and strength to the panel, while aluminum is the preferential energy dissipation area. The device has been optimized in order to have a wide plastic behaviour together with a low yielding interstory drift. The energy dissipating devices described above are mounted on the top of two stiff V-inverted steel braces (HEA100), as shown in Figure 6.1. Bolts ensure the rigid connection between the stiff braces and the experimental model. In order to ensure an adequate safety system, two additional V-inverted steel braces (UPN 80) have been constructed orthogonally to the test direction. The design criterion for all devices is to ensure the experimental model is maintained in its elastic condition during dynamic testing.

No.	Device Type	Manufacturer	Research Unit
1	Viscous fluids	FIP Industriale, Italy	University of Naples Federico II
2	Visco-elastic	Jarret	University of Udine
3	Magnetorheological fluids	Maurer&Söhne, Germany	University of Naples Parthenope
4	Magnetorheological fluids	LORD Corporation, USA	University of L'Aquila
5	Visco-re-centring	TIS Spa, Italy	University of Basilicata
6	Hysteretic	TIS Spa, Italy	Univ. of Basilicata and Univ. of Calabria
8	Hysteretic camper (TEC)	TEC S.r.l., Italy	Polytechnic of Bari

Table 6.2 Tested energy dissipation devices

6.5 DYNAMIC IDENTIFICATION TESTS

Structural dynamic identification tests of the JetPacs frame are carried out considering a number of different excitation sources: ambient noise, instrumental hammer impact excitations and sine-sweep ground motion induced by operating a nearby device test machine.

During the tests, three different mass configurations of the model are considered, obtained by using additional concrete blocks placed at each slab level, as shown in Figure 6.2: i) Basic Configuration (BC), with no additional masses; ii) Eccentric mass Configuration (NC), with two blocks at each storey level; iii) Symmetric mass Configuration (SC), with four blocks at each storey level (see Table 6.1 also). The model response is recorded by a total of 16 mono-directional servo-accelerometers (±0.1g, Columbia, model SA-107LN), of which 13 on the experimental model, 2 on the ground level and 1 on the test machine devices.

The experimental data acquired under various excitations for each mass configuration considered were used to obtain structural natural frequencies, masses, modal shapes and damping values. In order to obtain robust outcomes, the averaged values obtained from different only-output modal analyses techniques were considered.

In Table 6.3, dynamic test results are reported in terms of natural frequencies for each mass configuration. It is worth noting that almost identical results have been obtained by the research teams involved in the identification procedure.

Careful analysis of the results reported in Table 6.3 sheds light on the occurrence of two distinct experimental modes (denoted as IV°a and IV°b) instead of a single fourth mode, displaying relatively close frequencies and very similar modeshapes. These are clearly incompatible with the physical model and it appears that the global behaviour of the experimental model, in this configuration (without any dissipating device), is influenced by the transverse stiffness of the V-inverted rigid braces at the second floor, which acts as a Tuned Mass Damper (see Figure 6.1). In the dynamic test configuration of the controlled model this phenomenon vanishes because the V-inverted rigid braces are connected to the floor through the energy dissipation devices (see Figure 6.3). In Figure 6.5, the normalised shapes of the different modes, obtained by each Research Unit by means of an averaging procedure over the whole experimental test data, are shown and the model modal regularity is highlighted. In order to improve damping estimation accuracy, a rough calculation obtained from impact tests measurements yields a modal damping factor lower than 0.3-0.4% for the first three modes.

In Table 6.4, model mass identification parameters for each storey in the basic configuration are reported, as obtained by each Research Unit involved. The relatively small discrepancies observed can be accounted for by the different evaluation methods used [Ponzo *et al.*, 2007; Gattulli *et al.*, 2007; De Stefano *et al.*, 2008].

Configuration		BC	NC	SC
Mode	Dir.	Freq. (Hz)	Freq. (Hz)	Freq. (Hz)
I°	Uy	3.42	3.12	2.83
II°	Ux	4.20	3.81	3.61
III°	Rz	5.86	5.47	5.10
IV°a	Uy	9.40	8.90	8.42
IV°b	Ux	11.28	10.75	10.54
V°	Ux	14.65	12.99	12.41
VI°	Rz	18.75	17.39	16.40

Table 6.3: Natural frequencies of the experimental model

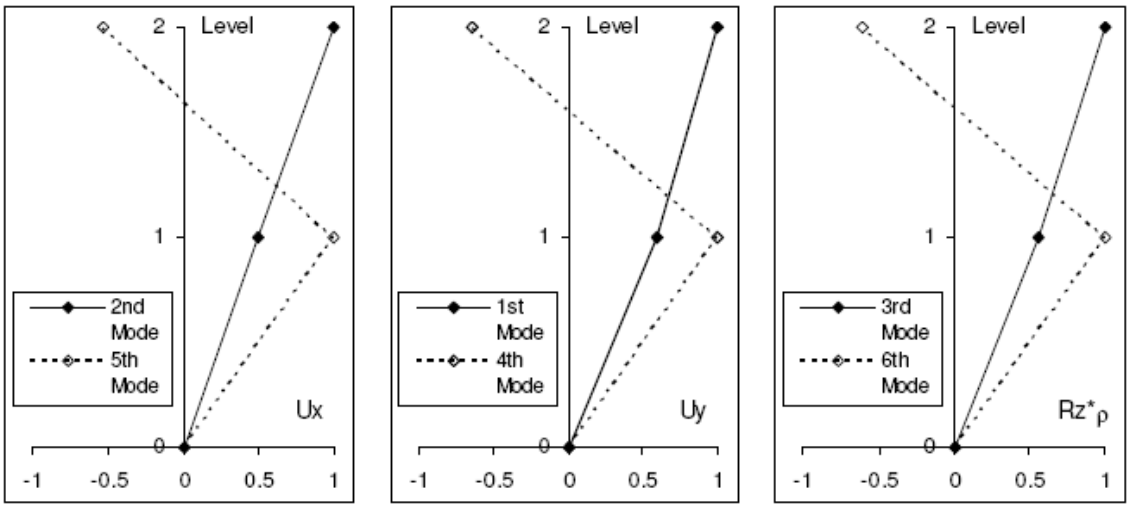

Figure 6.5: Model mode shapes of the SB configuration for the test direction

Configuration (BC)	UNIBAS	UNIAQ	POLITO	UNINA
Level	Mass (kg)	Mass (kg)	Mass (kg)	Mass (kg)
I°	3755	3391	3422	3607
II°	3412	3351	3214	3385

Table 6.4: Masses of the experimental model evaluated by different Research Units

6.6 DISCUSSION

An extensive dynamic experimental testing programme named JetPacs (Joint Experimental Testing on Passive and semi-Active Control Systems), involving partners

from several Italian Universities, has been scheduled to be carried out at the Structural Laboratory of the University of Basilicata.

In this section, the design of the JetPacs experimental scale model and the details regarding the model set up, seismic inputs used, test apparatus and sensor set up have been given. The results obtained from dynamic identification tests are reported, in terms of actual mass, fundamental periods of vibration, modal damping and mode shapes of the experimental model. It was shown that almost identical values of fundamental periods of vibration, modal damping and mode shapes have been obtained by each Research Unit. A lower than 10% difference in mass values has been observed, due to different evaluation methods adopted.

ACKNOWLEDGMENTS

The experimental seismic tests being carried out at University of Basilicata, in Potenza, as well as the dynamic characterisation tests already undergone on the scale steel model, are partially funded by the Italian Department of Civil Protection within the DPC-RELUIS 2005-2008 project (Research Line 7). Special acknowledgments are due to the researchers and technical staff involved in this project.

REFERENCES

9ISIED. (2005). Proc. 9th World Seminar on Seismic Isolation, Energy dissipation and active vibration control of structures. Kobe, Japan.

CEN, European Committee for Standardisation, TC340. (2004). Antiseismic devices. (Vers. 06-2004).

Cardone D., Di Cesare A., Dolce M., Moroni C., Nigro D., Ponzo F.C., Nicoletti M.. (2005). Dynamic tests on a 1:4 scaled r/c existing building: comparison of several isolation systems. 9th World Seminar on Seismic Isolation, Energy Dissipation and Active Vibration Control of Structures, Kobe, Japan.

Decreto Ministeriale 04/02/08 Norme Tecniche per le Costruzioni, Roma, 14 gennaio 2008.

De Stefano A., Matta E., Quattrone A.. (2008). Dynamic Identification and model-updating of the JETPACS prototype. DPC-RELUIS JETPACS Report No. 4.

Dolce M., Cardone D. and Ponzo F.. (2001). Comparison of different passive control systems for r/c frames through shaking table tests. Proc. 5th World Congress on Joints, Bearings and Seismic Systems for Concrete Structures, Rome, Italy.

Dolce, M., Cardone, D., Ponzo, F.C., Valente, C.. (2005). Shaking table tests on reinforced concrete frames without and with passive control systems. Int. Journ. of Earthquake Engineering and Structural Dynamics, Volume 34, Issue 14, Pages 1687-1717.

FEMA – ASCE 356. (2000). Prestandard and commentary for the seismic rehabilitation of buildings. Federal Emergency Management Agency and American society of civil engineering, Washington, DC, 2000.

Gattulli V., Lepidi M., Potenza F.. (2007). Identification of analytical and finite element models for the JETPACS three-dimensional frame. DPC-RELUIS JETPACS Report No. 2.

Ponzo F. C., Cardone D., Di Cesare A., Moroni C., Nigro D., Vigoriti G.. (2007). Dynamic tests on JET-PACS steel frame: experimental model set up. DPC-RELUIS JETPACS Report No. 3.

Ponzo F. C., Cardone D., Di Cesare A., Moroni C., Nigro D., Vigoriti G., Dolce M.. (2008a). JET-PACS project: dynamic test on steel frame equipped with hysteretic energy dissipating bracing system. 14th World Conference on Earthquake Engineering, October 2008, Beijing, China.

Ponzo F. C., Cardone D., Di Cesare A., Moroni C., Nigro D., Vigoriti G., Dolce M.. (2008b). JET-PACS project: dynamic test on steel frame equipped with visco-re-centring system. 14th World Conference on Earthquake Engineering, October 2008, Beijing, China.

CHAPTER 7

JET-PACS: AN AMBIENT VIBRATION TEST FOR BUILDING ROTATIONAL MODES IDENTIFICATION

Heavy structural damage on buildings subjected to seismic motion is frequently due to torsional effects. These effects have been extensively studied in the last years and incorporated in seismic codes. The standard approach for the experimental evaluation of such effects involves the installation of a multi-channel accelerometric system on buildings, either for continuous monitoring of earthquakes or to record forced vibrations. This time- and resource-consuming approach is usually applied to single buildings, but cannot be used in large scale studies in order to validate building code provisions or in quick estimations of building dynamic properties during vulnerability evaluations. In this section a simpler experimental set-up based on ambient vibration recordings, which is widely used for the identification of translational modes, is proposed. To validate the methodology the results with a full empirical and numerical experiment performed on a two-story steel frame were compared. A single high-resolution seismometer proves to be able to identify at least the first two torsional frequencies, while with more instruments it is possible to identify also the mode shapes.

7.1 INTRODUCTION

Heavy structural damage on buildings subjected to seismic motion is frequently due to torsional effects. In fact, due to torsional response, an uneven distribution of lateral loads can result, which can increase damage at key points in a structure, particularly when subjected to strong earthquakes.

Torsional effects can be caused by:

- irregular configuration in plan and/or in elevation;
- irregular distribution of masses and stiffnesses in plan and/or in elevation.

The configuration of a structure can significantly affect its behavior under seismic actions. Past earthquakes have frequently shown that buildings having an irregular configuration suffer higher damage than the regular ones.

The evaluation of torsional effects is an important topic in modern seismic engineering, both for new (e.g. CEN, 2003; UBC, 2000) and existing buildings having poor seismic design (e.g. NZEES, 2006; CEN, 2004, OPCM, 2003). Among the basic principles governing the conceptual design of new buildings, some are relevant to building configuration and regularity, such as uniformity, symmetry, torsional resistance and

stiffness. Specifically, uniformity in plan is achieved through an even distribution of the structural members, so that a short and direct transmission of the inertia forces created in the distributed masses of the building is allowed. Further, besides adequate lateral resistance and stiffness, building structures should possess also adequate torsional resistance and stiffness in order to limit the development of torsional motions which tend to stress the different structural members in a non-uniform way.

Criteria for regularity in plan and in elevation are provided in Eurocode 8 (CEN 2003), so that building structures can be classified as regular or non-regular. As regards to plan regularity, an important condition is minimizing the distance between the center of mass, where horizontal seismic floor forces may be assumed to be concentrated, and the center of stiffness. This result can be achieved if the distribution of lateral stiffness and mass of the building structure are approximately symmetrical in plan with respect to two orthogonal axes. As regards to elevation regularity, both the lateral stiffness and the mass of the individual story should remain constant or reduce gradually, without abrupt changes, from the base to the top. The distinction between regular and non-regular buildings has major implications on the design process, specifically concerning the choice of the structural model (planar or spatial), the method of analysis to be adopted, and the value of the behavior factor (i.e. the factor used for design purposes to reduce the forces obtained from a linear analysis in order to account for the non-linear response of a structure) which shall be decreased for buildings non-regular in elevation.

In NZEES (2006), plan and vertical irregularities are considered among the critical structural weaknesses in the assessment of performance of existing buildings.

While modern standards discourage design of irregular buildings, existing buildings designed without seismic criteria, may have severe plan and elevation irregularities. As already said, such irregularities can give rise to higher than normal ductility demands on some structural members. Post-earthquake field inspections show many cases of structural damage, up to partial or total collapse, that can be attributed to torsional effects, particularly in building structures with L and U-shaped plans or having a very stiff off-center core (see Fig 7.1a and b).

A remarkable example of such a behavior is provided by the damage distribution detected after the Mexico City earthquake, where torsional effects were recognized as one of the main factors causing building failure (Rosenblueth and Meli 1986).

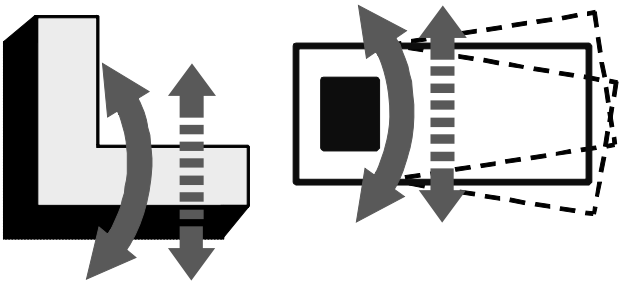

a) b)

Figure 7.1: a) Torsional effects created by irregular shape of building plan (L configuration) and by irregular distribution of plan stiffness (Bertero, 1985); b) Torsional failure of the second story of the Hotel Terminal, Guatemala City, during the 1976 Earthquake (courtesy of USGS Photo Library).

Torsional effects have been extensively studied in the last years. Many analytical and experimental works (e.g. Stathopoulos and Anagnostopoulos 2005) have been carried out in order to tackle this question. In particular, in the last years, laboratory experiments have been carried out by using shaking-table or pseudodynamic tests to better understand the seismic behavior of structures subjected to torsional effects as well as to improve the efficiency of structural models and code provisions.

The standard seismological contribution to this topic is the continuous monitoring of structures with permanent accelerometric arrays and the subsequent analysis of the recorded earthquakes. In the meantime, the research group of DiSGG (Department of Structure, Geotechnics and Engineering Geology) carried out both experimental (Mucciarelli and Gallipoli, 2007) and numerical studies (Masi and Vona, 2008) to evaluate the translational dynamic behavior of the existing buildings in a simplified and cheaper way. This approach could be beneficial for large-scale seismic vulnerability studies, because of the current developments of new methods for seismic risk estimation based on the dynamic properties of existing buildings.

Of course, this goal cannot be attained with continuous earthquake monitoring of building. Modern technologies allow to perform in a relatively short time (10-15 minutes) an assessment of the translational dynamic properties of a single building with ambient noise, thus allowing to study a large number of constructions with a limited effort.

This section describes a fast experimental set-up aimed at identifying also the structural torsional effects. The main aim of this work is to investigate the dynamic properties of a 2/3 scaled 3D frame in the Structural Laboratory of the University of Basilicata using a low level of excitation (ambient noise) and an simple instrumentation. In this work, the microtremor measurements on the steel frame are compared with the experimental results obtained by a classic dynamic identification technique using accelerometers and forced vibrations. The proposed methodology has some advantages; among them, the simplicity of instrumentation set-up, and the reduced amount of data and, therefore, of time and money resources required.

7.2 EXPERIMENTAL TECHNIQUE

In order to identify the dynamic characteristics of the structures, different techniques can be used depending on types and location of the structures, required range of motion amplitude and available economic resources. In seismic areas, the structures can be instrumented to record their response to a seismic input. This requires earthquake occurrence to gather data, thus in the past 50 years (since Sparks, 1935) alternative techniques were proposed to evaluate the dynamic behavior of buildings.

With regard to excitation source, the main difference concerns the location of structures to be tested. In a laboratory, the motion is controlled by means of shaking tables or hydraulic jacks. These methods cannot be applied on an existing building in the field, where three different kinds of excitation are used: shocks or impact action (transient), harmonic forcing induced by shaker (sinusoidal), ambient vibrations (random). These techniques have been used for decades, since the pioneering works of Blume (1935) with vibrodynes, and of Crawford and Ward (1964) with ambient (wind) excitation.

Shock tests are performed by impacting the upper part of the building in the two main directions by means of a backhoe. This method is used if the building has to be demolished, as it could cause heavy damage on the structure. Otherwise, tests can be realized by means of a mass impacting on the ground nearby the building. In both methods the excitation is a short impulsive action with a peak ground acceleration approximately equal to 10^{-2}g. A mechanical shaker (vibrodyne) can be used to induce a frequency-varying, constant-amplitude sinusoidal horizontal acceleration to identify the dynamic behavior of the building using a resonance approach. The peak ground acceleration obtained with this technique is about $10^{-4} – 10^{-3}$g. A less common approach is the pull and release test, that can be applied either to base isolated buildings

(Mucciarelli *et al.*, 2003) or also to buildings to be demolished (Gallipoli *et al*., 2006). Ambient noise technique is often disregarded, as it is a low accuracy (the peak acceleration ground is about 10^{-5}g), even though it shows the lowest costs and the greatest simplicity. This is probably due to the same reason that adversely affected noise techniques for the study of soil properties: the widespread use of accelerometers instead of high resolution seismometers (Mucciarelli, 1998). Recent works have demonstrated the reliability of ambient vibration. Yuen *et al*. (2002) proved that the stationarity hypothesis is not needed, and that transient-rich noise can provide building identification with a single output measurement without knowing the input motion. Gallipoli *et al*. (2004) showed that with ambient noise it is possible to detect the presence of soil-structure interaction and also to detect structural damage by determining the frequency shift of the buildings. Hans *et al.* (2005) demonstrated how the estimated fundamental frequency is substantially invariant when using impacts, forced vibration or ambient noise.

Ambient vibration is the most promising solution when large sets of building are examined for vulnerability studies considering the possible presence of soil-building resonance (Navarro *et al.*, 2004, Mucciarelli and Gallipoli, 2007).

7.3 DESCRIPTION OF THE EXPERIMENTAL MODEL

The test structure, known as Mock-up Frame (Ponzo *et al.*, 2007), is a two-storey 3D steel frame (Figure 7.2). This model is a part of an extensive program of dynamic experimental tests, named Jet-Pacs (Joint Experimental Testing on Passive and semi Active Control Systems), carried out at the Structural Laboratory of the University of Basilicata, developed within the DPC – RELUIS 2005-08 Project, Research Line 7. The frame, with one bay in each horizontal direction, is a 2/3 scaled model of a full-scale frame. The plan frame dimensions are 3.00 m × 4.00 m, and the inter-story height is 2.00 m. Floors are made of a 100 mm thick steel-concrete slab connected to the main beams in the longer direction. The floors can be considered as infinitely stiff in their own plane. The beams have the same section (IPE 180) in both directions and at both stories, as well as the four columns that have constant cross section (HEB 140) at both stories. Fe360 grade steel has been used for the structural members, having Young modulus E=206000 N/mm^2 and yield strength f_y=235 N/mm^2. All structural members have been designed considering dead and live loads for civil residential buildings. Moreover, because the 3D frame has been mainly designed to test the effectiveness of

seismic control techniques based on different energy dissipating bracing systems, at both stories two stiff V-inverted steel braces have been mounted, on top of them the energy dissipating devices will be placed during the seismic tests. Finally, the test structure has been bolted on steel beams (HE220B section) used to connect it to the hydraulic jack for forced vibrations.

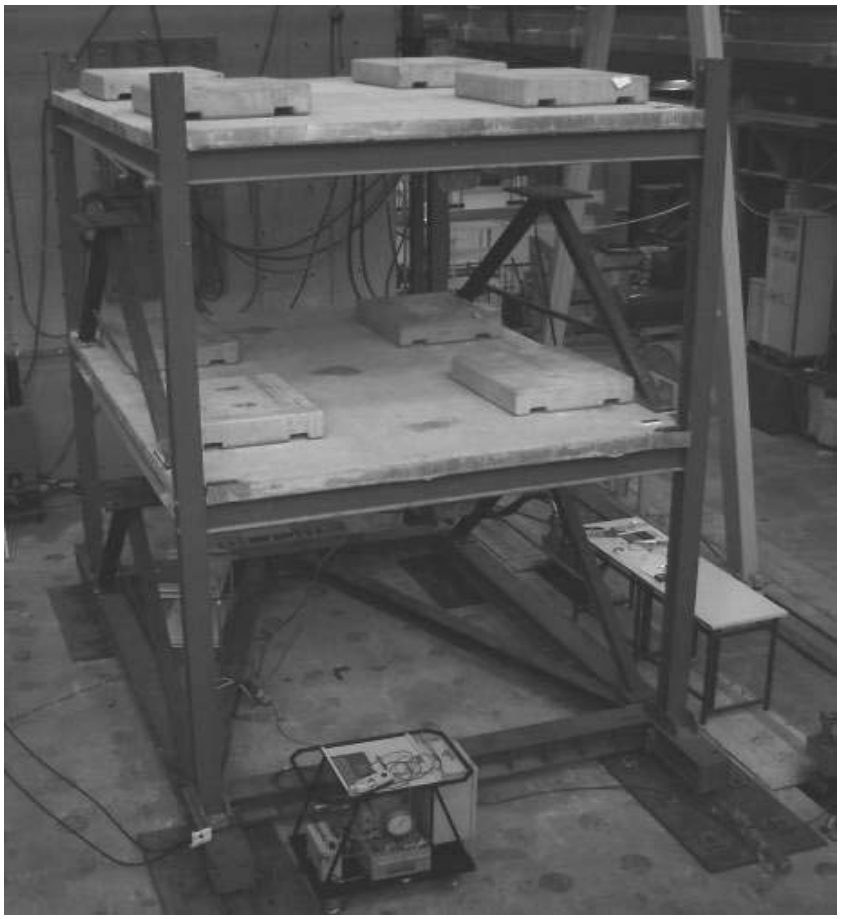

Figure 7.2: The two-story, 3D steel frame with additional masses in places, ready for the tests. Note the four inverted-V-shape supports for the damping system, not yet mounted.

The experimental tests have been carried out with additional lumped masses located at each story. These masses are 8 concrete blocks (4 on each story) of equal weight (about 3450 N), representing both dead and live loads considered in seismic design.

7.4 RESULTS OF TESTS

To validate the methodology proposed in this section, the results obtained have been compared with those obtained by a standard method based on an accelerometer apparatus. The dynamic identification (Ponzo *et al.*, 2007) was carried out using 15 acquisition channels to adequately capture the structural response due to forced vibrations.

The dynamic characteristics of the 3D frame, have been identified carrying out a measurement campaign using a digital tri-directional tromometer (Tromino Micromed) that is a tri-directional geophone attached to a 24 bit A/D converter whose dynamic is devoted to measure the lowermost part of the amplitude range. Compared with standard accelerometers used for building monitoring, this kind of instrumentation could easily saturate if used for recording earthquakes, but has better performances when used to record ambient noise. 10 minutes of ambient noise at 256 Hz have been sampled (thus allowing to resolve the second decimal digit in frequency analysis). In the first experimental set-up, four instruments were synchronized using a built-in GPS receiver. In such a way, the records have been processed with an unique reference time. One digital tri-directional tromometer has been placed in the corner of each floor from the bottom to the top along the same vertical (Fig. 7.3, top), and another tromometer has been placed in the center of last story.

With this first experimental set-up both the natural frequencies and the modal shapes of the first six modes have been identified. The results are synthesized in Fig. 7.4, where the continuous and dotted line are relevant to the FFT of recordings at middle and top level of the frame respectively, normalized to the corresponding component at the base. The frequency of the first mode (f1=2.84 Hz) is characterized by translation in Y direction while the frequency of the second mode (f2=3.56 Hz) is characterized by translation in X direction. The third mode is a torsional one characterized by a frequency equal to 5.12 Hz. The three higher modes repeat the same sequence (Y, X, R) of the fundamental ones. Moreover, a frequency attributed to the inverted-V steel brace is identifiable. In order to confirm this identification, a measurement has been carried out directly on V-inverted steel braces, and has provided an out-of-plane frequency equal to 10.53 Hertz.

Mode shapes have been estimated in time domain. Once the mode frequencies had been determined, the time histories were filtered with a pass-band filter, with 1 Hz band amplitude centered around each frequency. Overlapping all the time histories recorded at different levels, the mode shape was estimated normalizing each curve at a given instant. The timing for the normalization can be selected according different criteria, e.g. maximum value at the last level, local maximum, etc. In this study the maximum value at the last level was used.

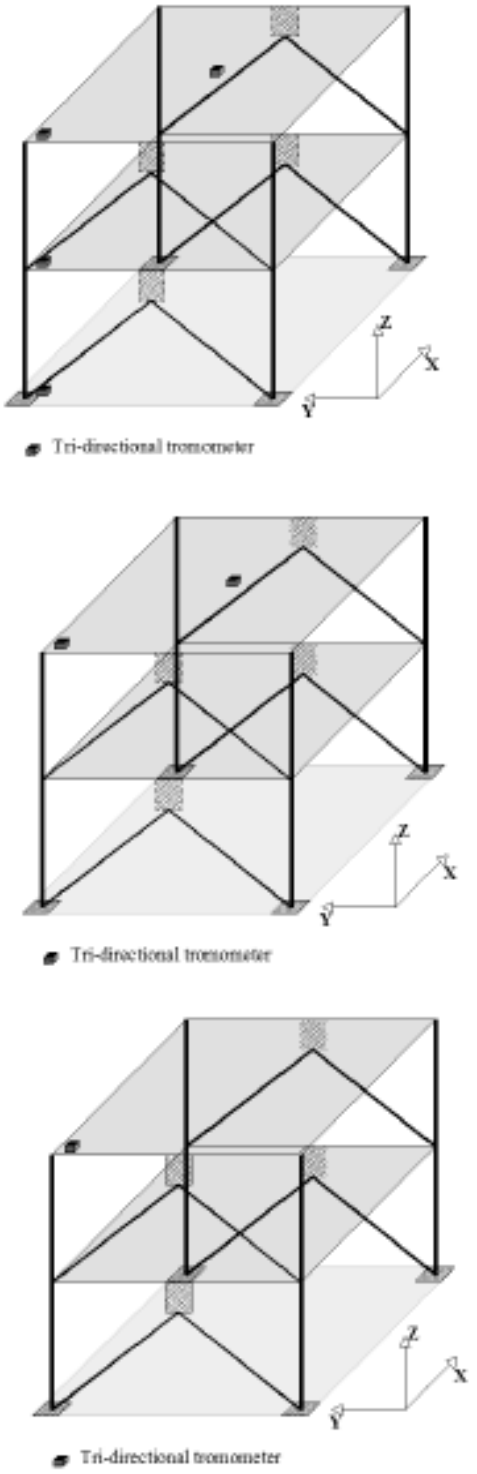

Figure 7.3: The three different set-up of the instrumentation used in the experiment. Top, with four tromometers; middle, with two instruments; bottom, the stand-alone configuration.

The results obtained using ambient noise and tromometers are in good agreement with those obtained by the accelerometer monitoring of forced vibrations; the differences between natural frequencies are negligible (Table 7.1) and the modal shapes are practically coincident (see Figure 7.5).

	I Mode	II Mode	III Mode	IV Mode	V Mode	VI Mode
	Trasl. Dir Y	Trasl. Dir X	Rot. Z	Trasl. Dir Y	Trasl. Dir X	Rot. Z
	f (Hz)	f (Hz)	f (Hz)	f (Hz)	f (Hz)	f (Hz)
Tromometer	2.83	3.56	5.12	8.43	12.38	16.34
Accelerometers	2.83	3.61	5.08	8.40	12.41	16.22

Table 7.1: Comparison between the frequencies obtained using ambient noise recorded by tromometers and those from the accelerometric monitoring of forced vibrations.

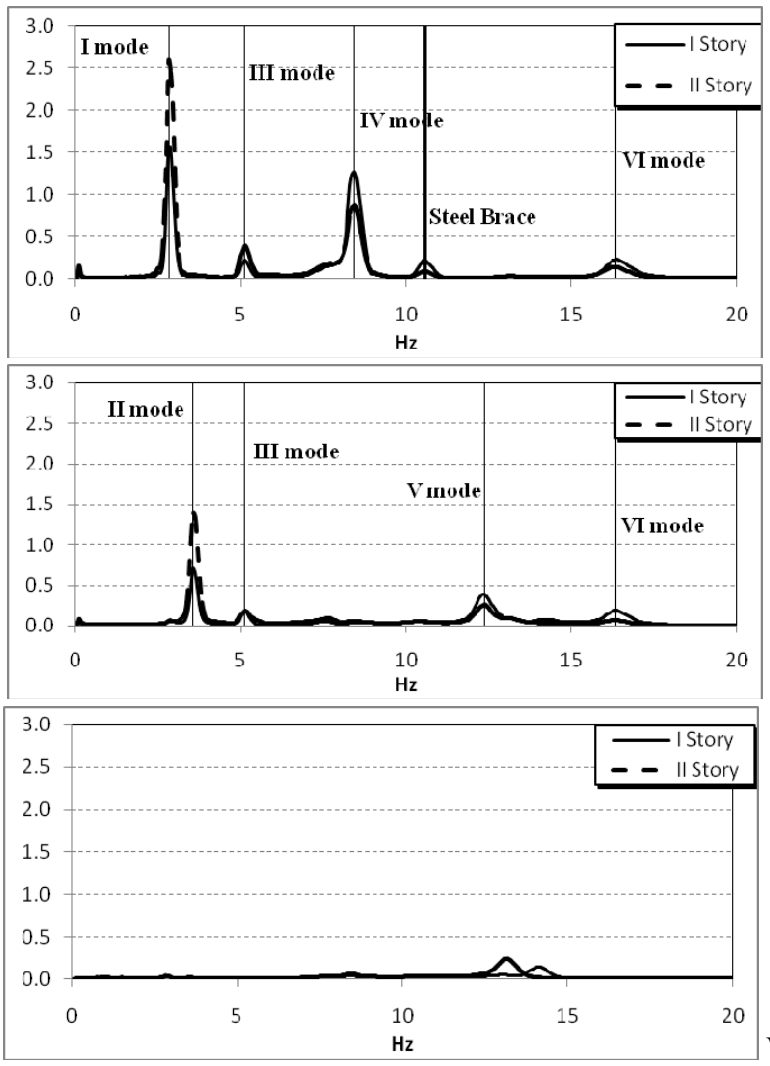

Figure 7.4: Frequency identification for the steel frame using the instrument configuration of fig. 3-top. Each FTT is normalized to the corresponding component at the base level.

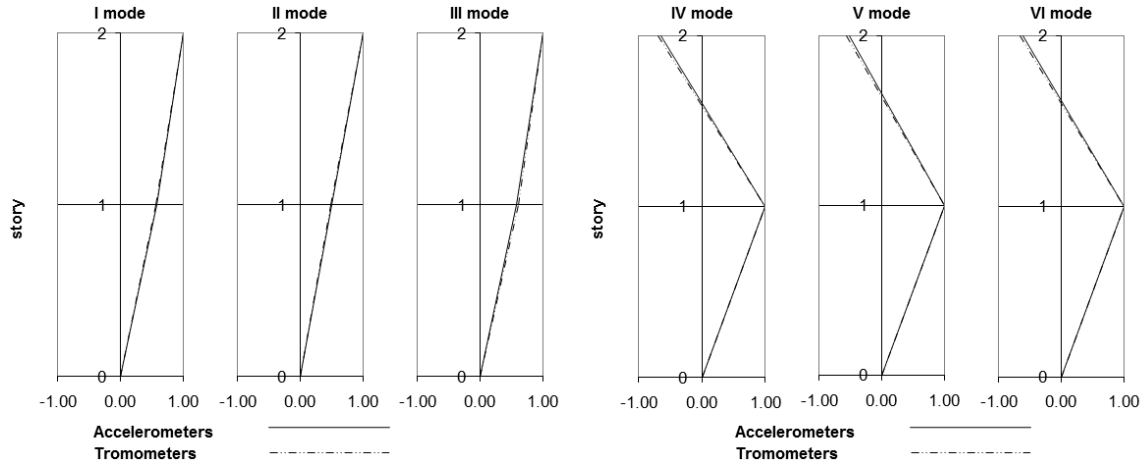

Figure 7.5: Comparison between the mode shapes obtained using ambient noise recorded by tromometers and those from the accelerometric monitoring of forced vibrations.

This result encouraged to try different procedures to perform the ambient noise measurements with a simpler instrumental set-up.

The procedure based on a tromometer at each floor is very accurate but time-consuming when applied on existing buildings. One instrument could be left at the base while another one is moving across upper floors, but for a building of ***N*** floors this would require at least ***N*** x 10 min. Moreover, a good knowledge of the first six frequency (including the two rotational ones) would be more than enough for several practical applications, even without complete knowledge of the mode shapes.

Different procedures based on two or one tromometer located at the last floor have thus been investigated, in order to check whether these methods are able to predict at least the frequency of the torsional fundamental mode. In a first step, one tromometer was placed in the corner and another in the center of the upper story (Fig. 7.3, middle). The ratio between the FFT of the 10 minutes time histories, using the central instrument as a reference (hereinafter Corner to Center Ratio, CoCeR) was then evaluated. Fig. 7.6 shows the CoCeR for one of the two components (the other returns obviously the same frequencies). The results obtained agree with those of Tab. 7.1, with the first and the second rotational frequency slightly above 5 and 16 Hz, respectively. It is interesting to note that an additional peak appears at about 13 Hz, corresponding to the frequency of the vertical component (see Fig. 7.4), that can be interpreted as the frequency of a rocking mode.

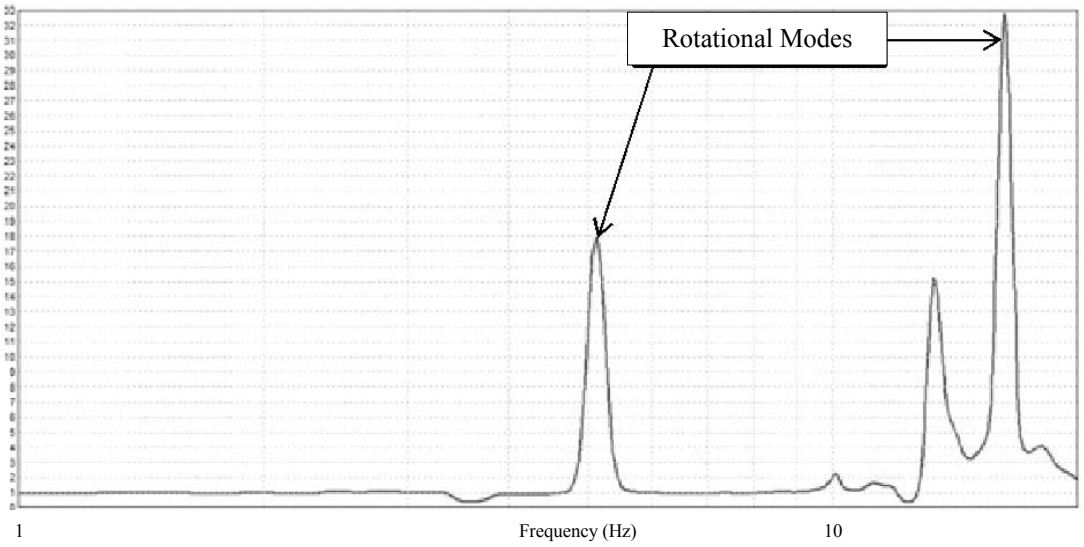

Figure 7.6: Corner to Center Ratio for one horizontal component at the last floor.

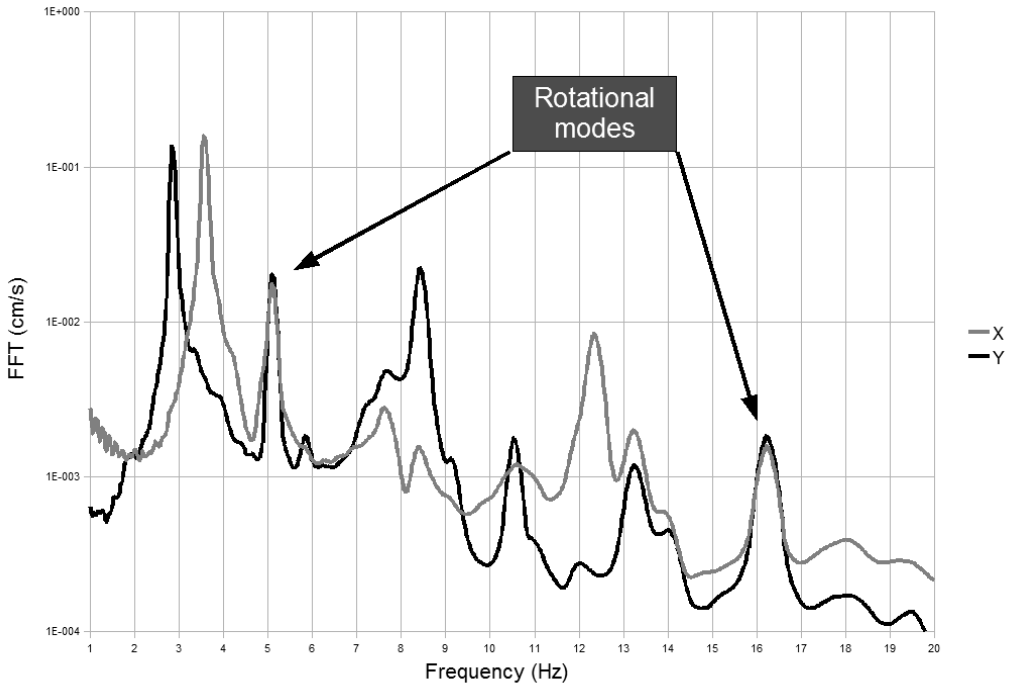

Figure 7.7: FFT of the horizontal components; ambient noise, 10 minute recording at the top level.

Finally, the capability of this methodology to identify the frequency of the first six vibration modes using just one tromometer placed in the corner of the upper story has been checked. Figure 7.7 shows the results. The six frequencies identified with the first set-up are clearly visible. The two fundamental translational frequencies are the easiest to be identified. The second translational modes are clearly visible, even if it is obviously impossible to demonstrate that their amplitude is larger at mid-height. The

rotational modes are perfectly identified, since their amplitude is equal on both components.

7.5 DISCUSSION

The identification of torsional modes is very important in the seismic vulnerability assessment of existing buildings. In the practice it would be desirable to perform quick but reliable empirical estimate of building dynamic characteristics, in order to study large sets of building structures. The results of a laboratory experiment based on forced vibrations of a 3D steel frame with three different set-ups recording ambient noise were compared. With the most complete system it is possible to retrieve mode shapes that are practically identical to those ones obtained by forced vibrations. With two instruments located at the top floor, using CoCeR it is possible to separate global rotational modes from rocking modes. Even with the stand-alone configuration it is possible to retrieve the six first modes of the structure in the horizontal plane, including the first two rotational modes.

REFERENCES

Bertero, V.V., (1985), Introduction to Earthquake Engineering, National Information Service for Earthquake Engineering (NISEE) Web site (http://nisee.berkeley.edu/bertero/).

Blume J. A. (1935) A machine for setting structures and ground into forced vibration, Bull. Seism. Soc. Am.; 25, 361-379

Bousias S. N., Fardis M. N., Spathis A.L., Kosmopoulos A. J. (2007), Pseudodynamic response of torsionally unbalanced two-storey test structure, Earthquake Engineering And Structural Dynamics ; 36:1065–1087.

CEN (2003). Eurocode 8: Design of structures for earthquake resistance, Part 1: General rules, seismic actions and rules for buildings, Final Draft, Comite Europeen de Normalisation (CEN), Brussels, December 2003.

CEN (2004). Eurocode 8 - Design of structures for earthquake resistance - Part 3: Assessment and retrofitting of buildings (draft n. 6), Comite Europeen de Normalisation (CEN), Brussels, May 2004.

Crawford, R. and H. S. Ward (1964). Determination of the natural periods of buildings, Bull. Seism. Soc. Am. 54, 1743-1756.

Gallipoli M. R., M. Mucciarelli, R. R. Castro, G. Monachesi, P. Contri, (2004), Structure, soil-structure response and effects of damage based on observations of horizontal-to-vertical spectral ratios of microtremors, Soil Dyn. Earthq. Eng., 24, 487-495.

Gallipoli M. R. , M. Mucciarelli, F. Ponzo, M. Dolce, E. D'Alema, M. Maistrello (2006) Buildings as a seismic source: analysis of a release test at Bagnoli, Italy, Bull. Seism. Soc. Am., 96, 2457–2464.

Hans S., Boutin C., Ibraim E., Roussillon P. (2005), In situ experiments and seismic analysis of existing buildings. Part I: Experimental investigations, Earthquake Engineering And Structural Dynamics; 34:1513–1529.

Hudson, D. E. (1962). Dynamic tests of buildings and special structures, Experimental Techniques in Shock and Vibration, Am. Soc. Mech. Engr., 81-91.

Mucciarelli M., 1998, Reliability and applicability range of the Nakamura's technique, Journ. Earthq. Eng., 2, 4, 625-638

Mucciarelli M. Gallipoli M. R., Ponzo F.C., Dolce M., (2003), Seismic waves generated by oscillating buildings: analysis of a release test, Soil Dynamics and Earthquake Engineering, 23 255–262.

Mucciarelli M., M. R. Gallipoli, (2007), Non-parametric analysis of a single seismometric record to obtain building dynamic parameters, Ann. Geoph., 50, 259-266

Navarro M., F. Vidal, M. Feriche, T. Enomoto, F. J. Sánchez, I. Matsuda (2004) Expected ground–RC building structures resonance phenomena in Granada city (Southern Spain), Proc. 13th World Conference on Earthquake Engin.,Vancouver, B.C., Canada, August 1-6, 2004, Paper No. 3308.

NZSEE (2006). Assessment and improvement of the Structural Performance of Buildings in Earthquakes, Recommendations of a NZSEE Study Group on Earthquake Risk Buildings, June 2006.

OPCM 3274 (2003). Ordinanza del Presidente del Consiglio dei Ministri del 20 marzo 2003 "Primi elementi in materia di criteri generali per la classificazione sismica del territorio nazionale e di normative tecniche per le costruzioni in zona sismica", May 2003, (in Italian).

Ponzo F.C., Cardone D., Di Cesare A., Moroni C., Nigro D., Vigoriti. G. (2007) Dynamic tests on jetpacs steel frame: experimental model set up, Executive Project DPC – Reluis 2005 – 2008 Research Project No. 7, Report No. 3 .

Rosenblueth E. and Meli R. (1986). The 1985 Earthquake: Causes and Effects in Mexico City, Concrete International, Vol. 8, No. 5, May 1986, pp. 23-34.

Sparks N. R. (1935) Building vibrations, Bull. Seism. Soc. Am.; 25, 381-386.

Stathopoulos K.G. and Anagnostopoulos S.A. (2005). Inelastic torsion of multistorey buildings under earthquake excitations, Earthquake Engineering and Structural Dynamics, No. 34, pp. 1449–1465.

UBC, (2000). Uniform Building Code. International Conference of Building-IBC, California, U.S.A..

Yuen K.-V., J. L. Beck and L. S. Katafygiotis (2002) Probabilistic approach for modal identification using non-stationary noisy response measurements only, Earthquake Engng Struct. Dyn. 31:1007–1023 (DOI: 10.1002/eqe.135)

CHAPTER 8

EXTRACTING MODAL PARAMETERS BY USING A BAND-VARIABLE FILTER

One of the main tools used to study the dynamic response of systems is certainly the Fourier transform. This tool is very useful and reliable if one wants to investigate the response of a stationary system, i.e. a system that does not change its characteristics over time. Conversely, when one wants to study the evolution of the dynamic response of a system whose features vary with time, the Fourier transform is no longer reliable. In this regard, several mathematical tools were developed to study time-variable dynamic responses. Soil and buildings, subject to transient forcing such as an earthquake, may change their characteristics over time with the initiation of nonlinear phenomena. In most cases, both for soil and buildings, abandoning the linear elastic field could represent a problem. This paper proposes a methodology to approach the study of non-stationary response of soil and buildings: a band-variable filter based on S-Transform. In fact, thanks to the possibility of changing the bandwidth over time, it becomes possible to extract from a generic signal only the response of the system focusing on the variation of individual modes of vibration. This section starts from examples and applications on synthetic signals and then examines possible applications to the study of the non-stationary response of soil and buildings.

8.1 INTRODUCTION

Generally, the study of the evolution over time of dynamic characteristics of a system has been addressed in an approximate way trying to stationarize it by using techniques that might not be appropriate. For example, one of the main tools used to analyze dynamical systems is the Fourier transform, which for a function h(t) holds:

$$H(f) = \int_{-\infty}^{+\infty} h(t) \cdot e^{-\mathrm{i} \cdot 2 \cdot \pi \cdot f \cdot t} dt \qquad \text{(Equation. 1)}$$

This technique, like all tools which have their basis on the assumption of stationary behavior of the system, appears to be not appropriate when one wants to perform studies on systems that change over time. In this context the concept of change is considered as the time evolution of dynamic parameters that characterize the system under study. In fact, passing to evaluate the Fourier Transform of a non-stationary

signal, what ensues is a graph in the frequency domain which allows to evaluate the average size of each spectral amplitude, assessed on the entire length of the analyzed signal. It is immediately obvious that the transient phase of the signal, which appears to be a fraction of the whole signal, it is completely distorted.

Another tool widely used to study the transients is the STFT (Short Time Fourier Transform) (Gabor 1946). This technique exceeds certain limits of the simple Fourier transform, giving us some indications on the variation over time of the spectral characteristics of analyzed signal. For a signal h(t) the SFTF is defined as:

$$STFT(\tau, f) = \int_{-\infty}^{+\infty} h(t) \cdot w(t-\tau) \cdot e^{-\mathrm{i} \cdot 2 \cdot \pi \cdot f \cdot t} dt \qquad \text{(Equation. 2)}$$

Unfortunately also this integral transformation has some limits which tend to distort the result. Indeed, the values of the moving-averaged spectral magnitudes have no absolute value, but may be used only for relative comparing. In order to assess the STFT it is necessary to choose the length of the time-window; this choice cannot be done arbitrarily, but it is bound by the necessity of having a good resolution both in time and in frequencies domain. In order to have a good time resolution, choose a very narrow short time-window has to be selected, but this would result in a very low resolution in the frequency domain. On the contrary, in order to have a good frequency resolution, a very wide time-window should be used. In the end, depending on the problem that one wants to address, it is necessary to perform a suitable choice of the time-window length. In recent decades, several techniques for time-frequency signals analysis have been developed. The most widely used are the Wavelet Transform and the Wigner-Ville Distribution. These transformations, for a signal h(t) are defined respectively as:

$$F(a,b) = |a|^{-\frac{1}{2}} \int_{-\infty}^{+\infty} h(t) \cdot w^*\left(\frac{t-b}{a}\right) dt \quad \text{where a and b are two scale factors} \qquad \text{(Equation. 3)}$$

$$WD(\tau, f) = \int_{-\infty}^{+\infty} h\left(\tau + \frac{t}{2}\right) \cdot h\left(\tau - \frac{t}{2}\right) \cdot e^{-\mathrm{i} \cdot 2 \cdot \pi \cdot f \cdot t} dt \qquad \text{(Equation. 4)}$$

These other transformations present a number of advantages compared with the Fourier transform and the STFT, but do not allow a fair assessment of the local spectrum. In other words, these instruments are insufficient to a correct evaluation of the spectral characteristics taking into account the instantaneous variations.
A tool that overcomes these limitations and allows to assess accurately both the spectral characteristics and their local variation over time is the S transform (Stockwell *et al.*, 1996). This transformation, for a signal h(t), is defined as:

$$S(\tau, f) = \frac{|f|}{2\pi} \int_{-\infty}^{+\infty} h(t) \cdot e^{-\frac{(\tau - t)^2 \cdot f^2}{2}} \cdot e^{-i \cdot 2 \cdot \pi \cdot f \cdot t} dt \qquad \text{(Equation. 5)}$$

where t is time, f is frequency and τ is a parameter that controls the position of Gaussian window along the time axis. As it has been defined in the transformation, the properties of Gaussian window scale derive from the continuous wavelet (Mallat 1998). However, the condition of zero mean for the wavelets it is not satisfied. Furthermore, compared to the wavelet transform, the S-Transform changes the shape of the real and imaginary coefficients over time together with the temporal translation of the Gaussian window. On the contrary, the wavelet transform does not have this property: the entire waveform translates over time, but never changes its shape (Parolai 2009). The S-Transform has also many important properties. For example, the S-Transform can be written as an operator that is function of the Fourier spectrum (Stockwell *et al.*, 1996):

$$S(\tau, f) = \frac{|f|}{2\pi} \int_{-\infty}^{+\infty} H(\alpha + f) \cdot e^{-\frac{2 \cdot \pi^2 \cdot \alpha^2}{f^2}} \cdot e^{-i \cdot 2 \cdot \pi \cdot \alpha \cdot \tau} d\alpha \qquad \text{with } f \neq 0 \qquad \text{(Equation. 6)}$$

Furthermore, it can be shown that (Stockwell *et al.*, 1996):

$$H(f) = \int_{-\infty}^{+\infty} S(\tau, f)\, d\tau \qquad \text{(Equation. 7)}$$

It is thus possible to completely recover the function h(t) by using the following relation (Stockwell *et al.*, 1996):

$$h(t) = \int_{-\infty}^{+\infty}\left(\int_{-\infty}^{+\infty} S(\tau, f)\, d\tau\right) \cdot e^{i\cdot 2\cdot\pi\cdot f\cdot t}\, df \qquad \text{(Equation. 8)}$$

The last, but not the least important property is the linearity of the S-Transform (Stockwell *et al.*, 1996):

$S\{data(t)\} = S\{signal(t)\} + S\{noise(t)\}$ where *S* stands for *S-Transform*

(Equation. 9)

Thanks to this property it is possible to extract the processed information by the signal of interest, without altering its characteristics.

8.2 BAND-VARIABLE FILTER (S-filter)

In the past, many authors have tried to develop methods to clean up a generic recorded signal from noise (Weaver *et al.*, 1991; Donoho and Johnstone, 1994; Donoho, 1995; Douglas, 1997; Galiana-Merino *et al.*, 2003). Eq. 9 suggested the possibility to filter the signals using the Stockwell transform (Pinnegar and Eaton, 2003; Schimmel and Gallart, 2005; Ascari and Siahkoohi, 2007; Simon *et al.*, 2007; Parolai, 2009).

This section discusses the possibility to use the S-filter to extract the dynamic characteristics of systems, in particular for soil and buildings, that evolve over time by acting simultaneously in both frequency and time domain. The filter was built using the properties of convolution, linearity and invertibility of the S-Transform. The algorithm on which the method for filtering is based can be summarized in a few steps:

1- Assessment of S-Transform $S(\tau, f)$ of the signal *h(t)*;

2- Generating the matrix filtering $G(\tau, f)$;

3- Calculating convolution in the frequency domain $M(\tau, f) = G(\tau, f) * S(\tau, f)$;

4- Assessment of the filtered signal $h_f(t)$ through the calculation of the inverse S-transform matrix $M(\tau, f)$.

$$h_f(t) = \int_{-\infty}^{+\infty}\left(\int_{-\infty}^{+\infty} [S(\tau, f) * G(\tau, f)]\, d\tau\right) \cdot e^{i\cdot 2\cdot\pi\cdot f\cdot t}\, df \qquad \text{(Equation. 10)}$$

Several kind of windows were tested, but in order to obtain a both flexible and dynamic tool and considering the results obtained from each test (not shown here), the tapered-cosine window shown in Figure 8.1 was used to build the filtering matrix $G(\tau, f)$.

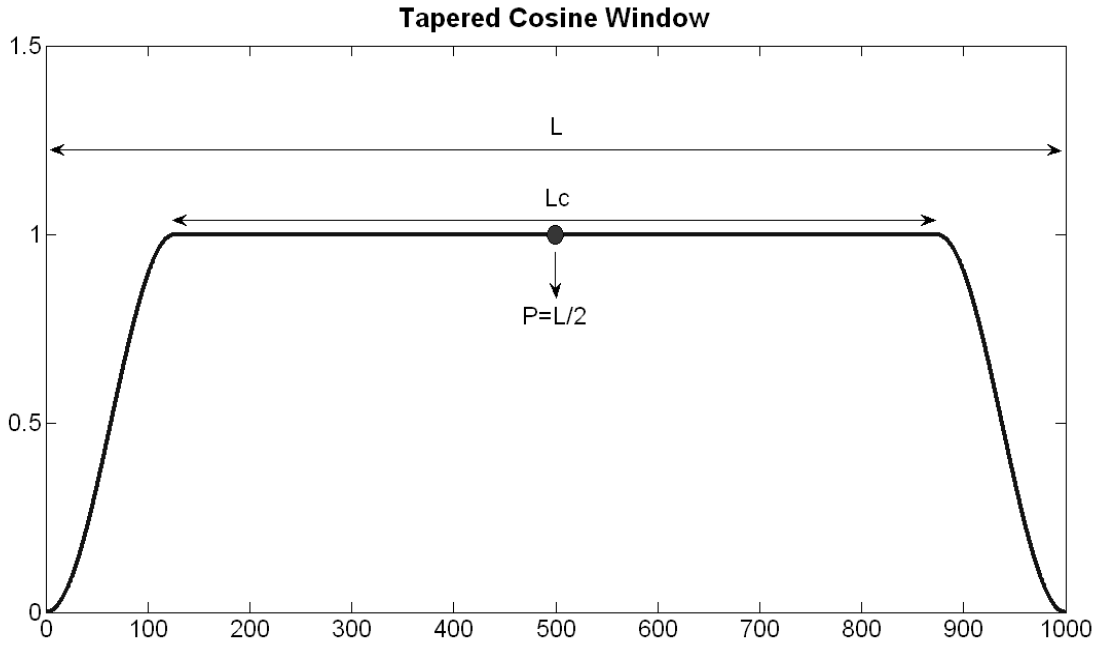

Figure 8.1: Example of tapered-cosine window used for build the filtering matrix.

This window identifies a generic $G(\tau_k, f)$. For the correct definition of the filtering window it is necessary to define the total width of the window (L) and the width of the constant section identified by Lc. In this work, after several tests a constant was chosen:

$$r = \frac{L - Lc}{L} = 0.25 \qquad \text{(Equation. 11)}$$

Moreover, it is necessary to define from time to time, the total width of the window. This width can be chosen bearing in mind that the number of points that make up a single window can be evaluated using the following relation:

$$Np(1Hz) = \frac{Lt}{fs} \qquad \text{(Equation. 12)}$$

where *Lt* is the signal length in time domain (expressed in percentage) and *fs* is the frequency sampling. In fact, if the window filtering has sizes smaller than $S(\tau, f)$ it is

necessary to insert zeros up to the length (in frequency) of the matrix. The definition of the filtering matrix could be a time-demanding operation. In order to simplify this process, it is convenient to try to automate it. The implementation proposed defines the array selecting the local spectrum using a graphical user interface (GUI). The selection of points is done by clicking with the mouse cursor on the screen window where the time-frequency matrix is plotted. The cursor represents the midpoint *P* of the window filtering. The routine is designed so that the user can select a few points and the computer performs a linear interpolation. The algorithm was implemented in Matlab ©.

8.3 APPLICATION ON SYNTHETIC SIGNAL

In order to demonstrate the functionality of this tool several tests on different kinds of non-stationary signals have been performed.

A synthetic non-stationary signal, with a superimposed transient is considered first. Consider a synthetic non-stationary signal, that it is slowly changing frequency over time. The signal length is equal to 22 sec with 1 sec of zeros at beginning and end. Apart from the zeros, the initial frequency is 11 Hz, in the central part reaches the minimum frequency, equal to 3 Hz, and then returns at a frequency equal to 11 Hz. The frequency variation follows a parabolic law. The signal is plotted in Figure 8.2a. This signal was summed with a signal with unitary amplitude, like the former one, and a constant frequency equal to 9 Hz. The result is a non-stationary signal with frequency variable with a strong disturbance in the central part, corresponding to the minimum values of the frequency of the main signal. It should be noted that the frequency of the disturbance is contained within the range of variation of the main signal, and this could be an insurmountable problem when using a classical approach.

Figure 8.3a reports the sum of the signals, while Figure 8.3b shows the Fourier spectrum of the same signal.

It is evident from the spectrum shown in Figure 8.3b, that looking only at the Fourier spectrum it is impossible to distinguish the main signal from noise, and using a traditional filter it would be impossible to eliminate the interference without affecting the original signal. It is in situations like this one, that a filter with variable band-pass can allow to isolate the main signal from noise. To identify the different components from the signal, the S-Transform has to be evaluated.

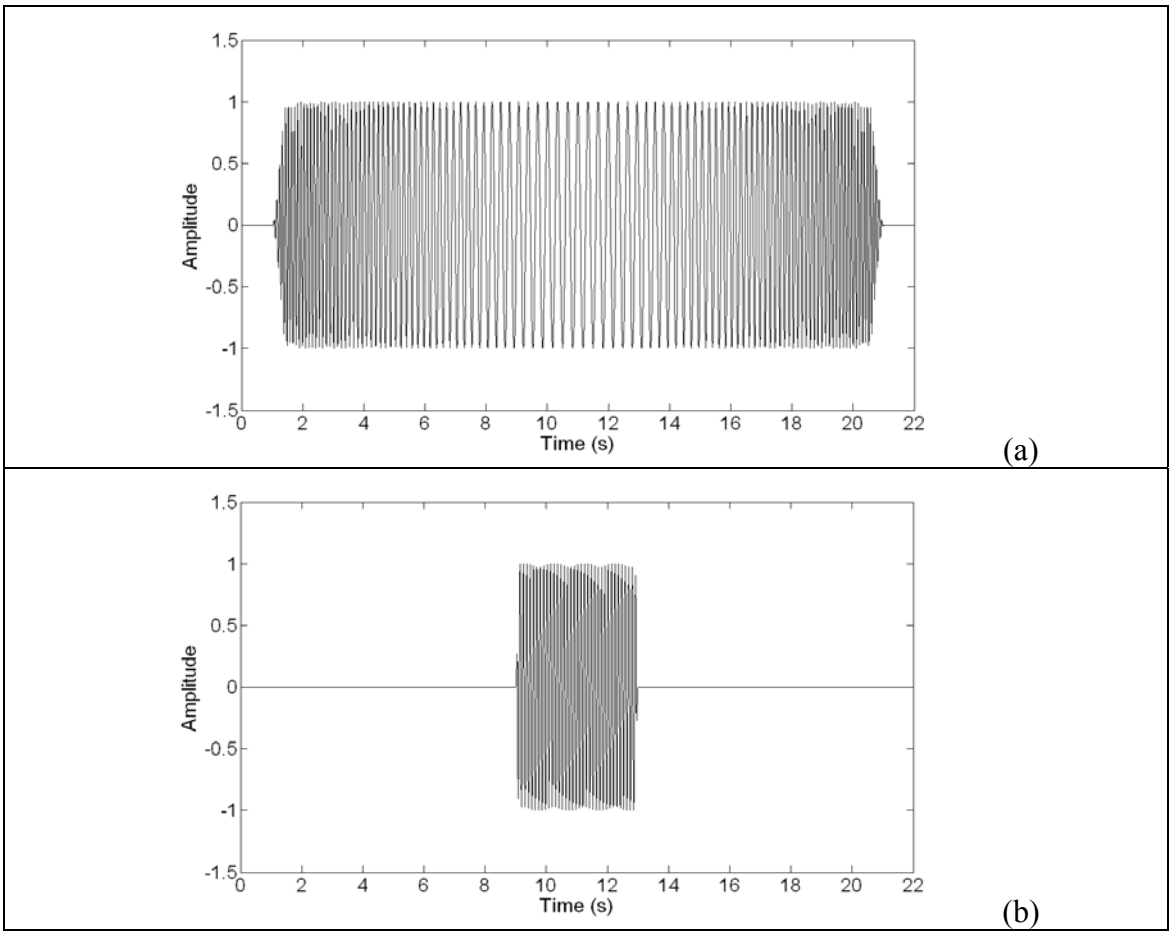

Figura 8.2: (a) Frequency variable sinusoid. (b) Constant amplitude sinusoid

From Figure 8.4a it is evident the advantage of using the S-Transform in place of the classical Fourier transform. In fact, observing the figure enables to distinguish clearly the two signals and the variation of the energy content over time.

As an example the filtering matrix used to eliminate the interference is shown in Figure 8.5b.

Figure 8.5a shows the GUI construction of a filtering matrix. The local spectrum is selected using the mouse cursor. The green curve represents the set of points P, central to the filtering window. The width of the window, as mentioned above, is chosen so as to be able to isolate the spectrum of interest; in this case, based on the information extracted from S-Transform, a width of 3.60 Hz was chosen, corresponding to a number of Np points equal to

$$Np = \frac{Lt}{fs} \cdot 3.63 = 80 \qquad \text{(Equation. 13)}$$

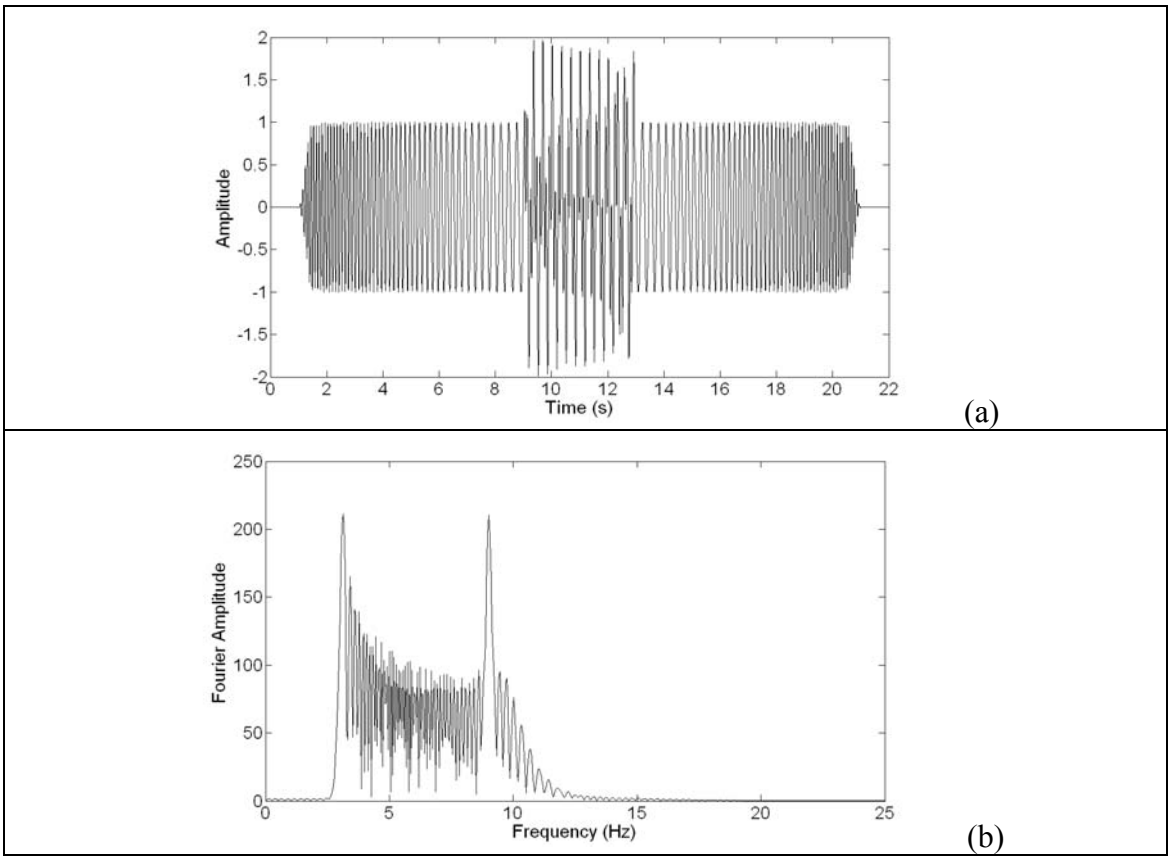

Figure 8.3: (a) Signal and noise. (b) Fourier spectra.

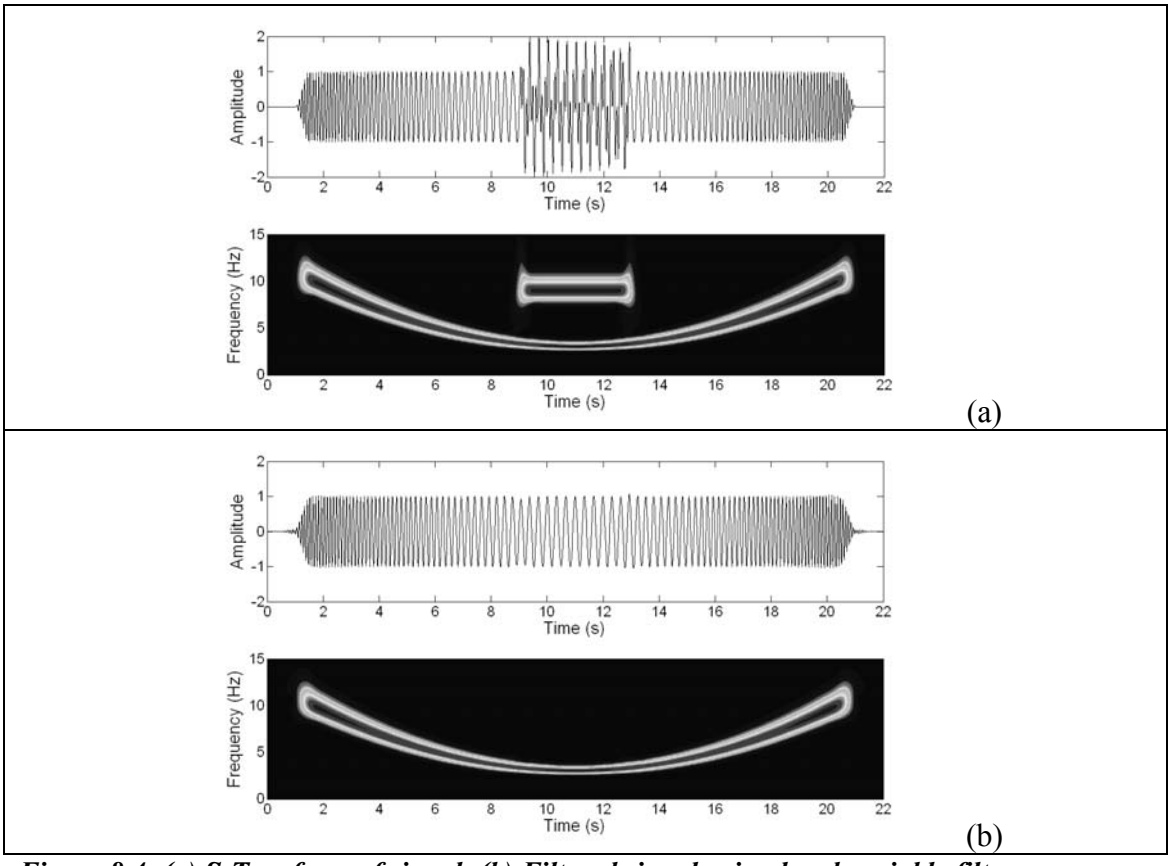

Figure 8.4: (a) S-Tansform of signal; (b) Filtered signal using band-variable filter.

Obviously, the remaining part of each local spectrum, is filled with zeros (Figure 8.5c). It is important to underline that the values used to construct the filter box are all real numbers, then the part of the complex matrix resulting from the calculation of the S-Transform is not altered. The result is a matrix filtering that changes the amplitude without altering the phases of the signal (Figure 8.5b). This procedure provides a variable band-pass filter that yields a filtered signal with the phases corresponding to those of original signal. Similarly to what was done to extract the variable frequency signal, the component that have been referred to as interference can be easily extracted.

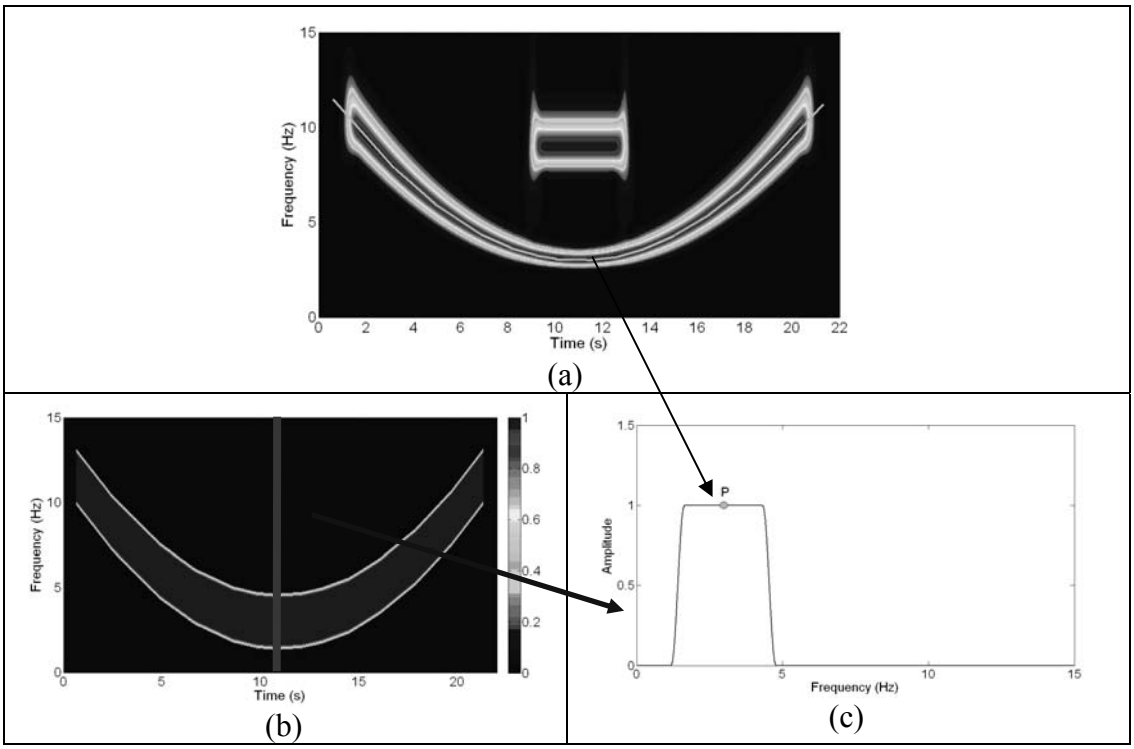

Figure 8.5: Example of filtering procedure.

8.4 APPLICATION ON REAL DATA: SOIL AND BUILDINGS

To demonstrate how it is possible to pick from a real recording only the information of interest, three real case histories are presented: the first signal was recorded during an experimental campaign on a full-scale structure, the second one was recorded on a building while it was being damaged by an aftershock of the Molise earthquake (Italy) in 2002 and the third one was registered during the Kobe earthquake in 1995 in a site where soil suffered severe non-linearity leading to liquefaction.

During the Bagnoli experiment (Gallipoli *et al.*, 2006), developed in order to test several shape-memory devices for retrofitting buildings, it was also possible to study the radiation effects of buildings on the free-field ground motion (Ditommaso *et al.*, 2009a). Several release tests were performed on the monitored building, thanks to a

contrast frame structure that was moved from the equilibrium condition and was left moving in free oscillations. The tests were numerous and in different conditions of degradation of the building. In order to monitor the behavior of the structure in different conditions and equipped with various devices, several control devices have been installed on the building and on the surrounding area. Thanks to the presence of the accelerometers installed in the surrounding area it was possible to record the ground motion caused by the oscillating building. Figure 8.6 shows the displacements recorded at a station placed 10 m away from the building, the S-Transform for registration and a zoom in the frequency range 0-3 Hz where most of the energy released from the structure was detected.

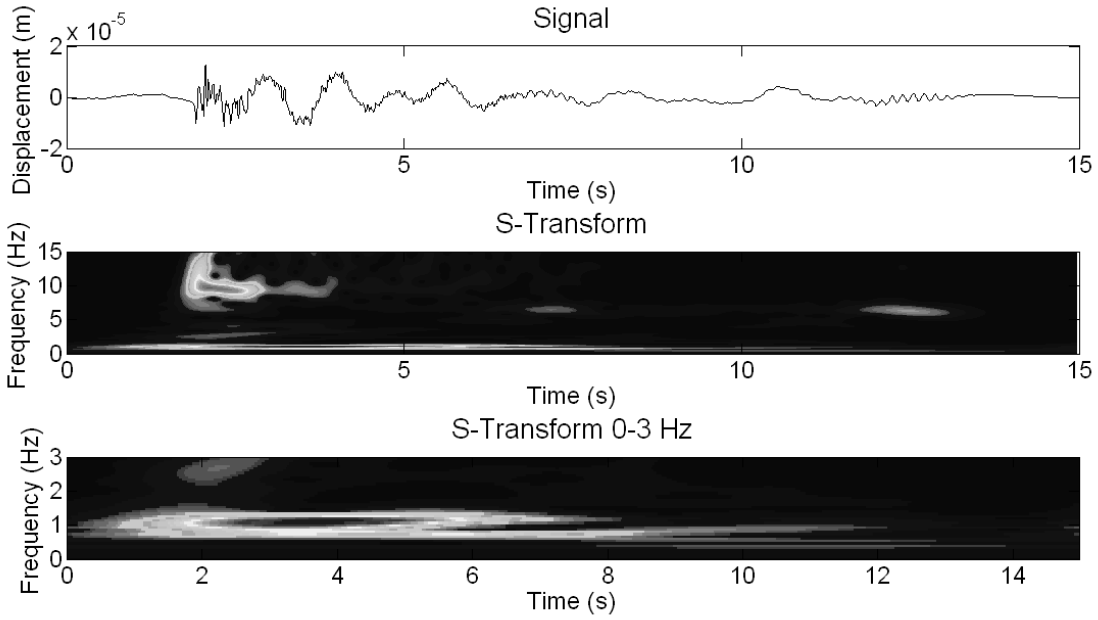

Figure 8.6: Free-field recording at 10 m from building.

At this point, using the band-variable filter it was tried to isolate the principal mode of vibration from higher modes and noise content. In order to extract the local spectrum varying over time a total width for the window filtering equal to 1 Hz was set.

The result (Figure 8.7) shows that it is possible to extract from a real signal the local spectrum with higher energy content that is varying over time as expected, due to the stiffening of the system caused by the shape-memory devices. Moreover, it is possible to avoid the phase distortions that can be introduced by standard causal filters.

The second example is taken form the seismic sequence in Molise (Italy). The town of Bonefro suffered as little damage (I_{MCS} = VII) except for two reinforced concrete buildings that have suffered serious damage. These buildings are very similar, both as

design and construction, and are located near to each other in an area where the surface layers appear to be formed by soft sediment.

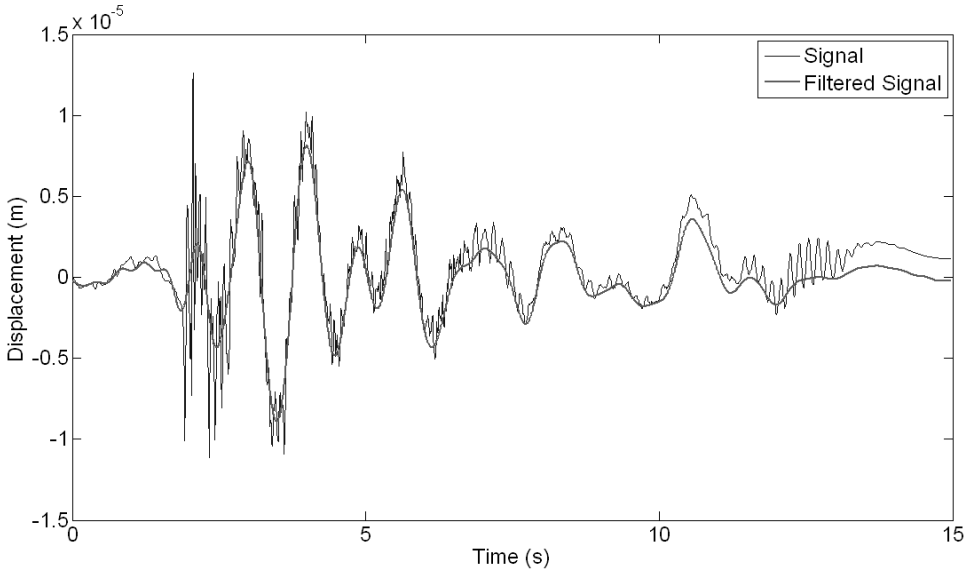

Figure 8.7: Comparison between filtered and original signal.

The main difference between the two buildings appears to be the height. The most damaged building has 4 floors, while the less damaged has three floors, and hence should be stiffer. As a result of the earthquake of the first of November (M 5.3) the tallest building had an additional damage to structural parts. Fortuitously, a seismometer located within the building recorded the seismic response of the building during the progression of damage (Mucciarelli *et al.*, 2004). Obviously, the building has exhibited a strongly non-linear behavior, leading to a 40% decrease of the frequency of the fundamental mode. Event recordings for the two orthogonal components in the horizontal plane are shown in Figure 8.8 with the respective S-Transform.

It is clear that notwithstanding the saturation of the seismometer during the event, it is possible to follow the evolution of the seismic behavior of the building in the time-frequency domain. A detailed study, of the behavior of this building and the possible effects of double resonance soil-structure carried out according to different methodologies was performed by Mucciarelli *et al.* (2004). At this point the attention is focused on the NS component of the recorded motion of building. Using the S-Transform analysis it is evident that the building starts from a frequency equal to 2.2 Hz, reaches the minimum frequency during the maximum excitation around 1.2 Hz before recovering in the final part of the signal at about 1.8 Hz. At this point it was tried to isolate the response of the building using the band-variable filter. Looking the S-

Transform result for the signal, it is clear that to isolate the building response is sufficient to take a width of the filtering window equal to 1 Hz.

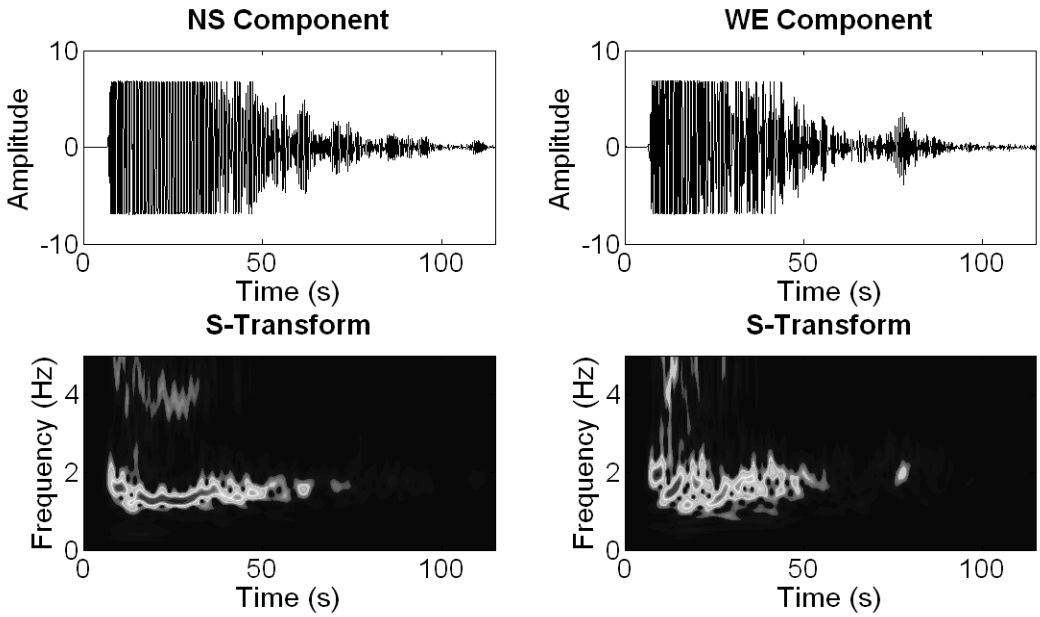

Figure 8.8: Velocimetric recordings within the building (Bonefro).

The result of filtering is shown in Figure 8.9. It is very interesting to see that, thanks to the selection of the local spectrum, the S-filter tool is able to reconstruct the dynamic response of the structure, with a negligible amount of noise even during non-stationary response. If the recordings at all levels of the building are available, it is possible to study the behavior of individual modes of vibration and their variation over time.

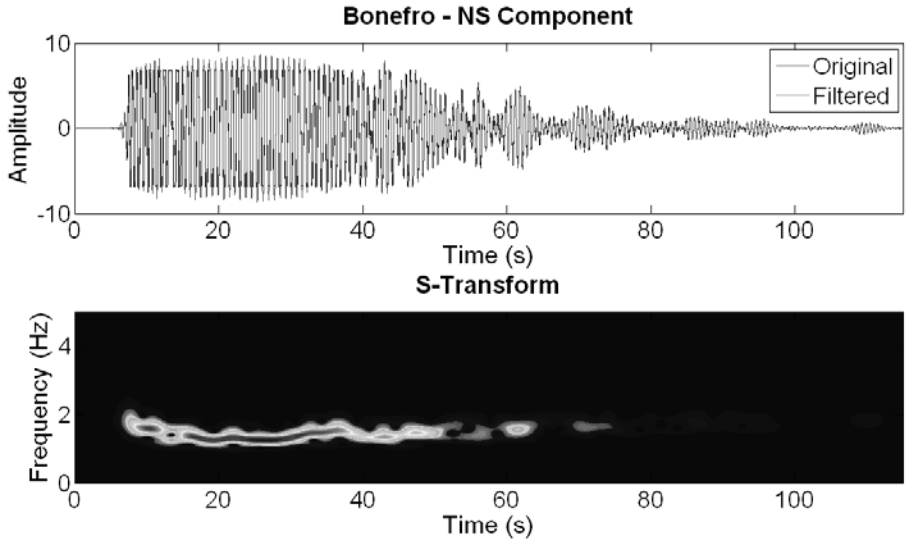

Figure 8.9: Extracting non-stationary behavior of the main mode of the structure.

It is obvious that if, during the seismic response of a building changes in the dynamic behavior of individual modes of vibration are observed, the structure is changing its dynamic characteristics, very likely due to damaging.

The band-variable filter has been finally used to extract the fundamental ground response during the Kobe earthquake (Japan) in 1995. The site of Port Island during the earthquake experienced soil liquefaction and thus a large variation of stiffness for the surface layers resulting in a variation of the main frequency of oscillation.

Figure 8.10 reports the NS component of the recording for Kobe earthquake at Port Island site, acquired in free-field conditions. The signals recorded during this earthquake have been extensively studied (Aguirre and Irikura 1997) along with all the data acquired, even at different depths.

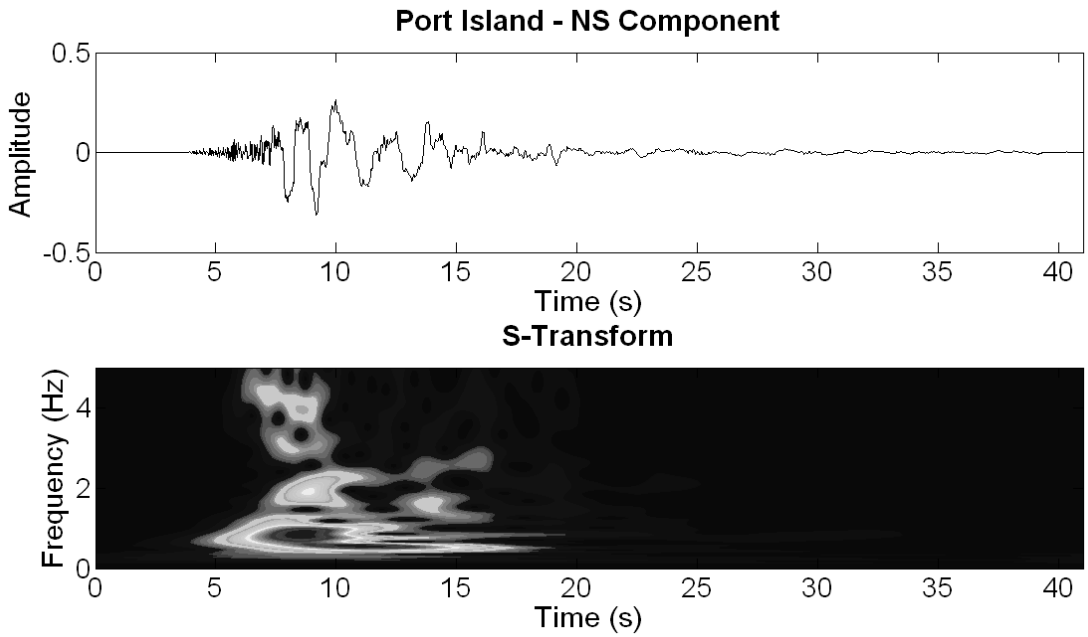

Figure 8.10: NS Component of Kobe earthquake recording.

Analyzing the S-Transform of the signal it is clear that most of the energy is concentrated in a single mode of vibration, and sharp frequency changes after just one cycle are observed. Following the frequency change, which known to be due to liquefaction of the subsoil, no stiffness recovery is observed, at least in this short period of time. It was tried to extract information about the characteristics of the first mode of vibration of the soil, trying to remove from the registration all the noise and the response of potential higher modes. For this purpose a filter with a window width equal to 1 Hz was used. S-Transform of the filtered signal and the comparison between the

two signals is shown in Figure 8.11. It is evident that also in this case the filter yields very interesting results.

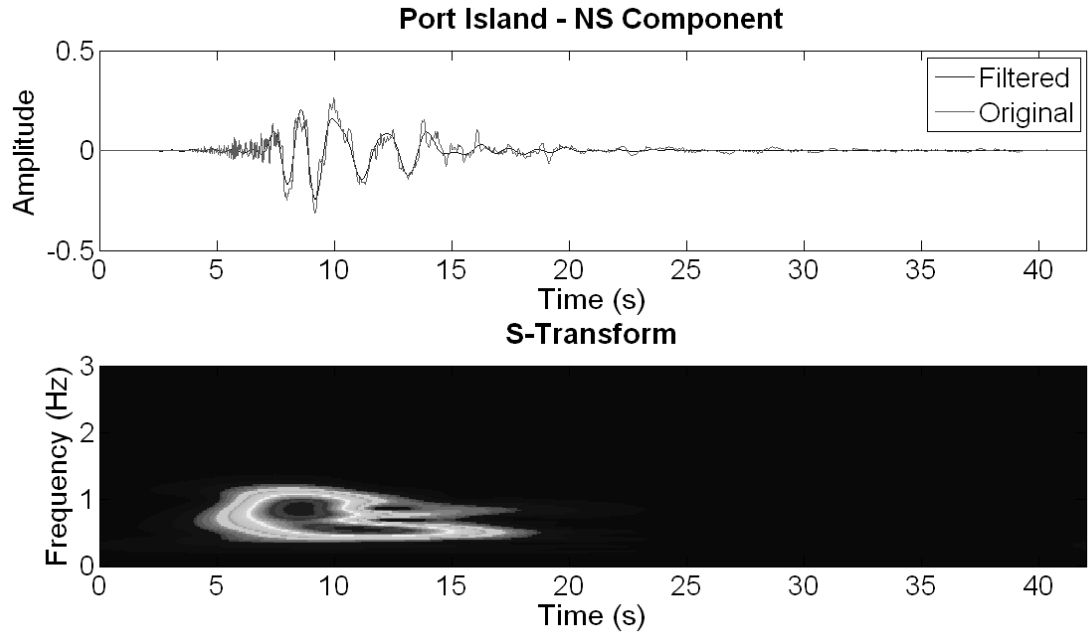

Figure 8.11: Band-variable filter application on Kobe earthquake recording (NS component).

As depicted in Figure 8.11 only the response of the main mode of vibration was extracted and the signal phase was preserved. This important characteristic had already been observed for the previous comparisons.

The possibility to extract the main modes of vibration preserving the signals phase allows to study a multiple degree of freedom systems, observing the time-variable dynamic response of each oscillating mode.

8.5 DISCUSSION

Researchers who deal with signal analysis and dynamic characterization of systems are in search of mathematical tools that enable them to study in detail the phase of non-stationary response of a dynamic systems. It is well known that classical techniques based on Fourier transform provide good results when the response of the system is stationary, but completely fail when the system exhibits a nonlinear behavior. In order to have classical techniques fail, it is not necessary that a building reaches damage: even the non-stationarity of the input and the possible interaction with the ground and/or adjacent structures can show the uselessness of classic techniques (Ditommaso *et al.*, 2009b) .

In 1996, Stockwell introduced a new powerful tool for the signals analysis: the S-Transform. Compared with the classical tecniques for the time-frequency analysis, this

transformation shows a much better resolution and also offers a range of fundamental properties, such as linearity and invertibility. By exploiting these properties, it was possible to developed a filter whose band varies both in time and in frequency domains, which is very useful to study the characteristics of nonlinear signals. This tool becomes necessary if it is required to isolate the response of individual modes of vibration, of soil and buildings, their dynamic characteristics evolving over time as a result of vibration due to seismic events. The ability to investigate the nonlinear response of soils and buildings opens new scenarios, gives us the opportunity to explore new possibilities. For example, the ability to isolate individual modes of vibration of a building makes possible to explore their variation over time, evaluating the change in modal curvature. It is known that this parameter is strongly linked to the building damage during a seismic event (Pandey *et al.*, 1991). Therefore, being able to evaluate the modal curvature during the maximum excursion in nonlinear field and isolating it from superimposed signals, a better understanding of the mechanisms of damage can be obtained and a more precise location of the damage on the structure can be achieved.

REFERENCES

Aguirre, J., and K. Irikura (1997). Nonlinearity, Liquefaction, and Velocity Variation of Soft Soil Layers in Port Island, Kobe, during the Hyogo-ken Nanbu Earthquake. Bulletin of the Seismological Society of America, Vol. 87, No. 5, pp. 1244-1258, October 1997.

Askari, R., and H. R. Siahkoohi (2007). Ground roll attenuation using the S and x-f-k transforms. Geophys. Prospect., Vol. 55, pp. 1–10.

Ditommaso, R., M. Mucciarelli, M. R. Gallipoli and F. C. Ponzo (2009a). Effect of a single vibrating building on free-field ground motion: numerical and experimental evidences. Bulletin of Earthquake Engineering. DOI: 10.1007/s10518-009-9134-5.

Ditommaso, R., S. Parolai, M. Mucciarelli, S. Eggert, M. Sobiesiak and J. Zschau (2009b). Monitoring the response and the back-radiated energy of a building subjected to ambient vibration and impulsive action: the Falkenhof Tower (Potsdam, Germany). Bulletin of Earthquake Engineering. DOI: 10.1007/s10518-009-9151-4.

Donoho, D. (1995). De-noising by soft-thresholding. IEEE Trans. Inf. Theory, Vol. 41, pp. 613–627.

Donoho, D., and I. M. Johnstone (1994). Ideal spatial adaptation by wavelet shrinkage. Biometria. Vol. 81, pp. 425–455.

Douglas, A.. (1997). Bandpass filtering to reduce noise on seismograms: is there a better way?. Bulletin of the Seismological Society of America, Vol. 87, pp. 770–777.

Gabor, D. (1946). Theory of communications. J. Inst. Electr. Eng, Vol. 93, pp. 429–457.

Galiana-Merino, J. J., J. Rosa-Herranz, J. Giner, S. Molina, and F. Rotella (2003). De-noising of short period seismograms by wavelet packet transform. Bulletin of the Seismological Society of America, Vol. 93, pp. 2554–2562.

Gallipoli, M. R., M. Mucciarelli, F. Ponzo, M. Dolce, E. D'Alema, and M. Maistrello (2006). Buildings as a Seismic Source: Analysis of a Release Test at Bagnoli, Italy. Bulletin of the Seismological Society of America, Vol. 96, No. 6, pp. 2457–2464.

Mallat, S. (1998). A Wavelet Tour of Signal Processing. Academic, New York.

Mucciarelli, M., A. Masi, M. R. Gallipoli, P. Harabaglia, M. Vona, F. Ponzo, and M. Dolce (2004). Analysis of RC Building Dynamic Response and Soil-Building Resonance Based on Data Recorded during a Damaging Earthquake (Molise, Italy, 2002). Bulletin of the Seismological Society of America, Vol. 94, No. 5, pp. 1943–1953.

Pandey, A. K., M. Biswas, M. M. Samman (1991). Damage detection from changes in curvature mode shapes. Journal of Sound and Vibration, Vol. 145, Issue 2, pp. 321-332.

Parolai, S. (2009). Denoising of Seismograms Using the S Transform. Bulletin of the Seismological Society of America, Vol. 99, No. 1, pp. 226–234.

Pinnegar, C. R., and D. E. Eaton (2003). Application of the S-transform to prestack noise attenuation filtering. J. Geophys. Res. , Vol.108, no. B9, 2422, doi 10.1029/2002JB00002258.

Simon, C., S. Ventosa, M. Schimmel, A. Heldring, J. J. Dañobeitia, J. Gallart, and A. Manuel (2007). The S-Transform and its inverses: side effects of discretizing and filtering. IEEE Trans. Signal Process. , Vol. 55, pp. 4928–4937, doi 10.1109/TSP.2007.897893.

Stockwell, R. G., L. Mansinha, and R. P. Lowe (1996). Localization of the complex spectrum: the S transform. IEEE Trans. Signal Process., Vol. 44, pp. 998–1001.

Weaver, J. B., X. Yansun, D. M. Healy Jr, and L. D. Cromwell (1991). Filtering noise from images with wavelet transforms. Magn. Reson. Med. , Vol. 24, pp. 288–295.

CONCLUSIONS

This thesis addressed issues concerning the monitoring and dynamic characterization of structures, taking into account their interaction with the ground, and some original techniques have been proposed for the signal treatment and to extract the dynamic characteristics of non-stationary systems.

The discussion concerning the dynamic soil-structure interaction was done using an original approach based on the model proposed by Şafak. This original approach has also allowed an assessment of the radiation transmitted from building to the ground. Following this approach the ability of buildings to change the free-field ground motion has been evaluated, taking into account also the interaction between the buildings, when there is more than one structure. Moreover, considering a single building, and basing on a experimentally calibrated model, a statistical estimates of the possibility of observing a given ground motion was proposed. The latter allows to assess in an approximate but quantitative way, the influence that a building of small and large size, taking into account the distance variation, could have on: PGA, Housner intensity and spectral acceleration. Moreover, during the experimental campaign on the Falkenhof Tower it was possible, on the one hand, to compare the results of different techniques used to study the dynamic characteristics of the tower, and on the other hand, to verify experimentally that a building is able to modify the free-field ground motion from multiple points of view. Beside a change in frequency content and amplitude, it is able to contribute to the dissipation of energy thanks to its damping. It should be kept in mind, however, that this effect is not always beneficial. In fact, as proved by analysis of experimental dataset, it is true that the total energy tends to decrease, but it is also true that a peak amplification of motion close to the natural frequencies of the structure can be observed.

Parallel to these aspects, in order to refine the methods and techniques for dynamic characterization, innovative methods for both detailed studies and for fast analysis were proposed. Moreover, using the innovative accelerometric stations, some tests to monitor large structures, such as the Fatih Bridge, and structures with normal size, in the Municipality of Navelli, were performed. The good quality of the results obtained from the tests, allows to state that these sensors are adequate for structural monitoring. They are cheap, and have the great advantage of communicating with each other and create a mesh that allows to connect to one station and communicate with all the other stations.

This allows to monitor the dynamic response of structures that are also in conditions of incipient collapse. Obviously, the stations must be already installed inside the building well before damage starts. In this case, taking the advantage to connect only to one station belonging to the network, it is possible to download the data without going inside a damaged structure. In particular, as regards to the fast methods, two techniques were proposed. The former is for the assessment of health status of a building subjected to earthquake, the latter aim at the frequencies characterization and the identification of torsional modes of structures. The former technique lends itself well to monitoring of strategic structures, for which it is certainly possible to install few sensors and then to assess in quasi-real-time, although in approximate way, the damage level suffered by the structure. In fact, the proposed method belong to the first level methods, and therefore, does not allow the damage localization, but a sufficiently accurate estimate of the damage level. The latter technique is useful for the expeditious evaluation of existing buildings. Indeed, the torsional modes are not always easy to identify if a large number of sensors are not available, therefore, below an adequate budget it is not always possible to go beyond the simple frequencies characterization of a structure. With the proposed technique, using only two tri-directional velocimeters it is not only possible to estimate the main frequencies of vibration, but it is also possible to evaluate the importance of torsional modes for the seismic response of the structure. The amount of data that are obtained allows to get the results in quasi-real-time if a laptop is available. Regarding the detailed studies, with particular reference to the analysis of non-stationary systems, a method for filtering and extrapolation of the dynamic characteristics of soil and buildings was implemented in a Graphical User Interface (GUI). Using the mathematical characteristics of the Stockwell transform, a band-variable filter that allows to isolate individual modes of vibration and to study their evolution over time has been tested. This methodology was successfully applied to study the signals recorded on soil, during the Kobe earthquake, where the deposit was subjected to liquefaction, and to study the signals recorded on instrumented buildings damaged during the Molise seismic sequence.

ACKNOWLEDGEMENTS

The successful completion of this thesis would not have been possible without the cooperation and help of a great many people.
I thank my supervisors V. Caputo, M. Mucciarelli, S. Parolai and F.C. Ponzo for stimulating discussion and for their invaluable advice and support.
Last but not least, I like to thank my family and my girlfriend for all their love and support given to me all my life.

I'd also like to thank all this people:

Chapter 1: thanks to M. R. Gallipoli, M. Mucciarelli, F. C. Ponzo

Chapter 2: thanks to S. Parolai, M. Mucciarelli, S. Eggert, M. Sobiesiak and J. Zschau

Chapter 3: thanks to M. Picozzi, C. Milkereit, C. Zulfikar, K. Fleming, M. Erdik, J. Zschau, J. Fischer, E. Safak, O. Özel, N. Apaydin

Chapter 4: thanks to M. Picozzi, S. Parolai, M. Mucciarelli, C. Milkereit, M. Sobiesiak and J. Zschau

Chapter 5: thanks to F. C. Ponzo, G. Auletta., A. Mossucca

Chapter 6: thanks to M. Dolce, F. C. Ponzo, A. Di Cesare, C. Moroni, D. Nigro, G. Serino, S. Sorace, V. Gattulli, A. Occhiuzzi, A. Vulcano, D. Foti

Chapter 7: thanks to M. Vona, M. Mucciarelli, A. Masi

Chapter 8: thanks to M. Mucciarelli, F. C. Ponzo